Department of Food and Nutrition
University of Helsinki
Dissertationes Universitatis Helsingiensis
100/2023

Mining for carbohydrate-active oxidoreductases in CAZyme family AA3

Hongbo Zhao

ACADEMIC DISSERTATION

To be presented, with the permission of the Faculty of Agriculture and Forestry of the University of Helsinki, for public examination in Walter hall, EE-building, Viikki,
on 8 December 2023, at 1 pm.

Helsinki 2023

Custos

Professor Marko Virta
Department of Microbiology
University of Helsinki

Supervisors

Professor Maija Tenkanen
Department of Food and Nutrition
University of Helsinki

Professor Emma Master
Department of Bioproducts and Biosystems
Aalto University, Finland
Department of Chemical Engineering and Applied Chemistry
University of Toronto, Canada

Docent Anna Happonen
Plant genetics and genomics
Natural Resources Institute Finland, Finland

Preliminary examiners

Professor Craig Faulds
Department of Biotechnology
Aix-Marseille University, France

Research Professor Aniko Varnai
Faculty of Chemistry, Biotechnology and Food Science
Norwegian University of Life Sciences, Norway

Opponent

Associate Professor Roland Ludwig
Department of Food Science and Technology
University of Natural Resources and Life Sciences, Vienna, Austria

Publisher: University of Helsinki
Series: Dissertationes Universitatis Helsingiensis 100/2023

ISBN 978-951-51-9540-1 (print)
ISBN 978-951-51-9541-8 (online)
ISSN 2954-2898 (print)
ISSN 2954-2952 (online)
PunaMusta, Joensuu 2023

Abstract

Hemicelluloses, particularly xylans, are a significant component of lignocellulosic biomass, and they constitute up to 50% of its composition in both grasses and deciduous trees. Biocatalysts have primarily focused on deconstructing hemicellulosic polysaccharides into fermentable sugars to produce fuels and chemicals. However, there is potential in enzymatically oxidizing hemicellulosic fragments to enable their further modification or polymerization into higher-value bio-based chemicals and materials, while retaining the carbon and energy stored in the original carbohydrate structures. The carbohydrate-active enzyme (CAZy) database categorizes oxidoreductases targeting lignocellulosic substrates into various auxiliary activity (AA) families. Notably, the AA3_1 and AA3_2 subfamilies comprise carbohydrate oxidoreductases that possess the ability to oxidize diverse carbohydrates at different positions. These enzymes have been studied for applications such as lignocellulose saccharification, biosensing, enzymatic anodes, dye decolorization, pulp bleaching, and gelling agents. Given their properties, AA3_1 and AA3_2 enzymes are promising candidates for upgrading hemicellulosic fragments. However, their specificity and regioselectivity in oxidizing oligosaccharides, particularly hemicellulosic oligosaccharides, remain largely unknown. Furthermore, despite a total of 2838 AA3_1 and AA3_2 sequences being recorded in the CAZy database, only a few dozen have been biochemically characterized, and novel activities are still to be discovered.

Therefore, this thesis focused on the discovery and characterization of fungal AA3 oxidoreductases with the ability to functionalize carbohydrates, especially xylooligosaccharides. Specifically, two previously studied pyranose dehydrogenases from the AA3_2 subfamily, *Ab*PDH1 and *Am*PDH1, were examined for their activity and regioselectivity towards linear xylooligosaccharides and xylooligosaccharides substituted with arabinofuranosyl or 4-O-(methyl)-glucopyranosyluronic acid residues. Both *Ab*PDH1 and *Am*PDH1 showed decreasing activity with increasing xylooligosaccharide length and acidic substrates. Oxidation of linear xylooligosaccharides primarily occurred at the secondary hydroxyls and the reducing end C-1, providing an opportunity to synthesize bifunctional molecules directly from hemicellulose fragments. Subsequently, a protein from the AA3_1 subfamily was produced and identified as a xylooligosaccharide dehydrogenase and named *Tm*XdhA. Like other characterized AA3_1 cellobiose dehydrogenases, *Tm*XdhA showed a preference for linear saccharides with β-(1→4) linkages, specifically targeting the hydroxyl group on the reducing anomeric carbon. Notably, *Tm*XdhA was distinguished, however, by its preferential activity towards xylooligosaccharides over cellooligosaccharides. Furthermore, 27 AA3_2 members were recombinantly produced to screen for novel activity. With a total of 52 electron donors and three electron acceptors being tested, seven active AA3_2 oxidoreductases were discovered, including two glucose dehydrogenases (*Ta*GdhA and *Mc*GdhA), a glucose oxidase (*Ap*GoxA), an oligosaccharide dehydrogenase (*Ki*OdhA) that primarily oxidizes gentiobiose, and three aryl alcohol oxidoreductases (*Ps*AaoA, *As*AadhA, and *As*AadhB). Notably, AA3_2s were found to utilize phenoxy radicals as an electron acceptor; thus, they may mitigate the potential cytotoxicity of radicals and prevent the reformation of semiquinones and other lignin radicals.

The discovery and characterization of these AA3_1 and AA3_2 enzymes offer new biocatalysts for biotechnology applications and provide insights into upgrading oligosaccharides to valuable chemicals.

Preface

The work presented in this doctoral thesis was conducted at the Department of Food and Nutrition in the Faculty of Agriculture and Forestry at the University of Helsinki, Finland. I am grateful for the financial support received from the following organizations: the Academy of Finland (COCOA project – 308996 & 308997), the Finnish Cultural Foundation (individual research grant – 00211192), the Novo Nordisk Foundation (ARADOX project – 0070816), and the Doctoral Programme in Microbiology and Biotechnology.

I owe my deepest gratitude to my supervisors, Professor Maija Tenkanen, Professor Emma Master, and Docent Anna Happonen, for their insightful feedback and continuous support along the way. Maija, your mentorship has been truly inspiring. I am particularly grateful for the freedom that you offered me to develop my own research ideas and explore uncharted territories in our field. I feel privileged to have had the opportunity to work under your tutelage. Emma, thank you for your guidance in protein production and enzyme characterization, and for consistently motivating me with your enthusiasm for science. To Anna, I offer my gratitude for your instruction on plant cell wall structure and lignin biosynthesis. I would also like to extend my appreciation to my thesis committee members, Docent Miia Mäkelä and Associate Professor Ndegwa Maina, for their expert insights, which enriched this work.

I would like to express my gratitude to Associate Professor Roland Ludwig (University of Natural Resources and Life Science, Vienna, Austria) for agreeing to be my opponent. I also thank Professor Craig Faulds (Aix-Marseille Université, France) and Research Professor Aniko Varnai (Norwegian University of Life Sciences, Norway) for their roles as pre-examiners. I am deeply grateful for the valuable feedback that has contributed to the continued enhancement of this thesis.

I would like to thank Professor Kirsi Mikkonen and Dr. Mari Lehtonen for their warm welcome and support upon my arrival in Helsinki for an internship when I was a master's student. It has been a pleasure to work with my current and former group members, Sun-Li Chong, Johanna Karppi, Minna Juvonen, Tanja Paasela, Daria Poshina, Mengyi Sun, and Jenny Svartström. Thank you all for the time we spent together and the support I got from you. Additionally, I would like to thank all the former and current colleagues and friends in the department of Food and Nutrition (FAN). Engaging in scientific discussions and casual conversations with each of you has been a true pleasure, and I have thoroughly enjoyed working alongside you. I would like to offer a special thanks to our lab technicians, Miikka Olin, Taru Rautavesi, Jutta Varis, and Mikko Kangas for their invaluable

assistance in the laboratory. To my Chinese friends and colleagues I met in the department – Xie Chong, Yang Zhen, Wang Yaqin, Liu Chang, Lyu Jian, Han Xiaocui, Wang Min, Liu Fengyuan, Li Binbin, and Zhang Ruoxi – I would like to acknowledge the challenges of being far away from home. With your presence, the distance seemed to fade away. Your friendship has been a source of comfort and support during my time in Helsinki.

I am deeply grateful for all my co-authors and collaborators across research institutes. I would like to thank Filip Mollerup, Ville Aumala, Amin Leamon, Leena Penttinen, Eleni Ioannou, Deepika Dahiya, Taru Koitto, and Majid Haddad Momeni for your support during my visits to Aalto University. It was a pleasure to have the chance to work with all of you. I also appreciate the cooperation in enzyme characterization from Owen Mototsune and Xuebin Feng from the University of Toronto. I am delighted that you visited Helsinki and we had the opportunity to work together. I extend my thanks to Professor Adrian Tang, Thi Truc Minh Nguyen, and Annie Bellemare from Concordia University for the collaboration in bioinformatic work.

I would never have made it this far without the love and support of my parents. Mom and Dad, you consistently backed my decisions throughout my growth and education. You urged me to follow my passions and forge my own unique path, ultimately making me who I am today. Your optimism also impacted me, providing me with the strength to confront and overcome the challenges I have encountered on my journey.

Finally, I wish to express my profound gratitude to my wife, Wei Wei. Maintaining a long-distance relationship for eight years, particularly with the added challenges of a pandemic limiting our chances to visit each other, was no easy feat. I am so happy that we made it through. You are the biggest source of joy in my life. Thank you for all your love and unconditional support.

Hongbo Zhao

Helsinki, Oct 2023

List of publications

This doctoral dissertation consists of a summary and the following publications, which are referred in the text by their number in this list.

1. Karppi, J., **Zhao, H.**, Chong, S.-L., Koistinen, A. E., Tenkanen, M., & Master, E. (2020). Quantitative comparison of pyranose dehydrogenase action on diverse xylooligosaccharides. *Frontiers in Chemistry, 8*, 11. https://doi.org/10.3389/fchem.2020.00011

2. **Zhao, H**., Karppi, J., Nguyen, T. T. M., Bellemare, A., Tsang, A., Master, E., & Tenkanen, M. (2022). Characterization of a novel AA3_1 xylooligosaccharide dehydrogenase from *Thermothelomyces myriococcoides* CBS 398.93. *Biotechnology for Biofuels and Bioproducts, 15*(1), 135. https://doi.org/10.1186/s13068-022-02231-w

3. **Zhao, H.**, Karppi J., Mototsune, O., Poshina, D., Svartström, J., Bellemare, A., Nguyen, T.T.M., Master, E., & Tenkanen, M. Substrate specificity mapping of fungal CAZy AA3_2 oxidoreductases. *Manuscript submitted*.

Author contributions

1. HZ participated in the design of the study, activity measurements, and substrate deletion analysis. HZ performed the quantitative analysis of the degree of oxidation and the oxidation position identification. HZ also took charge of interpreting the results of those analyses. Furthermore, HZ collaborated with coauthors in the process of writing the research article.

2. HZ planned the research with MT, with assistance from EM. HZ conducted most of the experimental work except for the cloning, transformation, and production of recombinant proteins. HZ interpreted all results and had preliminary responsibility for writing the article under the supervision of MT.

3. HZ planned the research with MT, with assistance from EM. HZ participated in most of the experimental work except for the cloning, transformation, and production of recombinant proteins. HZ interpreted all results and had preliminary responsibility for writing the article under the supervision of MT.

List of Abbreviations

AA	Auxiliary Activity
AADH	Aryl alcohol dehydrogenase
AAO	Aryl alcohol oxidase
ABTS	2,2′-azino-bis(3-ethylbenzothiozoline-6-sulfonic acid)
AOx	Alcohol oxidase
Ara*f*	arabinofuranosyl
A^3X	3^2-α-L-arabinofuranosyl-xylobiose
A^2XX	2^3-α-L-arabinofuranosyl-xylotriose
BQ	Benzoquinone
C_2	Cellobiose
C_3	Cellotriose
C_4	Cellotetraose
CAZy	Carbohydrate Active Enzymes Database
CBLM	5-amino-5-deoxy-cellobiono-1,5-lactam
CBM	Carbohydrate binding module
CDH	cellobiose dehydrogenase
CE	Carbohydrate esterase
DCIP	Dichlorophenolindophenol
DFF	furan-2,5-dicarbaldehyde
ELSD	Evaporative light scattering detector
EO	Ecdysone oxidase
ESI	Electron spray ionization
FAD	Flavin adenine dinucleotide
FDCA	2,5-furandicarboxylic acid
FFCA	2,5-formylfurancarboxylic acid
GalOx	Galactose oxidase
GH	Glycoside hydrolase
GMC	Glucose-methanol-choline
GOx	Glucose oxidase
GT	Glycosyl transferase
G unit	Guaiacyl unit
HILIC	Hydrophilic interaction chromatography

HMF	hydroxymethylfurfural
HPAEC	High Performance Anion-Exchange Chromatography
HQ	Hydroquinone
HRP	Peroxidase from horseradish
H unit	*p*-hydroxyphenyl unit
JGI	US Joint Genome Institute (jgi.doe.gov)
k_{cat}	Turnover rate
K_M	Michaelis-Menten constant, affinity of an enzyme for its substrate
LPMO	Lytic polysaccharide monooxygenase
MALDI	Matrix-assisted laser-desorption-ionization
MS	Mass spectroscopy
ODH	Oligosaccharide dehydrogenase
PAD	Pulsed amperometric detection
PDA	Photodiode-array detector
PDH	Pyranose dehydrogenase
PFP	Pentafluorophenyl
PGC	Porous Graphitic Carbon
PL	Polysaccharide lyases
POx	Pyranose oxidases
SSN	Sequence similarity network
S unit	Syringyl unit
TEMPO	2,2,6,6-tetramethylpiperidine
TOF	Time of Flight
X_2	Xylobiose
X_3	Xylotriose
X_4	Xylotetraose
XA^3XX	3^3-α-L-arabinofuranosyl-xylotetraose
$XU^{4m2}XX$	2^3-(4-O-methyl-α-D-glucuronyl)-xylotetraose
Xyl*p*	Xylopyranosyl
U	Enzyme unit
UPO	Unspecific peroxygenase
UPLC	Ultra high-performance liquid chromatography
$U^{4m2}X$	2^2-(4-O-methyl-α-D-glucuronyl)-xylobiose
$U^{4m2}XX$	2^3-(4-O-methyl-α-D-glucuronyl)-xylotriose

Contents

Abstract 1
Preface 2
List of Abbreviations 6
1. Introduction 10
1.1 Plant cell wall as an important biomass resource 10
1.1.1 Cell wall composition 10
1.1.2 Forest biomass utilization 15
1.1.3 Chemical catalysis vs enzymes as biocatalysts 16
1.2 CAZy oxidoreductases 16
1.2.1 CAZy oxidoreductases in general 16
1.2.2 Fungal oxidoreductases 17
1.2.3 Carbohydrate-active oxidoreductases as biocatalysts and their applicable use 19
1.2.4 The genomic resource 20
1.3 AA3 oxidoreductases 21
1.3.1 Overview of CAZy family AA3 enzymes 21
1.3.2 AA3_1 cellobiose dehydrogenase 22
1.3.3 Diverse enzyme function within the AA3_2 subfamily 28
1.3.4 Glucose oxidase/dehydrogenase 29
1.3.5 AA3_2 pyranose dehydrogenase 31
1.3.6 AA3_2 aryl alcohol oxidase/dehydrogenase and other putative AA3_2 sequences 33
1.4 Biotechnology applications of fungal AA3_1s and AA3_2s 35
1.5 Biological function of fungal AA3s 37
2. Aim of the thesis 39
3. Materials and methods 40
3.1 Commercial enzymes and electron donors 40
3.2 Production and purification of fungal AA3 proteins 42
3.3 Enzymatic assays 42
3.4 Product identification and quantification 45
3.4.1 Product analysis of *Ab*PDH1 and *Am*PDH1 oxidized xylooligosaccharides (Study 1) 45
3.4.2 Product analysis of *Tm*XdhA oxidized oligosaccharides (Study 2) 45
3.4.3 Product analysis of AA3_2 oxidized carbohydrate and aryl alcohols (Study 3) 47
3.5 Utilization of phenoxy radicals by AA3_2s 47
3.6 Sequence and structure analysis 47
3.7 Statistical analysis 47
4. Results 48

4.1 Production and purification of fungal AA3 proteins 48
4.2 Oxidation of xylooligosaccharides by AA3_2 *Ab*PDH1 and *Am*PDH1 50
4.2.1 *Ab*PDH1 and *Am*PDH1 were able to oxidize xylooligosaccharides 50
4.2.2 *Ab*PDH1 and *Am*PDH1 introduced multiple oxidations to the xylooligosaccharides 52
4.2.3 *Ab*PDH1 and *Am*PDH1 oxidized xylooligosaccharides at both ends 55
4.3 Biochemical characterization of a novel AA3_1 xylooligosaccharide dehydrogenase, *Tm*XdhA 57
4.3.1 *Tm*XdhA oxidized diverse mono-, di- and oligosaccharides at the anomeric carbon 57
4.3.2 *Tm*XdhA prefers linear xylooligosaccharides over cellooligosaccharides 60
4.3.3 The structure model of *Tm*XdhA suggests that a glutamine residue could facilitate *Tm*XdhA's binding to pentose sugar 63
4.4 Screening for substrate specificity among AA3_2 subclusters 65
4.4.1 Sequence selection based on sequence similarity network 65
4.4.2 Primary activity screening 67
4.4.3 Secondary activity screening 67
4.4.4 Detailed characterization of the new carbohydrate oxidase and dehydrogenases 69
4.4.5 *Ps*AaoA is an aryl alcohol oxidase 70
4.5 AA3_2s can use phenoxy radical as electron acceptor 73
5. Discussion 75
5.1 *Ab*PDH1 and *Am*PDH1 for xylooligosaccharide conversion 75
5.2 *Tm*XdhA as the first xylooligosaccharide dehydrogenase in AA3_1 77
5.3 Mining for novel activities within AA3_2 78
5.3.1 Correlation between enzyme specificity and SSN clustering 78
5.3.2 AA3_2 GDH/GOx activities are not restricted to glucose 79
5.3.3 *Ps*AaoA oxidized a wide range of aryl alcohols 80
5.4 The biological function of AA3s 81
6. Future research aspects 82
7. Conclusions 85
References 86

1. Introduction

1.1 Plant cell wall as an important biomass resource

Forests hold immense importance for the history, identity, and economy of Finland and many other countries. In today's world, the global significance of forests is paramount, given that they act as crucial carbon sinks, effectively capturing atmospheric carbon to combat climate change and to support life on our planet. Additionally, forests offer abundant opportunities for sustainable and renewable bioproducts, such as pulp, paper, timber, bioenergy, and biomaterials. This growing demand presents countries worldwide with a valuable chance to leverage their forest resources for economic and environmental benefits.

1.1.1 Cell wall composition

The forest biomass, predominantly composed of lignocellulose, is primarily stored in the plant cell wall. The plant cell wall consists of various polysaccharides, aromatic substances, and proteins that form a functional matrix comprising the middle lamella, primary cell wall, and secondary cell wall (Figure 1A) (Carpita, Ralph, and McCann 2015). The middle lamella, situated between adjacent plant cells, is mainly composed of pectin, proteins, and lignin (Westermark 1985; Zamil and Geitmann 2017). The primary cell wall comprises a polysaccharide-based network with cellulose as the structural scaffold and hemicellulose and pectic polysaccharides cross-linking the cellulose fibers (Figure 1B). In some cases, aromatic substances can be incorporated into the primary cell wall through esterification with the polysaccharide chain (Carpita et al. 2015). During cell differentiation, the lignified secondary cell wall is formed, and simultaneously, the pectic polysaccharide content reduces (Figure 1C) (Ishii 1997; Vogel 2008).

While the composition of the plant cell wall varies among species and undergoes dynamic changes throughout the cell's life span, forest biomass can be primarily categorized into three main components: cellulose, hemicellulose, and lignin. Cellulose, the most abundant plant polysaccharide, is found in both the primary and secondary cell walls, accounting for 15–45% of plant dry weight (Vogel 2008). It consists of repeating β-(1→4)-linked D-glucopyranosyl units that form crystallized cellulose microfibrils. The arrangement and crystallinity of cellulose microfibrils differ between primary and secondary walls, as well as among different layers of the secondary cell wall and plant species (Barnett and Bonham 2004). These microfibrils provide structural support and contribute to the mechanical rigidity and stability of plant cells.

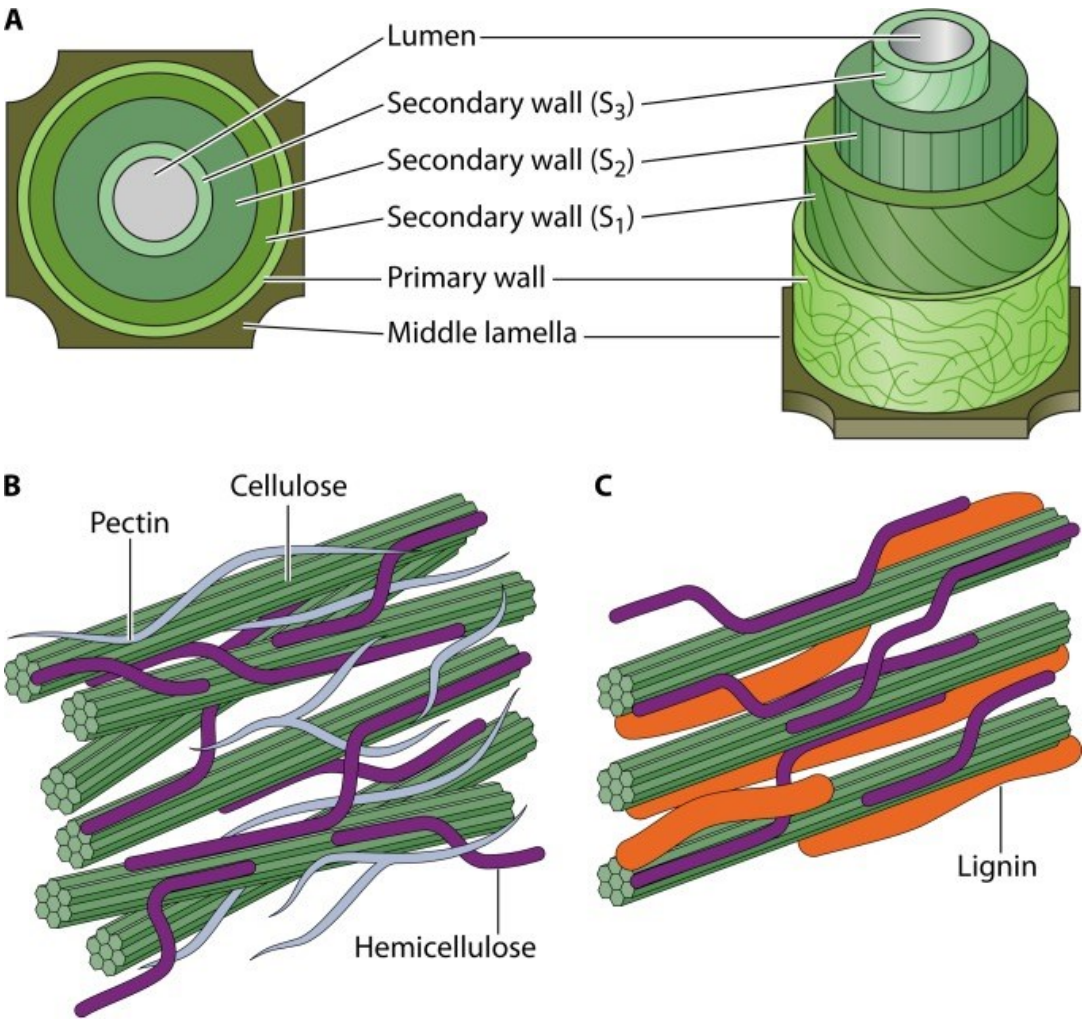


Figure 1. Simplified model of plant cell wall structure. A) The three main cell wall layers: the middle lamella and the primary and secondary walls. The angles and directions of the polysaccharide chains differ among the primary wall and the S1–S3 layers of the secondary wall. The main polysaccharides (cellulose, hemicellulose, and pectin) and lignin in B) the primary wall and C) secondary wall. The lignin content in the primary cell wall (not illustrated) varies notably depending on the plant species. The illustrations are not to scale. Figure adapted with permission from Rytioja et al. (2014).

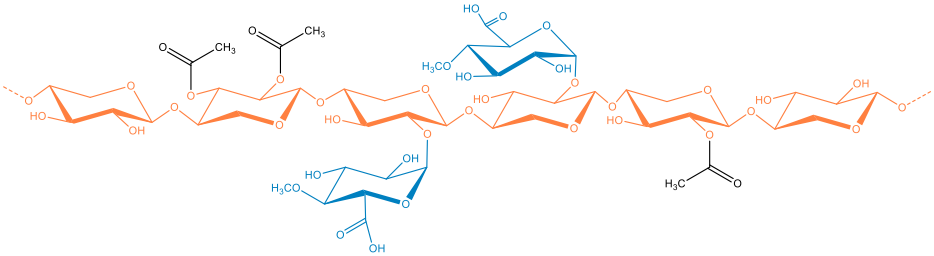
Hemicelluloses, which are classes of alkalic extractable polysaccharides, play a crucial role in cross-linking cellulose microfibrils along with uronic acid-rich pectin through hydrogen bonds (Carpita et al. 2015). There are four major types of hemicellulose: xyloglucan, heteromannan, β-glucan, and xylan, each composed of different sugar building blocks.

Xyloglucan is the main hemicellulose found in the primary cell wall of eudicots and approximately half of monocots. It consists of linear chains of β-(1→4)-linked glucan, and xylosyl residues have been found to attach to the O-6 position of the glucosyl residues (Carpita et al. 2015). Some xylosyl residues are further substituted with L-arabinose, D-galactose, or L-fucose. These substitutions play a crucial role in regulating water retention by the plant cell wall and enable dynamic enzymatic recognition and modification of the cell wall during growth (Scheller and Ulvskov 2010).

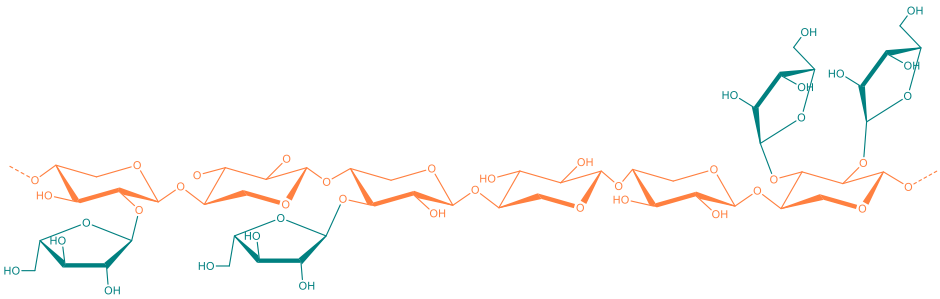
Xylan is a type of hemicellulose present in the primary cell wall of flowering plants and in the secondary cell wall of spermatophytes (seed plants). It generally accounts for 10–35%, 5–11%, and up to 30% of the total dry weight of angiosperms (hardwoods), gymnosperms (softwoods), and cereals, respectively (Vogel 2008). Xylan has a backbone of β-(1→4)-linked xylosyl residues, with the hydroxyl groups on the O-2 and O-3 positions typically substituted. There are three main types of xylans based on the abundance of substituents: arabinoxylan, glucuronoxylan, and glucuronoarabinoxylan/arabinoglucuronoxylan (Figure 2). Arabinoxylan, with L-arabinofuranosyl (Ara*f*) substitutions, is commonly found in cereals and grasses (Harris and Stone 2008). Glucuronoxylan, with 4-O-methyl-α-D-glucopyranosyl uronate (MeGlc*p*A) as the dominant carbohydrate side group, is commonly found in hardwoods. Softwoods often contain mixed substitutions of Ara*f* and glucuronic acid. Xylan can also be further substituted with functional groups such as acetyl groups and ferulate units such as ferulic acid (Oliveira et al. 2019).

Galactoglucomannan is the main type of hemicellulose found in softwoods, constituting 15–25% of their cell wall weight (Eriksson, Blanchette, and Ander 1990; Vogel 2008). Galactoglucomannan typically consists of β-(1→4)-linked D-mannose and D-glucose and is decorated with monomeric D-galactosyl branches and acetyl groups.

A) glucuronoxylan



B) arabinoxylan



C) arabinoglucuronoxylan/glucoronoarabinoxylan

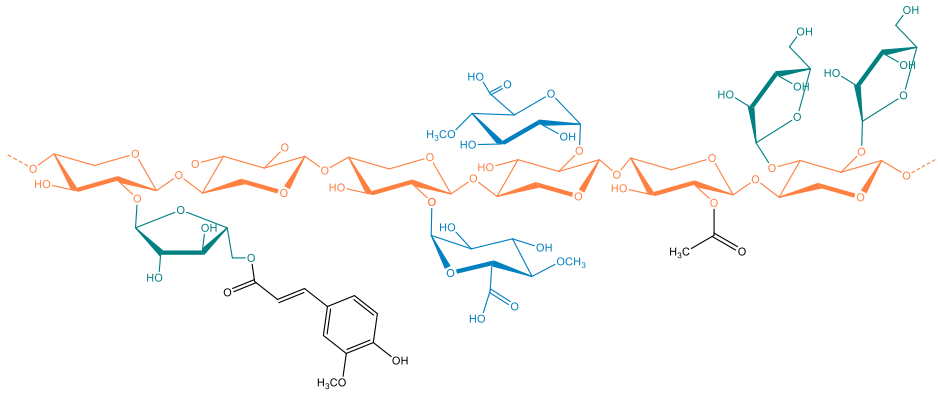


Figure 2. The simplified chemical structure of the three main types of heteroxylan: A) glucuronoxylan, B) arabinoxylan, and C) arabinoglucoronoxylan/glucuronoarabinoxylan. For clarity, the positions of the substitutions are illustrative. Figure adapted and modified from Vuong and Master (2022).

In addition to polysaccharides, aromatic and heterogenic lignin comprise a significant portion of forest biomass, accounting for 21–32% of dry weight in both softwoods and hardwoods (Eriksson et al. 1990). Lignin is mainly synthesized from three monolignols—*p*-coumaryl alcohol, coniferyl alcohol and sinapyl alcohol—which are derived from the phenylpropanoid biosynthetic pathway.

These monolignols are transformed to the *p*-hydroxyphenyl unit (H), guaiacyl unit (G), and syringyl unit (S), respectively (Figure 3). This transformation involves enzymes such as laccase, peroxidase, and other oxidoreductases, which convert monolignols into monolignol derivatives and radicals. These radicals then undergo coupling reactions to form lignin polymers. Furthermore, lignin polymers can also covalently bind to hemicellulose through two mechanisms. First is the radical coupling between monolignol radicals and feruloyl radicals on the hemicellulosic backbone. In the second mechanism, the hydroxyls on the hemicellulosic backbone act as nucleophiles to induce the re-aromatization of lignin residues (Terrett and Dupree 2019).

The composition of lignin monomers varies among plant species. In softwoods, lignin is predominantly composed of G units, while hardwood lignin contains both G and S units. In contrast, grass plants mainly consist of H units and they generally have less lignin content than woody plants (Lourenco and Pereira 2018). Some plants also incorporate various phenolic compounds and monolignin aldehydes in their lignin (Del Río et al. 2019).

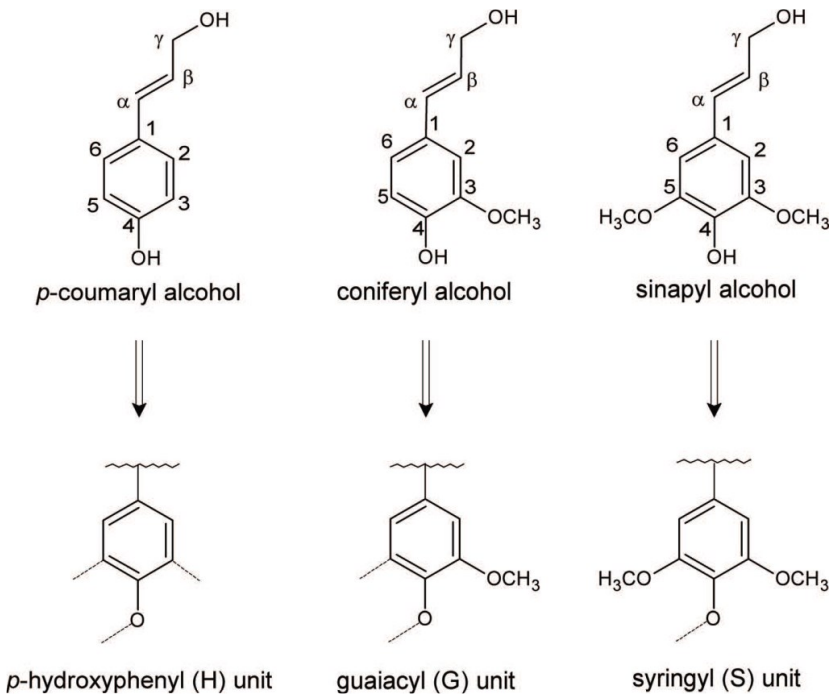


Figure 3. The chemical structure of the three main monolignols and their corresponding building blocks in lignin.

1.1.2 Forest biomass utilization

The direct combustion of forest biomass has a low energy conversion rate and results in the emission of harmful substances such as particulates and sulfur dioxide (Glushkov et al. 2021). Nowadays, the forest biomass is primarily harvested for particular products like pulpwood or sawn timber, which are used in paper production and the manufacture of wood-based panels and products. Pulp mills produce cellulose fiber as their primary output, and the hemicellulose fraction remains largely underutilized (Kumar et al. 2021). The limited utilization of hemicellulose fractions is partially due to the lack of a proper extraction method.

In recent years, a method known as pressurized hot water extraction has been developed as a sustainable and cost-efficient approach to increasing hemicellulose utilization. This method utilizes hot water as the extraction solvent and birch sawdust from sawmills as the raw material. The extraction yield can exceed 50%, and the high processing temperature leads to the depolymerization of hemicelluloses into hemicellulosic fragments or oligosaccharides with a molar mass ranging from 4 kDa to 20 kDa (Kilpeläinen et al. 2013). Complementing this method, enzymatic techniques have gained significant attention for the production of oligosaccharides from hemicellulose. These methods involving enzymes such as endo-xylanases and endo-mannanases are known for their higher selectivity, reduced energy consumption, and minimal environmental impact (Houfani et al. 2020).

Efforts to contribute to carbon neutrality and drive the bioeconomy have led to growing interest in utilizing forest biomass in a green and sustainable manner. Significant work has been devoted to converting forest biomass residues into biofuels and biochemicals by means of chemical or enzymatic depolymerization of the lignocellulosic materials. This approach involves breaking down the complex structure of lignocellulose into smaller molecules that can subsequently be transformed into biofuels and platform chemicals (Hayes 2009; Okolie et al. 2021; Sun and Cheng 2002; Yu et al. 2021). The production of biofuels, such as ethanol derived from cellulosic materials, has demonstrated the potential to slash greenhouse gas emissions by over 85% in comparison to fossil fuels (Adler, Del Grosso, and Parton 2007; Schmer et al. 2008). Platform chemicals derived from lignocellulose have been used for applications in various industries, including adhesives, paints, cosmetics, food, and pharmaceuticals (Okolie et al. 2021). However, this approach does not fully unlock the potential of plant biomass, as it sacrifices the polymeric structure of lignocellulose.

More recently, some focus has shifted to upgrading lignocellulosic substrates to added value materials while retaining their polymeric structure. For instance, cellulose nanofiber and hemicellulose, such as xylan, have emerged as promising biomaterials due to their exceptional mechanical properties and

environmental advantages when compared to petroleum-based polymers (Shaghaleh, Xu, and Wang 2018; Vuong and Master 2022). These biomaterials have potential applications as green alternatives to plastics, for example, biofilms and biodegradable, renewable bio-food packaging (Kisonen et al. 2015; Mikkonen et al. 2013; Parikka et al. 2017).

1.1.3 Chemical catalysis vs enzymes as biocatalysts

To modify plant biomass and achieve specific properties, the introduction of additional functional groups may be necessary. Although chemical oxidation methods, such as the use of 2,2,6,6-tetramethylpiperidine (TEMPO) or sodium periodate, have been effective in selectively oxidizing hydroxyl groups in carbohydrates, they are not always sustainable due to the use of harsh chemicals and the generation of side products (Johnson et al. 2009). TEMPO oxidation selectively targets primary hydroxyl groups at the C-6 position, while sodium periodate oxidizes both C-2 and C-3 secondary hydroxyl groups, resulting in cleavage of the link between these carbons (Kristiansen, Potthast, and Christensen 2010). However, these chemical methods lack the desired regioselectivity, often leading to polysaccharide degradation (Bragd, Besemer, and Van Bekkum 2000).

As a result, enzymes have emerged as attractive alternatives to conventional chemical conversions for biomass modification. They offer inherent specificity, require less energy input, and are environmentally friendly and sustainable. Enzymes serve as biocatalysts that can be utilized to tailor lignocellulosic materials, particularly targeting oligosaccharides derived from agricultural or forest sidestreams, to produce value-added materials.

1.2 CAZy oxidoreductases

1.2.1 CAZy oxidoreductases in general

Lignocellulose-targeting enzymes and their associated proteins are currently classified in the carbohydrate-active enzymes (CAZy) database (Drula et al. 2022). Based on their catalytic mechanism and sequence similarity, these enzymes are grouped into the families of glycoside hydrolase (GH), glycosyl transferase (GT), polysaccharide lyase (PL), carbohydrate esterase (CE), and auxiliary activity (AA). In addition, the non-catalytic carbohydrate-binding modules (CBMs) are also included in the class of associated modules. The inclusion of AA families in the CAZy database was due to their direct or indirect involvement in the modification and degradation of lignocellulosic biomass. Currently, 17 AA families are defined in the CAZy database, and subfamilies have been assigned to families AA1, AA3, and AA5 based on their homologous relationships (Table 1).

The oxidoreductases can be further categorized based on the nature of their electron acceptors. Enzymes that exhibit a preference for reducing organic compounds or ions that have little or no activity with molecular oxygen are referred to as **dehydrogenases**. Conversely, when oxygen is one of the primary electron acceptors and is reduced to hydrogen peroxide, the enzymes are referred to as **oxidases** (Mattevi 2006). **Laccases** also take oxygen as a primary electron acceptor, but they reduce oxygen to water. **Oxygenases** represent the enzymes that incorporate both atoms of molecular oxygen into the electron donor of the reaction, whereas **monooxygenases** incorporate only one atom of molecular oxygen into the electron donor of the reaction, with the other oxygen atom reduced to water. When hydrogen peroxide serves as the primary electron acceptor and is reduced to water, oxidoreductases are known as **peroxidases**. **Catalase** stands as a unique exception, functioning as a type of peroxidase that catalyzes the disproportionation of hydrogen peroxide into molecular oxygen and water.

Enzymes involved in the degradation and modification of aromatic compounds have been primarily identified in certain AA families, namely AA1 (comprising laccases and multicopper oxidases), AA2 (manganese and lignin peroxidases), AA3 subfamily 2 (aryl alcohol oxidases), AA4 (vanillyl alcohol oxidase), AA5 subfamily 2 (alcohol oxidases), and AA6 (1,4 benzoquinone reductases) (Table 1). In contrast, AA3, AA5, and AA7 include carbohydrate-active oxidases/dehydrogenases, which oxidize the hydroxyl groups of carbohydrate substrates to carbonyls. Lytic polysaccharide monooxygenases (LPMOs) have gained considerable attention over the past decade given their unique ability to cleave oligosaccharides and polysaccharides via oxidation of the glycoside bonds at either the C-1 or C-4 position, and some LPMOs have reportedly oxidized C-6 hydroxyl groups (Chen et al. 2018; Sun et al. 2022).

1.2.2 Fungal oxidoreductases

CAZy oxidoreductases have been identified in every kingdom of life, including fungi, plants, animals (particularly insects), and bacteria. Among these sources, fungi stand out for their remarkable ability to produce a wide range of extracellular oxidoreductases with diverse catalytic activities, making them valuable resources for biocatalyst discovery in biomass transformation (Cragg et al. 2015). Furthermore, fungal enzymes have gained attention due to their scalable production, cost-effectiveness, and easy genetic engineering, making them highly attractive for biotechnological applications (Singh, Singh, and Pandey 2019).

The fungal oxidoreductases are believed to play auxiliary roles in the degradation of plant biomass. For instance, enzymes such as laccases, lignin peroxidases, manganese peroxidases, and versatile

peroxidases are responsible for oxidizing lignin into smaller phenolic compounds, which facilitates the accessibility of hemicelluloses and cellulose to other enzymes (Zhou et al. 2022). LPMOs participate in cellulose fiber degradation together with the hydrolases. Additionally, various oxidases from the AA families oxidize diverse substrates and generate hydrogen peroxide, which in turn fuels the reactions of LPMOs and peroxidases. AA family dehydrogenases have been found to drive LPMO reactions through direct or phenol-mediated indirect electron transfer (Garajova et al. 2016; Haddad Momeni et al. 2021; Kracher et al. 2016). Interestingly, different fungal habitations are associated with distinct patterns of oxidoreductase expression. Wood decay and litter-decomposing fungi generally exhibit higher counts of extracellular oxidoreductases, while pathogenic fungi rely less on these enzymes (Mattila et al. 2022). Further biochemical characterization of oxidoreductases derived from diverse fungi will enhance understanding of their biological functions.

A uniform nomenclature for bacterial genetics and proteins was proposed in 1966, and the system has been adopted by some fungal researchers as well (Demerec et al. 1966). In this system, a gene is identified by a symbol consisting of three lowercase letters written in italics, with paralogs denoted by a single uppercase letter. The protein encoded by the gene carries the same three-letter symbol, but without italics, and with the first letter capitalized. The organism is represented by the first letter of the genus and species, with the first letter of the genus capitalized and italicized, and the first letter of species lowercase and italicized. For example, if the first cellobiose dehydrogenase gene characterized in *Aspergillus niger* is assigned the symbol *AncdhA*, the corresponding protein would be named *An*CdhA. Additionally, gene names are assigned only when the gene or its encoding product has been experimentally characterized, and it is typically assigned based on the characterized function rather than the predicted function solely based on the phylogenetic analysis. For example, a dehydrogenase that shows preferential activity for xylooligosaccharides should be named xylooligosaccharides dehydrogenase (XdhA) even though phylogenetic analysis predicts it to be a cellobiose dehydrogenase. However, this is not a system that every researcher follows. Some researchers use the conventional abbreviations for enzymes that are characterized, where the enzymes are denoted by three uppercase letters or the mix of uppercase and lowercase letters. For example, cellobiose dehydrogenase was conventionally named CDH, glucose oxidase is GOx, and galactose oxidase is GalOx. And if more than one putative sequence is identified from the genome of the organism, the paralogs are denoted by numbers. For instance, three pyranose dehydrogenases, identified from *Agaricus (Leucoagaricus) meleagris* are named *Am*PDH1, *Am*PDH2, and *Am*PDH3. To avoid further confusion, the enzymes that are newly characterized in this thesis are named

according to the Demerec nomenclature system, and the conventional abbreviations assigned by previous researchers were followed as originally proposed.

Table 1. Known activities, corresponding cofactor, and source organism in each AA (sub)family.

(Sub) Family	Known activities in each (sub)family	Cofactor	Source organism	Number of sequences*
AA1	**Multicopper oxidase**	Copper	fungi, plants, insects, bacteria	5135
AA1_1	Laccase			
AA1_2	Ferroxidase			
AA1_3	Laccase-like multicopper oxidase			
AA2	**Class II peroxidase**	Heme	fungi, plants, Oomycete	875
	Manganese peroxidase			
	Lignin peroxidase			
	Versatile peroxidase			
AA3	**GMC oxidoreductase**	FAD	fungi, plants, animals, Rhodophyta, Oomycete, Euglenozoa, Archaea	3240
	Details in Table 2			
AA4	**Vanillyl alcohol oxidase**	FAD	fungi	85
AA5	**Radical copper oxidase**	Copper	fungi, bacteria, plants, insects, Archaea	879
AA5_1	Glyoxal oxidase			
AA5_2	Galactose oxidase			
	Raffinose oxidase			
	(Aryl)alcohol oxidase			
AA6	**1,4 benzoquinone reductase**	NADP	fungi, plants, animals, Rhodophyta, Stramenopiles	839
AA7	**Oligosaccharide oxidase**	FAD	fungi, Oomycota, plants	137
AA8	**Iron reductase domain**	Heme	fungi	208
AA9–11	**Lytic polysaccharide monooxygenase**	Copper	fungi, bacteria, viruses	11561
AA12	**Sugar dehydrogenase**	Pyrroloquinoline quinone	fungi, animals, plants	117
13–17	**Lytic polysaccharide monooxygenase**	Copper	fungi, viruses, animals, Stramenopiles, algae, Oomycota	1079

*Number of sequences listed in the CAZy database as of July 2023.

1.2.3 Carbohydrate-active oxidoreductases as biocatalysts and their applicable use

Carbohydrate-active oxidoreductases are biocatalysts that operate under mild reaction conditions and exhibit high selectivity (Savino and Fraaije 2021). Glucose oxidase serves as a prominent example of a carbohydrate-active oxidoreductase that has found applications in diverse fields, including glucose biosensing (Tasca et al. 2007), production of glucosaminic acid for biomedical purposes (Zhang et al. 2010), and synthesis of gluconic acid as an antioxidant in the food industry (Godjevargova, Dayal, and Turmanova 2004). Moreover, carbohydrate-active oxidoreductases possess the capability to introduce functional groups into polysaccharides, leading to the creation of novel telechelic building

blocks. For instance, the AA5 galactose oxidase can introduce an aldehyde group at the C-6 position of terminal galactosyl residues within polysaccharides such as galactoglucomannan, galactomannan, and xyloglucan. These formed aldehydes can subsequently undergo allylation and propargylation for further functionalization (Leppänen et al. 2014; Parikka et al. 2010). Additionally, galactose oxidase, AA3_2 pyranose dehydrogenase, and transaminases have been employed in biocatalytic cascades to generate bifunctional carbohydrates containing diamine groups (Aumala et al. 2019). Such diacids, diamines, and molecules containing both carboxylic acid and amino groups can be utilized in the synthesis of polymers with unique properties (Chung et al. 2015; Froidevaux et al. 2016; Harmsen, Hackmann, and Bos 2014). However, research on the enzymatic derivatization of oligosaccharides, especially xylooligosaccharides, was limited. One of the reasons for this limitation was the scarcity of xylooligosaccharide oxidizing enzymes.

When work on this thesis began, xylooligosaccharide oxidizing enzymes were identified primarily in theAA7 and AA9 families (Hüttner et al. 2019; Vuong et al. 2013). The AA7 oligosaccharide oxidases solely target the reducing end C-1, and the AA9 LPMOs depolymerize xylooligosaccharides. Meanwhile, although the AA3 enzymes were known to oxidize at the different positions of carbohydrates, knowledge regarding the capability of existing AA3 enzymes to oxidize oligosaccharides, especially xylooligosaccharides, was still limited.

1.2.4 The genomic resource

Despite the significant potential of oxidoreductases as biocatalysts, their adoption in the chemical industry, especially for large-scale industrial chemical production, remains limited. Some of the main challenges lie in the lack of biocatalysts that possess the required selectivity, productivity, and stability under harsh process conditions involving high temperatures, high substrate concentrations, strong solvents, and oxidative environments (Martínez et al. 2017). To overcome these obstacles in oxidative enzymatic biotransformation, two complementary approaches can be pursued. The first is screening for novel oxidoreductases from diverse natural species, and the second is tailoring catalytic properties through enzyme engineering based on structural function information.

Past advancements in sequencing technology greatly facilitated screening for new biocatalysts in genomes. For example, the US Joint Genome Institute (JGI; jgi.doe.gov) has conducted extensive screenings of microorganism genomes, providing a vast resource of putative enzymes for the biocatalytic transformation of plant biomass. Therefore, the discovery of fungal CAZy oxidoreductases from the AA3 family can be leveraged by the abundance of sequence information.

1.3 AA3 oxidoreductases

1.3.1 Overview of CAZy family AA3 enzymes

The CAZy family AA3 is comprised of glucose–methanol–choline (GMC) oxidoreductases. The GMC oxidoreductase family was defined in the 1990s based on sequence similarities observed in enzymes such as glucose dehydrogenase from *Drosophila melanogaster*, choline dehydrogenase from *Escherichia coli*, glucose oxidase from *Aspergillus niger*, and methanol oxidase from *Hansenula polymorpha* (Cavener 1992). All enzymes in this family possess covalently or non-covalently bound flavin adenine dinucleotide (FAD) or its derivatives as a cofactor. Typically, AA3 GMC oxidoreductases consist of an FAD-binding domain and a substrate-binding domain. The FAD-binding domain contains a conserved Rossmann fold or βαβ mononucleotide-binding motif, while the substrate-binding domain exhibits more sequence variations, depending on the preferred substrate (Sützl et al. 2018).

The four subfamilies of AA3 enzymes exhibit a wide range of redox activities. Subfamily 1 includes cellobiose dehydrogenases (CDH, EC 1.1.99.18), subfamily 3 includes alcohol oxidases (AOx, EC 1.1.3.7), and subfamily 4 includes pyranose oxidases (POx, EC 1.1.3.10). Subfamily 2 is the most diverse and encompasses enzymes with different electron donors and acceptors. This subfamily includes aryl alcohol oxidase/dehydrogenases (AAO/AADH, EC 1.1.3.7), as well as carbohydrate-active enzymes such as pyranose dehydrogenases (PDH, EC 1.1.99.29), glucose oxidases (GOx, EC 1.1.3.4), glucose dehydrogenases (GDH, EC 1.1.5.9), oligosaccharide dehydrogenases (ODH, EC 1.1.5.-), and an ecdysone oxidase (EO, EC 1.1.3.16) until now (Table 2) (Cerutti et al. 2021; Sützl et al. 2019). Despite the diverse range of substrates accepted by AA3 oxidoreductases, they share a similar reaction mechanism. This mechanism involves two halves: a reductive half-reaction, where the electron donor (substrate) is oxidized while FAD is reduced to $FADH_2$, and an oxidative half-reaction, where $FADH_2$ is re-oxidized. The active site of these enzymes contains a catalytic His/His or His/Asn pair that is highly conserved and essential for their activity (Fernández et al. 2009; Hallberg et al. 2003; Tan et al. 2013).

The CAZy database currently contains a total of 3240 AA3 sequences, but only 41 of them have been biochemically characterized. This indicates a significant knowledge gap and highlights the importance of characterizing novel AA3 enzymes. Such research is crucial for gaining a better understanding of their biological functions and exploring their potential applications in industrial biocatalysis. In particular, there is a need to investigate the enzymatic activation of underutilized hemicellulosic oligosaccharides to create unique structures with high value.

Specifically, this thesis focused on the characterization of fungal AA3 GMC oxidoreductases from subfamilies 1 and 2, with a particular interest in their potential activity on oligosaccharides, particularly xylooligosaccharides. A review in 2018 provided a thorough discussion of the many functions of the AA3 oxidoreductases (Sützl et al. 2018), and a subsequent publication summarized their phylogenetic relationships and sequence space in more detail (Sützl et al. 2019). The following provides a detailed introduction to the enzymes detected in the CAZy AA3_1 and AA3_2 families, along with their relevant applications and biological functions.

1.3.2 AA3_1 cellobiose dehydrogenase

The AA3_1 subfamily consists primarily of cellobiose dehydrogenases, which were first discovered in the 1970s in the white-rot fungi *Trametes versicolor* (Westermark and Eriksson 1974) and *Phanerochaete chrysosporium* P127-1 (Westermark and Eriksson 1975). The *cdh* genes are predominantly found in fungi, with an equal distribution in Basidiomycota and Ascomycota. However, the presence of *cdh* genes varies significantly depending on the fungal habitations. White rot and litter-decomposing fungi typically have a higher number of cdh genes, while brown rot, soft rot, plant symbiotic, and pathogenic fungi rarely possess these genes (Mattila et al. 2022; Scheiblbrandner and Ludwig 2020).

CDHs can be single-domain or multidomain enzymes, consisting of at least a GMC dehydrogenase domain that binds non-covalently linked FAD as a cofactor. Some CDHs also contain an N-terminal cytochrome domain and a C-terminal cellulose-binding module (CBM1) (Sützl et al. 2019). The cytochrome domain, classified individually in the CAZy family AA8, contains a haem b cofactor and acts as a redox mediator that drives LPMOs for oxidative cellulose depolymerization (Felice et al. 2021; Tan et al. 2015). Notably, the cytochrome domain is not essential for the physiological function of all CDHs, as multidomain CDHs retain activity after proteolytic cleavage of the cytochrome (Henriksson et al. 1991; Kracher et al. 2020; Sygmund, Kracher, et al. 2012). Additionally, CDHs with only the dehydrogenase domain have been observed, yet no such native protein has been functionally characterized prior to the research in this thesis.

Phylogenetic analysis has identified four classes of CDHs, with class I originating from basidiomycetes and classes II, III, and IV from ascomycetes, with very few exceptions (Sützl et al. 2019). Class I CDHs were found to have a strong affinity for cellulose and bind cellulose via a cellulose-binding site on the surface of their DH domain (Hallberg et al. 2002). Class II CDHs, however, do not possess this binding site and rely on the C-terminal CBM1 for cellulose binding. Class II CDHs are further divided into subclass IIA (with CBM1) and subclass IIB (without CBM1),

with the latter lacking cellulose-binding capability (Harreither et al. 2011). While CDHs from class I and II have been biochemically characterized and shown preferential activity towards cellobiose, no CDHs from classes III and IV have yet been characterized with detectable activity.

CDHs characterized to date generally show preferential activity towards β-(1→4)-linked cellobiose, and they specifically oxidize the anomeric carbon, forming the corresponding lactone that spontaneously hydrolyzes to carboxylic acid in water (Figure 4) (Scheiblbrandner and Ludwig 2020). Lactose, which is not related to plant biomass, is also a good substrate for CDHs, possibly due to its structure that is similar to cellobiose, as they differ only by the orientation of the C-4 hydroxyl at the non-reducing end (Kracher and Ludwig 2016). CDHs from *Sclerotium (Athelia) rolfsii* CBS 191.62 (*Sr*CDH), *Trametes pubescens* MB 89 (*Tp*CDH), *Trametes villosa* MB 51 (*Tv*CDH), *Humicola insolens* (*Hi*CDH), and *Neurospora crassa* CBS 232.56 (*Nc*CDHs) act on xylooligosaccharides, including xylobiose and xylotriose, albeit with comparatively low catalytic efficiency relative to cellobiose (Baminger, Subramaniam, et al. 2001; Ludwig et al. 2004; Schou, Christensen, and Schülein 1998; Sygmund, Kracher, et al. 2012). Other oligosaccharides, including maltose, maltotriose, maltotetraose, galactobiose, mannobiose, and various monosaccharides, can also be accepted by some CDHs with relatively low affinity.

The first crystal structure of the DH domain was resolved in 2002 from a class I CDH from *Phanerochaete chrysosporium* (*Pc*CDH) (Hallberg et al. 2002; Hallberg et al. 2003). Subsequently, crystal structures for full-length CDHs were determined for two Class II CDHs: *Mt*CDH from *Crassicarpon hotsonii* (formerly *Myriococcum thermophilum*) and *Nc*CDH from *N. crassa* (Tan et al. 2015). The superposition of active sites of three CDHs (Figure 5A) revealed that the two Class II CDHs (*Mt*CDH and *Nc*CDH) were nearly identical in terms of amino acid composition and orientation. The bindings of 5-amino-5-deoxy-cellobiono-1,5-lactam (CBLM), a mimetic of cellobiose, to *Pc*CDH and *Mt*CDH are shown in Figures 5B and C. Both *Pc*CDH and *Mt*CDH bind the lactam moiety, corresponding to the reducing end of cellobiose, in a similar manner. In both enzymes, the catalytic His/Asn pair interacts with the hydroxyl groups of the reducing end, and the Asn688/Asn700 residue forms hydrogen bonds with the C3 hydroxyl groups. For the C6 hydroxyl groups of the reducing motif, a water-mediated hydrogen bond system involving specific amino acid residues is established. In *Pc*CDH, this includes T584 and Y609, while in *Mt*CDH, it involves T599 and Y619.

Regarding the non-reducing motif, although both *Pc*CDH and *Mt*CDH have an aromatic amino acid residue (F282/W295) to establish the CH-π interaction, the bindings between CDHs with cellobioses

are mainly dominated by hydrogen bonds. In *Pc*CDH, R586 rotates towards the non-reducing glycosyl unit for the hydrogen binding with hydroxyl groups of C2 and C3. Conversely, in *Mt*CDH, the amino acid residue in the same position interacts with C6 of the reducing moiety. Additionally, *Pc*CDH possesses E279 to establish additional hydrogen bonds towards hydroxyl groups on C2 and C3 of the non-reducing glycosyl unit. In contrast, *Mt*CDH binds the hydroxyl groups on C3 and C4 of the non-reducing glycosyl unit via direct hydrogen bond and a water-mediated hydrogen bond system involving E603 and Y549. This difference in substrate binding may explain the generally wider substrate spectrum of lass II CDHs than class I CDHs (Harreither et al. 2011).

The close proximity between substrate C1 and cofactor FAD N5 means the CDHs favor a base catalyzed hydride transfer mechanism (Figure 6A). The reaction starts with the base-assisted deprotonation of the C1 hydroxyl group by the catalytic histidine, while the catalytic asparagine assists the catalysis by forming a hydrogen bond with the C1 hydroxyl group. The resulting intermediate then undergoes a concerted process with the expulsion of 1-H as hydride in a planar transition state. However, a radical mechanism cannot be ruled out (Figure 6B). This type of reaction involves the transfer of one electron from the substrate O1 to the flavin N5, while simultaneously abstracting the O1-H proton through the catalytic histidine. This results in the formation of a flavin radical and a substrate radical. The next step involves the transfer of the 1-H as a hydrogen radical to flavin N5 and the redistribution of the remaining electron.

The two electrons transferred from the substrate to the flavin of CDH can be subsequently transferred to a wide range of electron acceptors, including one-electron acceptors like cytochrome *c*, ferric–ion complexes, Cu^{2+}, and two-electron acceptors like dichlorophenolindophenol (DCIP) and benzoquinone (BQ). Additionally, CDHs with the cytochrome domain can transfer the electrons from the oxidized flavin in the DH domain to the haem cofactor of the cytochrome domain, and further on to external electron acceptors. such as cytochrome *c*, LPMO, or an electrode surface (Felice et al. 2021; Laurent et al. 2019; Scheiblbrandner and Ludwig 2020; Tan et al. 2015).

Table 2. Known activities, main substrates, target carbons, end products, and the characterized crystal structures of enzymes in each AA3 subfamily.

Sub family	Enzymes	EC number	E-acceptor	Main substrate	Target carbon	Main end product	First crystal structure	Reference
AA3_1	Mainly cellobiose dehydrogenases	1.1.99.18	BQ/DCIP	Cellobiose	C_1	Lactone → carboxylic acid	1KDG	(Hallberg et al. 2002)
AA3_2	Aryl alcohol oxidases	1.1.3.7	O_2	Aromatic alcohol	–	Aromatic aldehyde	3FIM	(Fernández et al. 2009)
	Glucose 1-oxidases	1.1.3.4	O_2	D-glucose	C_1	Lactone	1CF3/1GPE	(Wohlfahrt et al. 1999)
	Glucose dehydrogenases	1.1.5.9	BQ/DCIP	D-glucose	C_1	Lactone	4YNT	(Yoshida et al. 2015)
	Oligosaccharide dehydrogenase	1.1.5.-	BQ	Laminaribiose	C_1	Lactone	6XUT	(Cerutti et al. 2021)
	Pyranose dehydrogenases	1.1.99.29	BQ/DCIP	Pyranose, pyranoside	C_1, C_2, C_3, C_4	Lactone/ (di)ketosugars	4H7U	(Tan et al. 2013)
	Ecdysone oxidase	1.1.3.16	O_2	Ecdysone	–	3-Dehydroecdysone	–	(Sun et al. 2011)
AA3_3	Alcohol oxidases	1.1.3.13	O_2	Primary alcohol	–	Aldehyde	5HSA	(Koch et al. 2016)
AA3_4	Pyranose 2-oxidases	1.1.3.10	O_2	Pyranose, pyranoside, C-glycoside	C_2	2-Ketoaldoses	1TZL	(Bannwarth et al. 2004)

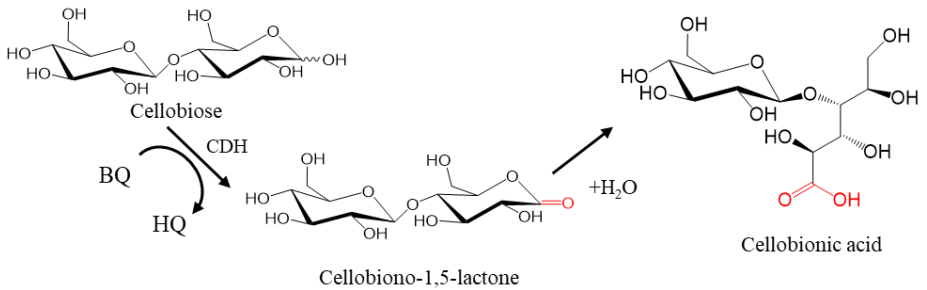


Figure 4. Reaction catalyzed by cellobiose dehydrogenase (CDH). Cellobiose is oxidized by CDH to cellobiono-1,5-lactone, which is not stable in water but further hydrates to cellobionic acid.

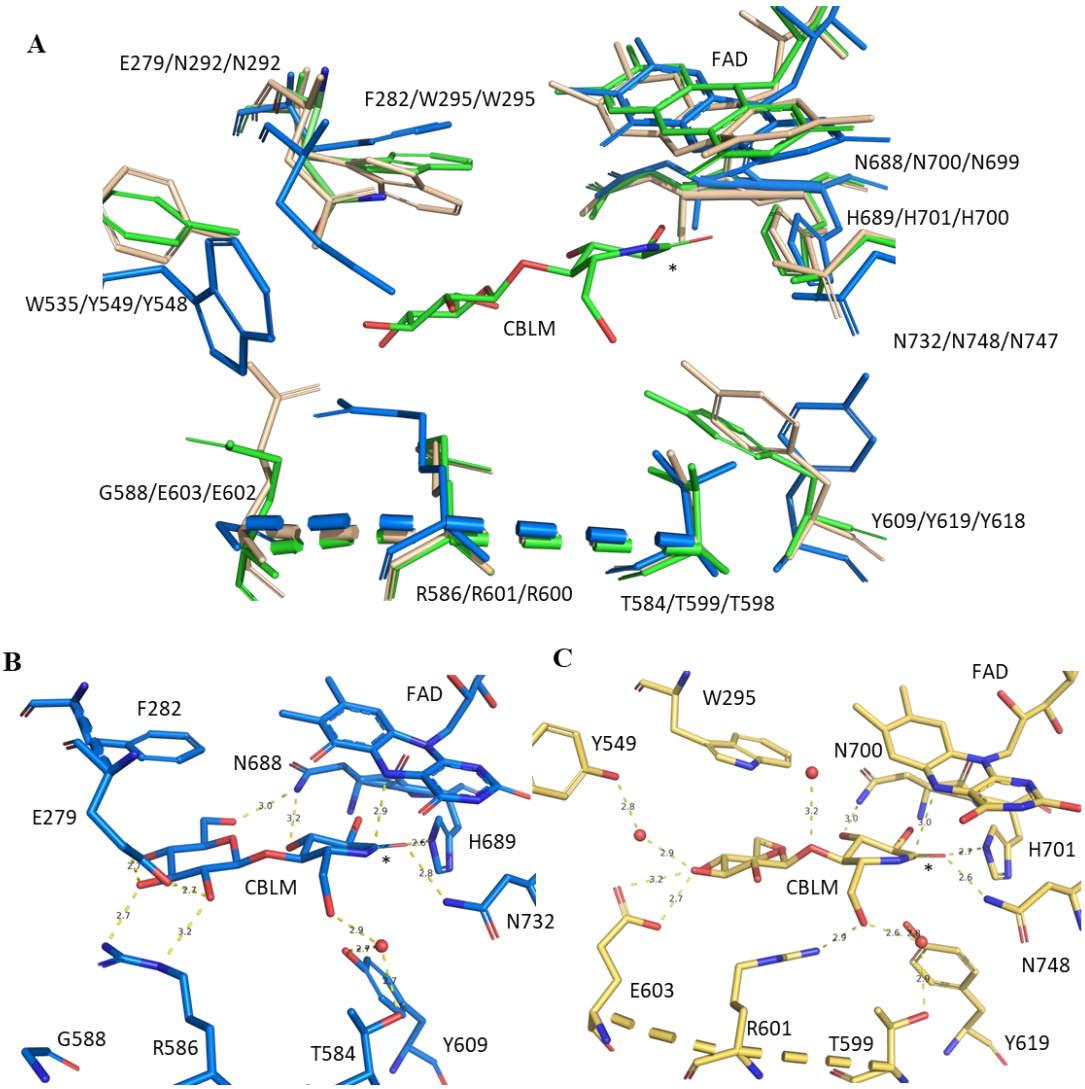


Figure 5. The active site orientation and ligand interactions of three cellobiose dehydrogenases. The inhibitor 5-amino-5-deoxy-cellobiono-1,5-lactam (CBLM) was used as the ligand for studying active site interaction. The asterisk denotes the position in the CBLM of the oxidation in cellobiose.

This figure was produced using the crystal structures of class I CDH from *Phanerochaete chrysosporium* (*Pc*CDH, PDB: 1KDG-ligand free, 1NAA-binding with CBLM), class II CDH from *Crassicarpon hotsonii* (*Mt*CDH, PDB: 4QI4-ligand free, 4QI5-binding with CBLM), and class II CDH from *Neurospora crassa* (*Nc*CDH, PDB: 4QI7-ligand free). A) Superposition of the active sites in *Pc*CDH (blue), *Mt*CDH (orange), and *Nc*CDH (green). The thick dashed line represents the hidden amino acid residues. B) Binding of CBLM in the active site of *Pc*CDH. C) Binding of CBLM in the active site of *Mt*CDH. Dashed lines are interatomic distances that meet the criteria for hydrogen bonds that are less than 3.2 Å in length.

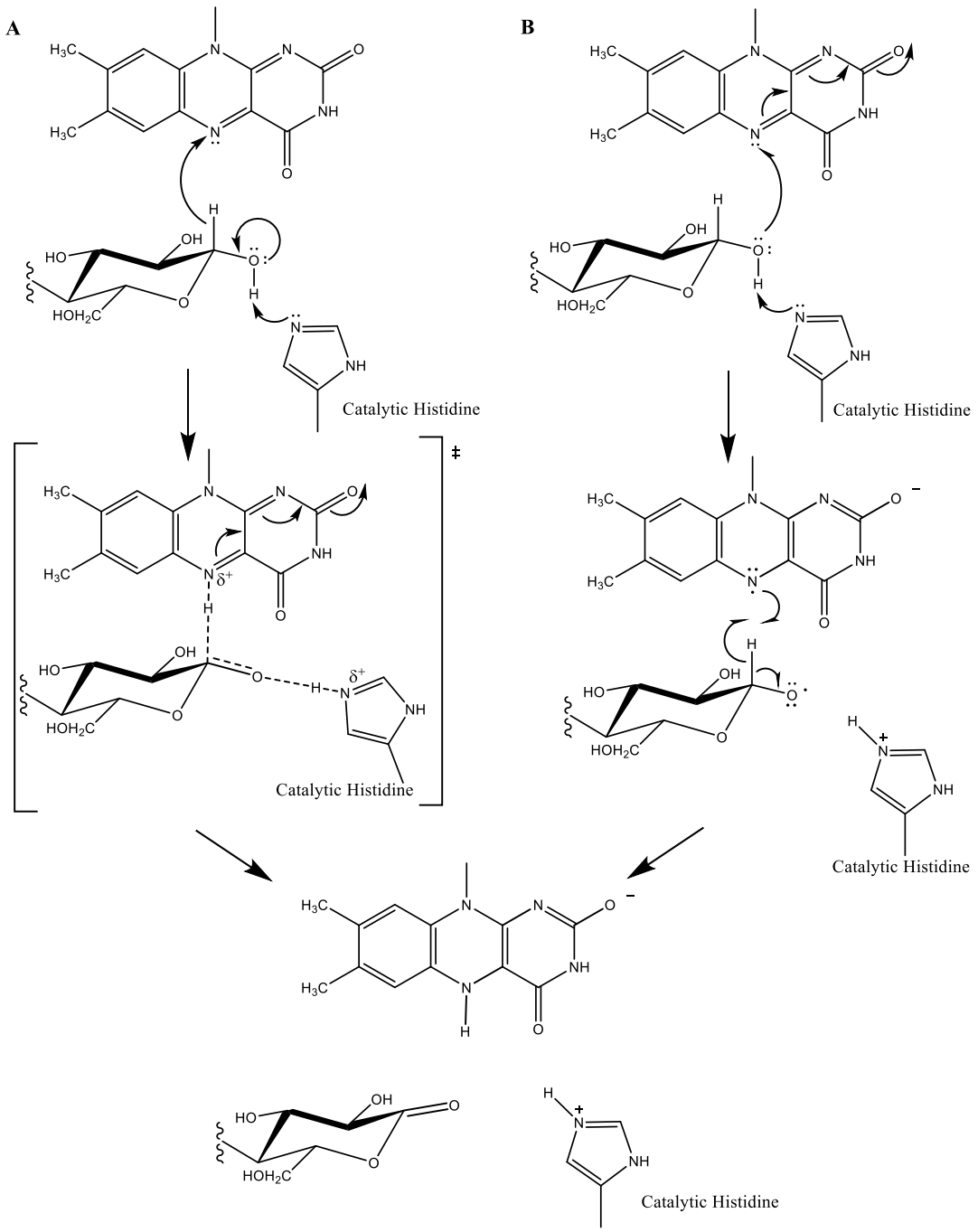


Figure 6. The two putative reaction mechanisms for cellobiose dehydrogenase oxidation. A) Hydride transfer mechanism. B) Radical mechanism. Reproduced from Hallberg et al. (2003).

1.3.3 Diverse enzyme function within the AA3_2 subfamily

According to the sequence similarity network (SSN) containing only fungal AA3 sequences generated by Sützl et al. (2019), the characterized AA3 enzymes are grouped into four clusters of sequences with high levels of sequence similarity (Figure 7). Specifically, the characterized AA3_2 enzymes are located within two subclusters of sequences that exhibit high levels of sequence similarity. One subcluster contains enzymes such as glucose oxidase and glucose dehydrogenase, while the other subcluster contains enzymes such as aryl alcohol oxidase/dehydrogenase and pyranose dehydrogenase. These characterized enzymes represent a subset of the AA3_2 subfamily and demonstrate known enzymatic activities in this subfamily. Importantly, there are still large regions of sequence space within the AA3_2 subfamily that remain uncharacterized, suggesting the presence of novel enzymatic activities waiting to be discovered. Further exploration and characterization of these uncharacterized sequences can provide valuable insights into the diversity and potential functionalities of AA3_2 enzymes.

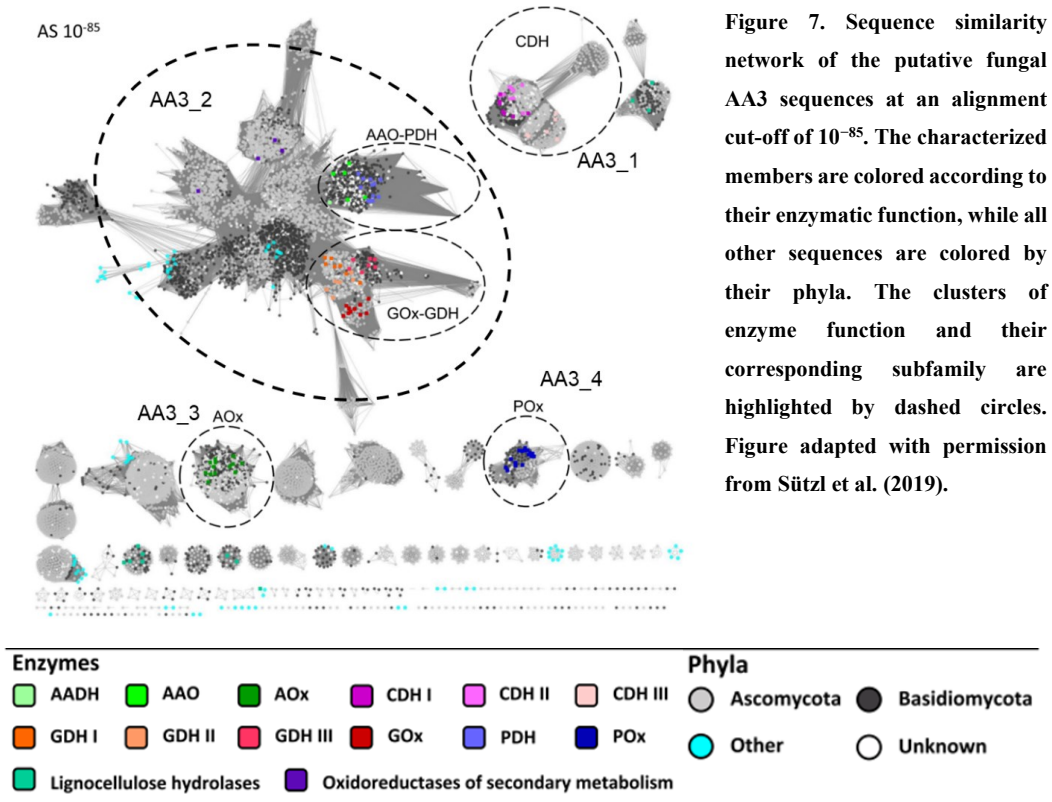


Figure 7. Sequence similarity network of the putative fungal AA3 sequences at an alignment cut-off of 10^{-85}. The characterized members are colored according to their enzymatic function, while all other sequences are colored by their phyla. The clusters of enzyme function and their corresponding subfamily are highlighted by dashed circles. Figure adapted with permission from Sützl et al. (2019).

1.3.4 Glucose oxidase/dehydrogenase

The GOx-GDH subcluster of AA3_2 primarily consists of two types of enzymes, glucose oxidase and glucose dehydrogenase. These enzymes possess non-covalently but tightly bound FAD and share a common reaction in which they oxidize D-glucose to D-glucono-1,5-lactone. The lactone subsequently hydrolyzed to gluconic acid in water (Figure 8). Although GOxs and GDHs have high levels of sequence similarity, they differ in their oxygen acceptability. GOxs use molecular oxygen as one of the primary electron acceptors and reduces oxygen to hydrogen peroxide. In contrast, GDHs have low levels of activity with oxygen and can utilize a range of other electron acceptors, including BQ, DCIP, and phenoxy radicals (Muller 1929; Piumi et al. 2014).

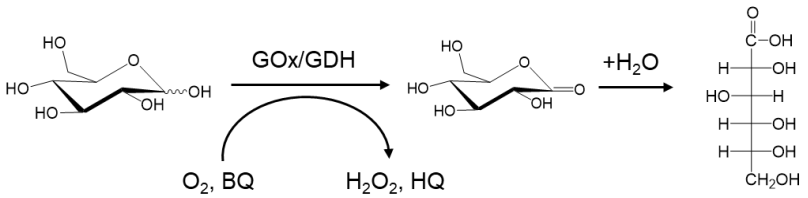


Figure 8. The oxidation of glucose by glucose oxidase (GOx) and glucose dehydrogenase (GDH) in the presence of oxygen or benzoquinone (BQ). The formed D-glucono-1,5-lactone is not stable in water and reacts with water to form gluconic acid.

The first glucose oxidase (*An*GOx) was identified from *A. niger* in 1928, and its high-resolution crystal structure (PDB_1CF3) was solved in 1999 (Wijayanti et al. 2021; Wohlfahrt et al. 1999). The GDHs were not included in the original description of subfamily AA3_2 in 2013. Since then, they have gained increasing attention due to their potential application in oxygen-independent glucose biosensors (Sode et al. 2017). The first crystal structure of GDH (*Af*GDH, PDB_4YNT) was resolved from *Aspergillus flavus* in 2015, providing crucial structural information about this enzyme (Yoshida et al. 2015). *Af*GDH was found to possess a domain architecture similar to *An*GOx and shared the same catalytic histidine pair, His505/His548 in *Af*GDH and His516/His559 in *An*GOx. The former histidine with *Af*GDH and *An*GOx performs a base-assisted deprotonation of the C1 hydroxyl group, followed by the hydride transfer from C1 of glucose to N5 of FAD, while the latter histidine is in a doubly protonated state formed through strong hydrogen bonds with the neighboring Glu residue (Glu399 for *Af*GDH and Glu412 for *An*GOx). The mutagenesis of both catalytic histidines to alanines either greatly reduces the enzymatic activity to near zero or eliminates it (Yoshida et al. 2015).

The sequences in the GOx-GDH subcluster were recently subdivided into four major clades, GOx I, GDH I, GDH II, and GDH III, and a minor clade, GOx II, that is phylogenetically close to GDH III

but displays oxidase activity (Sützl et al. 2019; Wijayanti et al. 2021). Prior to the start of this thesis, the biochemical characterization of GOx and GDH focused mainly on clade GOx I and GDH I, particularly their ability to oxidize various monosaccharides. The advantage and distinguishing characteristic of GOxs in GOx I clades is their high specificity for D-glucose. Although GOxs in GOx I can oxidize other monosaccharides, including 2-deoxy-D-glucose, D-galactose, D-mannose, and D-xylose, it is with lower catalytic efficiency (Adams, Mast, and Free 1960; Pazur and Kleppe 1964; Semashko, Mikhailova, and Eremin 2003; Wijayanti et al. 2021; Witt, Singh, and Kalisz 1998). However, GDHs in clade GDH I show significant activity with D-xylose, which can range from 2% activity relative to that with glucose to approximately equal activities for glucose and xylose (Mori et al. 2011; Sode et al. 2017; Sygmund et al. 2011; Wijayanti et al. 2021). For instance, *An*GOx from GOx I showed almost exclusive activity towards glucose, whereas *Af*GDH from GDH I displayed considerable specific activity towards xylose that was only four times lower than its activity with glucose (Loew et al. 2017; Pazur and Kleppe 1964).

Additional studies have revealed that enzymes within the clades GDH II, GDH III, and GOx II exhibit a broader substrate range beyond monosaccharides. A study conducted in 2014 characterized an enzyme in GDH III from *Pycnoporus cinnabarinus*, synonym *Trametes cinnabarina*, that showed activity towards various carbohydrates, including glucose, galactose, xylose, arabinose, lactose, maltose, and maltotriose (Piumi et al. 2014). Among all the substrates tested, the most activity was shown towards glucose with a K_M of 272 mM and a catalytic efficiency of 67 $M^{-1}s^{-1}$, followed by lactose with a K_M of 1.7 M and a catalytic efficiency of 4 $M^{-1}s^{-1}$ (Piumi et al. 2014). This enzyme was further studied for its activity towards an extended list of substrates, where it displayed the most activity towards laminaribiose (β-D-Glucosyl-(1→3)-D-glucose) with a K_M of 77 mM and a catalytic efficiency of 777 $M^{-1}s^{-1}$, leading to it being renamed *Tc*ODH (Cerutti et al. 2021). In the crystal structures, *Tc*ODH was observed to bind laminaribiose primarily through sugar–aromatic stacking with Phe416 and Trp430. Interestingly, upon binding, Phe421 shifted around 17 Å towards the active site, establishing sugar–aromatic stacking with the non-reducing glucosyl moiety. This phenylalanine residue is not conserved in *Af*GDH and *An*GOx, possibly explaining their lower activity towards laminaribiose (Cerutti et al. 2021). Two other enzymes from GDH III, *Rs*GDH from *Rhizoctonia solani* and *Um*GDH from *Ustilago maydis,* also exhibited significant activity towards laminaribiose and gentiobiose of at least five times higher than their activity towards glucose (Wijayanti et al. 2021). Furthermore, a recent study found that *Um*GDH is secreted by the maize pathogen *Ustilago maydis* together with a GH that has preferential activity towards β-(1→3) glucan with short β-(1→6) substitutions. Laminaribiose and gentiobiose are the typical dimers of the fungal cell wall

polysaccharide β-(1→3), (1→6)-linked glycan, which suggests that AA3_2s may participate in the modification of their fungal cell wall via interactions with other enzymes (Reyre et al. 2022).

Enzymes in GDH II and GOx II were not characterized until 2021. and they also displayed activity towards oligosaccharides (Wijayanti et al. 2021). For instance, *As*GOx from *Aureobasidium subglaciale,* the only characterized member of GOx II, showed preferential activity towards glucose (1.2 U/mg), with three times lower activity towards gentiobiose (β-D-Glucosyl-(1→6)-D-glucose, 0.4 U/mg). Additionally, *Tv*GDH from *Trichoderma virens* (GDH II) displayed a preference for maltose, followed by galactose, glucose, and xylose. These recent findings suggest that the oligosaccharide-oxidizing capacity of enzymes in the GOx-GDH subcluster has been overlooked in previous studies, highlighting the need for further research in this area.

1.3.5 AA3_2 pyranose dehydrogenase

Pyranose dehydrogenases (PDHs) have been identified in specific fungi in the Basidiomycota division, namely the *Agaricaceae* and *Lycoperdaceae* families, with *Ab*PDH1 from *Agaricus bisporus* the first to be isolated (Morrison, Wood, and Wood 1999; Peterbauer and Volc 2010; Volc et al. 1997; Volc et al. 1998). Other PDHs, including *Ax*PDH from *Agaricus xanthodermus, Ac*PDH from *Agaricus campestris,* and *Am*PDH1-3 from *Agaricus meleagris* (synonymous with *Leucoagarisu meleagris*), were later purified and characterized (Graf et al. 2017; Staudigl et al. 2013; Sygmund et al. 2008).

*Am*PDH1, for which the crystal structure (PDB_4H7U) was resolved in 2014, exhibits the typical two-domain architecture of AA3 enzymes, with an FAD-binding domain and a substrate-binding domain (Tan et al. 2013). *Am*PDH1 has a covalently tethered FAD attached to a histidine residue (His103) in the active site. Conversely, a valine or isoleucine residue occupies the same position for most other AA3s, leading to a non-covalently bound FAD. The covalent FAD attachment might improve the redox potential of an enzyme, and previous mutagenesis of His103 to residues, including Tyr, Phe, Trp and Met, led to increased oxygen reactivity (Graf et al. 2015; Krondorfer et al. 2014). The active site of *Am*PDH1 contains two conserved histidines. His512 of *Am*PDH1 acts as the main base in the first reductive half-reaction, while His556 together with Gln392 and Tyr510 take part in substrate interactions that likely affect the observed substrate-specific regioselectivity (Graf et al. 2013; Graf et al. 2015; Tan et al. 2013). After the first half-reaction, the reduced flavin is oxidized by an electron acceptor such as ferricenium, BQ, or DCIP. The active site of *Am*PDH1 is rather open, which might be attributed to its broad substrate reactivity and regioselectivity.

PDHs from different fungal sources vary in their ability to oxidize different sugar substrates and can catalyze monooxidation and dioxidation at different positions. L-arabinose is the favored substrate for *Am*PDH1, followed by glucose and galactose (Sygmund et al. 2008). Although the catalytic efficiency of *Am*PDH1 towards xylose (22.9 $mM^{-1}s^{-1}$) is only three times lower than that towards L-arabinose (57.5 $mM^{-1}s^{-1}$), it still had the greatest catalytic efficiency on xylose among all of the characterized PDHs (Morrison et al. 1999; Staudigl et al. 2013; Sygmund et al. 2008). *Am*PDH1 oxidizes L-arabinose and galactose in a monooxidation process, resulting in 2-keto sugars. In contrast, glucose and xylose undergo dioxidation at both the C-2 and C-3 positions, leading to the formation of 2,3-diketo-glucose and diketo-xylose as final products (Figure 9) (Sedmera et al. 2004; Sedmera et al. 2006). Based on the modeling of glucose and xylose at the active site, *Am*PDH1 was found to be able to oxidize at C-1, C-2, C-3, and C-4 of glucose and xylose, although oxidation at C-1 and C-4 has not been experimentally proven (Tan et al. 2013).

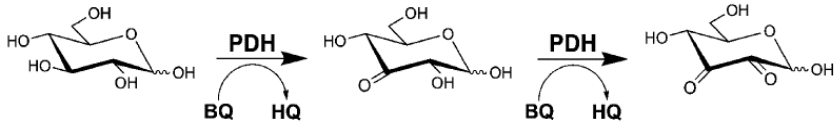


Figure 9. Dioxidation of D-glucose by *Am*PDH1. Glucose is double oxidized in C-2 and C-3 to diketo-glucose.

The two most studied PDHs are *Am*PDH1 and *Ab*PDH1 from *Agaricus bisporus*. Similar to *Am*PDH1, *Ab*PDH1 oxidizes L-arabinose and glucose at the highest initial rate, and *Ab*PDH1 oxidizes xylose to 2,3-diketo-D-xylose (Gonaus et al. 2016; Morrison et al. 1999; Volc et al. 2000). In addition to monosaccharides, both *Ab*PDH1 and *Am*PDH1 exhibit activity towards disaccharides and oligosaccharides, including cellobiose, cellotetraose, and maltotriose (Gonaus et al. 2016; Rafighi et al. 2019; Sedmera et al. 2006; Volc et al. 1997). *Am*PDH1 also shows activity towards maltooligosaccharides up to maltoheptaose and xylobiose (Sygmund et al. 2008).

The ability of PDHs to oxidize pyranose at multiple positions makes them potential candidates for generating novel classes of telechelic carbohydrate building blocks from forest biomass and agricultural resources. However, PDH action towards xylooligosaccharides derived from hardwood and agricultural resources has not been investigated. Moreover, the analysis of corresponding oligosaccharide products is challenging due to the multiple hydroxyl groups that can potentially be oxidized. Additionally, the oxidized products are inherently unstable in water, and they can further transform into various end products. For example, oxidation of the anomeric carbon leads to a lactone that spontaneously hydrolyzes to a carboxylic acid in water (Vuong et al. 2013). Furthermore,

secondary hydroxyls that are oxidized to ketones and primary hydroxyls that are oxidized to aldehydes exist primarily as hydrates (geminal diols) in water (Andberg et al. 2017; Volc et al. 2002). Developing analytical methods to simplify and clarify the analysis of these compounds is essential for understanding their biological significance and potential applications.

1.3.6 AA3_2 aryl alcohol oxidase/dehydrogenase and other putative AA3_2 sequences

In addition to the carbohydrate-oxidizing enzymes, AAOs/AADHs are classified in AA3 subfamily 2, which is most phylogenetically similar to PDHs. The first AAO activity was identified in the basidiomycete *Polystictus (Trametes) versicolor* in 1960, and AAO activity has since been found in many other basidiomycete and ascomycete fungal species (Farmer, Henderson, and Russell 1960; Urlacher and Koschorreck 2021).

The first AAO with a solved crystal structure was *Pe*AAO from *Pleurotus eryngii*, and its complex with an inhibitor in the active site was published in 2017 (Carro et al. 2017; Fernández et al. 2009). It contains two catalytic histidines (His502 and His546) that are highly conserved among all other AA3_2 enzymes and located in the *si* face of the non-covalently bound FAD cofactor's isoalloxazine ring. Despite its great phylogenetic similarity to PDHs, *Pe*AAO has a unique funnel-shaped tunnel to restrict access to the active site, created via a narrow hydrophobic entrance formed by three aromatic residues (Tyr92, Phe397, and Phe501). The absence of this narrow hydrophobic tunnel in PDHs might lead to a wider substrate entrance site, making it easier for sugar substrates to bind. Additionally, the bulkiness of the hydrophobic entrance impacts the oxygen acceptability of AAOs. Site-directed mutagenesis of F501A in *Pe*AAO resulted in a significant reduction in its oxygen reactivity (Hernández-Ortega et al. 2011). Moreover, the 202 times lower turnover rate on oxygen compared to *Pe*AAO for *Mt*AAOx from *Thermothelomyces thermophilus* may be related to its fully accessible catalytic tunnel containing none of the three amino acid residues conserved with *Pe*AAO (Ferreira et al. 2010; Kadowaki et al. 2020).

Typically, AAOs catalyze the oxidation of the primary alcohol group on different aromatic and aliphatic unsaturated alcohols to the corresponding aldehyde. Only in rare cases can the aldehydes be further oxidized to acids. Other than electrophilic C-H bond activation, the oxidation of aldehydes by AAOs was believed to be achieved with the formation of gemdiols by aldehyde hydration, and the later oxidation of the hydroxyl group in the gemdiol follows a mechanism analogous to alcohol oxidations (Ferreira et al. 2010). The stability of the gemdiol intermediate is influenced by the electron density around it, which in turn determines the aldehyde reactivity of AAOs. For example, the presence of electron-withdrawing groups, such as chloro and nitro at the para or ortho position,

increased aldehyde reactivity, while the presence of electron-donating groups such as methoxy resulted in low or no activity (Ferreira et al. 2010).

AAOs can accept a wide range of different substrates, and the substrate preference varies among AAOs from different organisms and even among different isoforms within the same organism. For *Pe*AAO, the best substrate tested to date was *p*-anisyl alcohol with a recorded catalytic efficiency of 5.23×10^6 $M^{-1}s^{-1}$. Other alcohols, including 3,4-dimethoxyl benzyl alcohol, cinnamyl alcohol, and 2,4-hexadien-1-ol, were also good substrates (Ferreira et al. 2006; Guillén, Martínez, and Martínez 1992). The substitution on the benzyl ring was found to impact the activity of AAOs. For instance, the presence of an electron-donating substituent like a methoxy group at the para position enhanced the enzyme activity compared to benzyl alcohol with no substitution, while the presence of an electron-withdrawing group like a nitro group at the same position reduced enzyme activity (Galperin et al. 2016; Guillén et al. 1992; Jankowski, Koschorreck, and Urlacher 2020; Varela et al. 2000). However, other AAOs, such as *Cc*AAO from *Coprinopsis cinerea*, BAO from *Botrytis cinerea*, and AOx from *Aspergillus terreus*, oxidized benzylic alcohols with and without methoxy substitution equally well at the para or meta position (Urlacher and Koschorreck 2021). The impact on AAO activity of a hydroxyl group at the para position is difficult to predict. For *Pe*AAO, the activity towards *p*-hydroxybenzyl alcohol was negligible compared to the activity towards benzyl alcohol, whereas *Cc*AAO oxidized *p*-hydroxyl benzyl alcohol at a higher rate than benzyl alcohol (Guillén et al. 1992; Tamaru, Umezawa, and Yoshida 2018). Additionally, some polyunsaturated aliphatic alcohols like trans, trans-2,4-hexadien-1-ol were also found to be oxidized by some AAOs, though with much less activity (Jankowski et al. 2020; Urlacher and Koschorreck 2021).

Multigenicity, a common feature in fungal enzyme systems, is characterized by the presence of multiple paralogous genes in an organism resulting from gene duplication and diversification. Among the AA3 genes, multigenicity is mostly pronounced for AAOs/AADHs, high rates of copies of AAO/AADH genes are normally recorded from white-rot decaying fungi and litter-decomposing fungi. For example, Basidiomycota *Armillaria mellea* has been found to possess 24 putative AAO/AADH genes (Mattila et al. 2022).

This phenomenon provides fungi with functional diversity and the ability to adapt to diverse natural substrates and environmental changes (Taylor 2011). Three aryl alcohol-oxidizing enzyme isomers from *Pycnoporus cinnabarinus* were found to be secreted during the degradation of biomass, and their variation in functional diversity supports this notion (Mathieu et al. 2016). These enzymes exhibited significant differences in reactivity towards various aromatic alcohols. While all three

isoforms could oxidize *p*-anisyl alcohol, only one of them showed activity towards *m*-anisyl alcohol. Moreover, two of these isomers had relatively low reactivity with oxygen, about 50 times less than their reactivity with BQ or DCIP, while the third enzyme acted purely as a dehydrogenase, with zero reactivity to oxygen (Mathieu et al. 2016). These findings suggest that the range of substrates AAOs/AADHs can act upon is highly variable, and yet the structure and function relationship for this group of enzymes is still not fully understood.

1.4 Biotechnology applications of fungal AA3_1s and AA3_2s

Studies on AA3_1 CDHs have explored their potential for diverse applications, including but not limited to biofuels, bioelectrochemical processes, and biomedical applications (Kracher and Ludwig 2016; Nyanhongo, Thallinger, and Guebitz 2017; Scheiblbrandner and Ludwig 2020). Cellobiose dehydrogenases initially drew attention for their ability to interact with quinones and to improve cellobiohydrolase activity by reducing product inhibition in lignocellulose degradation (Duarte, Costa-Ferreira, and Sena-Martins 1999; Igarashi, Samejima, and Eriksson 1998). Since the discovery of LPMOs, the ability of CDHs to drive LPMO reactions has greatly increased their potential use in lignocellulose saccharification. Furthermore, the unique ability of CDHs to directly transfer electrons to metallized and carbonous surfaces makes them highly suitable for bioelectronic applications, such as enzymatic biosensors and biofuel cells. This direct electron transfer eliminates the need for redox-active mediators, resulting in enhanced sensitivity and potential usage in living cells (Scheiblbrandner and Ludwig 2020). CDH-based biosensors could find applications in the food industry or environmental monitoring for measuring lactose or cellobiose concentrations. Additionally, CDHs have been explored as bioanodic elements in biofuel cells, enabling the conversion of glucose or lactose into electrical energy (Duarte et al. 1999).

Despite their limited ability to use molecular oxygen as an electron acceptor, CDHs still produce hydrogen peroxide to some extent. This property, along with the high oxidizing potential of hydrogen peroxide, makes CDHs suitable as antimicrobial and antioxidant agents (Sulej et al. 2019). Moreover, CDHs' preference for lactose makes them promising candidates for producing lactose-free galactose oligosaccharides (Maischberger et al. 2008). Galactose oligosaccharides are prebiotics that promote beneficial bacteria in the human colon and are usually produced by transgalactosylation of lactose using β-galactosides (Rastall and Maitin 2002). CDHs can also be utilized for producing aldonic acids, such as lactobionic acids, which have numerous applications as gelling and preservative agents in the food industry, bioactive agents in pharmaceuticals, and moisturizing agents in cosmetics (Alonso, Rendueles, and Díaz 2013; Nyanhongo et al. 2017).

AA3_2 GOxs and GDHs have shown great potential as enzymatic anodes in enzymatic biological fuel cells for electricity generation (Cinquin et al. 2010; Ivnitski et al. 2006; Milton et al. 2013; Zebda et al. 2011). In addition, GOxs and GDHs have been used in the biosensors of blood glucose meters for diabetes self-monitoring (Tonyushkina and Nichols 2009). Moreover, researchers have explored their use in cancer treatment by delivering GOx and hemoglobin to cancer cells to initiate nutrient starvation and cytotoxic Fenton reactions, leading to in vitro tumor destruction (Ranji-Burachaloo et al. 2019).

PDHs offer an alternative enzyme to GOx and GDHs for sugar detection in biosensors. Unlike GOxs and GDHs, which only oxidize at the reducing end C-1 of sugars, PDHs have more relaxed substrate recognition and can also oxidize other positions, enabling the detection of various sugars and sugars without the anomeric center (Peterbauer 2020). Additionally, PDHs can be combined with GOx/CDHs in biofuel cells to enhance power density. While GOx alone yields two electrons per glucose molecule by oxidizing at the reducing end C-1, the incorporation of PDHs allows for further oxidation at positions C-2 and C-3, leading to the generation of more electrons for energy harvesting (Tasca et al. 2010).

AA3_2 AAOs have extensive potential in various biotechnological processes, including dye decolorization, pulp bleaching, and synthesis of flavors and polymer building blocks (Urlacher and Koschorreck 2021). Their ability to catalyze stereoselective reactions towards secondary alcohols, such as (*S*)-(*p*-fluorophenyl)ethanol, is particularly interesting for organic synthesis (Hernández-Ortega et al. 2012). A potential application of AAOs is in the conversion of hydroxymethylfurfural (HMF) into a bio-based alternative platform chemical for sustainable bioeconomy. HMF can be enzymatically oxidized to furan-2,5-dicarbaldehyde (DFF), which can further be converted to 2,5-formylfurancarboxylic acid (FFCA) and, finally, to 2,5-furandicarboxylic acid (FDCA), a bio-based alternative to terephthalic acid for producing polyester-type plastics (Figure 10). Initial enzyme cascades for this conversion involved the combination of AA3_2 AAO and the unspecific peroxygenase (UPO), where AAO oxidized HMF and DFF to FFCA, and UPO catalyzed the conversion of FFCA to FDCA. Recently, some AA5_2 copper radical oxidases from fungi have shown excellent activity on HMF and directly oxidized HMF to FFCA, offering alternative biocatalysts for this conversion (M. Cleveland et al. 2021; M. E. Cleveland et al. 2021). Researchers are also screening new oxidoreductases and undertaking engineering efforts to create biocatalysts with the ability to directly oxidize HMF to FFCA (Serrano et al. 2019; Viña-Gonzalez et al. 2020).

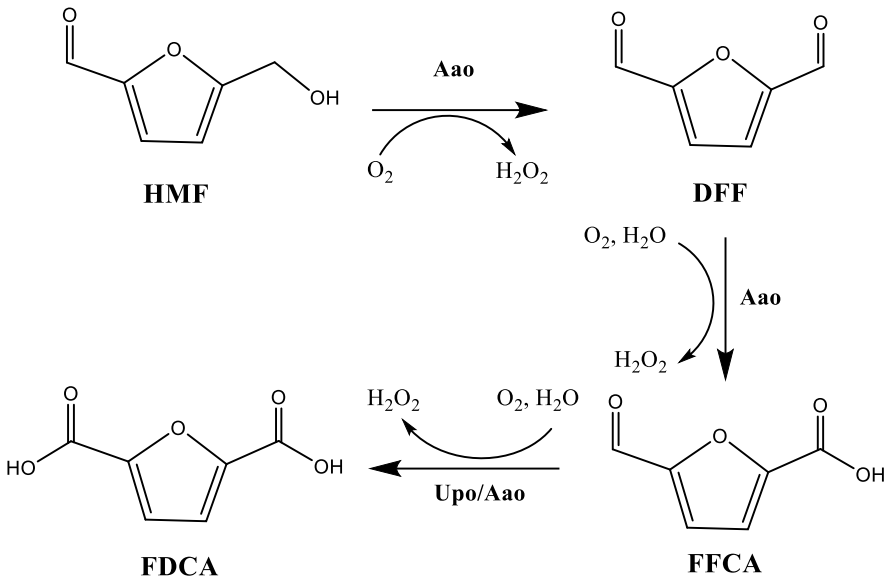


Figure 10. Biocatalytic reaction pathways for production of FDCA from HMF via three-step oxidation.

1.5 Biological function of fungal AA3s

Fungal AA3 enzymes do not directly participate in the degradation of lignocellulosic materials. Instead, they are believed to work in cooperation with other enzymes to facilitate lignocellulose degradation through the direct transfer of electrons or by supplying hydrogen peroxide or hydroquinone. One well-known example of interprotein direct electron transfer is the enzymatic cascade between CDH and LPMO, mediated via the cytochrome domain. In this cascade, electrons from cellobiose are first accepted by the DH domain of CDH and then transferred to the cytochrome domain, facilitated by a closed enzyme conformation that brings the FAD and heme *b* cofactor into close contact. The heme *b* cofactor in CDH undergoes reduction, leading to a conformational change in CDH from a closed to an open state, exposing the heme *b* to the copper center of LPMO for interprotein electron transfer (Felice et al. 2021; Tan et al. 2015).

Hydrogen peroxide, a reactive oxygen species, plays a crucial role in the fungal extracellular redox cycle and enables fungi to decompose plant biomass (Bissaro et al. 2018). Many proposed physiological roles of AA3 oxidases are related to their ability to generate hydrogen peroxide. Hydrogen peroxide can initiate the Fenton reaction in the presence of ferrous ions, generating hydroxyl radicals that aid in lignocellulose degradation. With the phytopathogenic fungus *Ustilago maydis*, a significant number of putative oxidoreductases, including AA3_2 aryl alcohol oxidase, were secreted when grown on maize bran (Couturier et al. 2012). One of the most abundant

oxidoreductases is an AA3_2 aryl alcohol oxidase that was hypothesized to play a role in pathogenicity by contributing to the formation and expansion of lesions via the generation of hydrogen peroxide (Couturier et al. 2016). Additionally, hydrogen peroxide can activate enzymes, including lignin-modifying peroxidase and LPMOs, to further degrade lignin and polysaccharides (Bissaro et al. 2017). The interplay between LPMOs and AA3s is supported at the genomic and secretory levels. Co-regulation and co-secretion of AA9 LPMO and AA3_2 enzymes have been observed in *Aspergillus nidulans* and *Pycnoporus cinnabarinus* (Miyauchi et al. 2017; Nekiunaite et al. 2016). Moreover, high copy numbers of AA3 oxidase-encoding genes are often accompanied by high copy numbers of LPMO-encoding genes in Basidiomycota fungi (Mattila et al. 2022).

Instead of reducing oxygen to form hydrogen peroxide, the AA3 oxidoreductases may reduce various quinones and iron compounds as electron acceptors (Sygmund et al. 2011). This reduction of quinones may serve as a defense mechanism employed by fungi to detoxify quinones generated by plants during defense, converting them to less toxic hydroquinones. The hydroquinones can then further reduce ferric ions to ferrous ions, forming semiquinone radicals. These semiquinone radicals react with oxygen to generate hydroperoxyl radicals, which can then produce hydrogen peroxide for the Fenton reaction. The semiquinone radicals can also reduce another Fe^{3+} to regenerate the original quinone. This proposed quinone redox cycle may also play a role in driving LPMO reactions with quinones as mediators (Garajova et al. 2016; Kracher et al. 2016).

Some plants actively release phenoxy radicals to reinforce lignin and impede fungal invasion. In this context, AA3 enzymes may have additional functions in promoting fungal growth during plant infection through their ability to reduce laccase-generated phenoxy radicals. This ability of AA3 enzymes to utilize laccase-generated radicals was first identified in the plant pathogen *Glomerella cingulata*, where *Gc*GDH was found to inhibit the generation of guaiacol radical and 2,6-dimethoxyphenol radical by *Trametes pubescens* laccase (Sygmund et al. 2011). Similar observations were made for *Trametes cinnabarina*, a white-rot fungus that secretes AA3 enzymes, including *Tc*ODH (previously known as *Pc*GDH), and three aryl alcohol dehydrogenases (AAQO1, AAQO2, and AAQO3), all of which were found to utilize laccase-generated radicals to varying degrees (Mathieu et al. 2016; Piumi et al. 2014). However, only a limited number of AA3 enzyme sequences have been biochemically characterized, and the characterized members usually come from a small sequence space with high levels of similarity to each other. This limitation hinders our understanding of the diverse biological roles of AA3s. Therefore, there is a clear need for more detailed biochemical characterization of AA3 enzymes from different fungal organisms adapting distinct lifestyles and exhibiting greater sequence diversity.

2. Aim of the thesis

The primary objective of this thesis was to explore and characterize carbohydrate-active enzymes from the fungal CAZy subfamilies AA3_1 and AA3_2 for the development of innovative lignocellulose-based biomaterials. While the primary focus was on oxidation toward oligosaccharides, particularly xylooligosaccharides, this thesis also encompasses the study of other carbohydrates with varying linkages and aryl alcohols.

The specific aims were as follows:

- To investigate the properties and capabilities of two previously studied AA3_2 pyranose dehydrogenases regarding their conversion of xylooligosaccharides [1].

- To characterize a novel AA3_1 xylooligosaccharide dehydrogenase and to gain insights into its preferential conversion towards xylooligosaccharides [2].

- To mine for enzymes from different subclusters of CAZy AA3_2s for their substrate specificity towards a broad spectrum of substrates [3].

- To study the ability of AA3_2s to utilize laccase-generated phenoxy radicals as an electron acceptor [3].

3. Materials and methods

3.1 Commercial enzymes and electron donors

Catalase (C100, Merck, Germany), peroxidase from horseradish (HRP, 77332, Merck, Germany) and laccase from *Trametes versicolor* (38429, Sigma-Aldrich, Germany) were used in the reactions to remove hydrogen peroxide, to couple the hydrogen peroxide formation to 2,2′-azino-bis(3-ethylbenzothiozoline-6-sulfonic acid) (ABTS) oxidation, and to recycle the electron acceptors or to generate radicals, respectively. Various electron donors, including carbohydrates, alcohols, and furan compounds used in this thesis, are listed in Table 3. All other buffering chemicals and electron acceptors were procured from Sigma-Aldrich (Germany).

Table 3. Electron donors used in tests discussed in this thesis.

Electron donors	Structure	Manufacturer	Study
Monosaccharide			
Glucose	D-Glc	Sigma-Aldrich, USA	2, 3
Mannose	D-Man	Sigma-Aldrich, USA	2, 3
L-Arabinose	L-Ara	Sigma-Aldrich, USA	2, 3
Xylose	D-Xyl	Sigma-Aldrich, USA	1, 2, 3
Galactose	D-Gal	Sigma-Aldrich, USA	2, 3
Fructose	D-Fru	Sigma-Aldrich, USA	3
β-Methyl-glucose	1-O-methyl-β-D-Glcp	Sigma-Aldrich, USA	3
Disaccharide			
Trehalose	α-D-Glc*p* -(1→1)-α-D-Glc*p*	Sigma-Aldrich, USA	3
Kojibiose	α-D-Glc*p* -(1→2)-D-Glc	Megazyme, Ireland	2, 3
Nigerose	α-D-Glc*p* -(1→3)-D-Glc	Megazyme, Ireland	2, 3
Maltose	α-D-Glc*p* -(1→4)-D-Glc	Sigma-Aldrich, USA	2, 3
Isomaltose	α-D-Glc*p* -(1→6)-D-Glc	Megazyme, Ireland	2, 3
Sophorose	β-D-Glc*p* -(1→2)-D-Glc	Megazyme, Ireland	2, 3
Laminaribiose	β-D-Glc*p* -(1→3)-D-Glc	Megazyme, Ireland	2, 3
Cellobiose (C_2)	β-D-Glc*p* -(1→4)-D-Glc	Merck, Germany	2, 3
Gentiobiose	β-D-Glc*p* -(1→6)-D-Glc	Megazyme, Ireland	2, 3
Xylobiose (X_2)	β-D-Xyl*p* -(1→4)-D-Xyl	Megazyme, Ireland	1, 2, 3
Galactobiose	β-D-Gal*p* -(1→4)-D-Gal	Megazyme, Ireland	2, 3
Mannobiose	β-D-Gal*p* -(1→4)-D-Gal	Megazyme, Ireland	2, 3
Glucosyl-mannose	β-D-Glc*p* -(1→4)-D-Man	Megazyme, Ireland	2
Melibiose	α-D-Gal*p* -(1→6)-D-Glc	Sigma-Aldrich, USA	3
Lactose	β-D-Gal*p* -(1→4)-D-Glc	Sigma-Aldrich, USA	3
Sucrose	α-D-Glc*p* -(1→2)-β-D-Fru*f*	Sigma-Aldrich, USA	3
D-turanose	α-D-Glc*p* -(1→3)-D-Fru*f*	GLYCON, Germany	3
Lactulose	β-D-Gal*p* -(1→4)-D-Fru*f*	Sigma-Aldrich, USA	2
Methyl-lactose	β-D-Gal*p* -(1→4)-D-Glc-1-O-methyl	In-house production	2
Methyl-cellobiose	β-D-Glc*p* -(1→4)-D-Glc-1-O-methyl	In-house production	2

Electron donors	Structure	Manufacturer	Study
Oligosaccharide			
Cellotriose (C_3)	β-D-Glc*p*-β-D-Glcp -(1→4)-D-Glc	Megazyme, Ireland	1, 2
Cellotetraose (C_4)	β-D-Glc*p*-β-*D-Glcp*-β-D-Glcp -(1→4)-D-Glc	Megazyme, Ireland	1, 2
Glucosyl-(1→3)-β-D-cellobiose	β-D-Glc*p*-(1→3)-β-D-Glcp-(1→4)-D-Glc	Megazyme, Ireland	2
Xylotriose (X_3)	β-D-Xyl*p* -β-D-Xyl*p*-(1→4)-D-Xyl	Megazyme, Ireland	1, 2
Xylotetraose (X_4)	β-D-Xylp-β-D-Xyl*p*-β-D-Xyl*p*-(1→4)-D-Xyl	Megazyme, Ireland	1, 2
3^2-α-L-arabinofuranosyl-xylobiose (A^3X)	α-L-Ara*f* -(1→3)-β-D-Xylp -(1→4)-D-Xyl	Megazyme, Ireland	1, 2
2^3-α-L-arabinofuranosyl-xylotriose (A^2XX)	α-L-Ara*f* -(1→2)-β-D-Xyl*p*-(1→4)-β-D-Xylp -(1→4)-D-Xyl	Megazyme, Ireland	1, 2
3^3-α-L-arabinofuranosyl-xylotetraose (XA^3XX)	β-D-Xyl*p* -(1→4)- [α-L-Ara*f* -(1→3)]-β-D-Xyl*p*-(1→4)-β-D-Xylp-(1→4)-D-Xyl	Megazyme, Ireland	2
2^3-(4-O-methyl-α-D-glucuronyl)-xylotriose ($U^{4m2}XX$)	4-O-methyl-α-D-GlcA*p*-(1→2)-β-D-Xyl*p*-(1→4)-β-D-Xylp -(1→4)-D-Xyl	In-house production	1, 2
2^3-(4-O-methyl-α-D-glucuronyl)-xylotetraose ($XU^{4m2}XX$)	β-D-Xyl*p*-(1→4)-[4-O-methyl-α-D-GlcA*p*-(1→2)]-β-D-Xyl*p*-(1→4)-β-D-Xylp-(1→4)-D-Xyl	In-house production	1, 2
Acetylated sugar			
N-acetylglucosamine	GlcNAc	GLYCON, Germany	3
N-acetylmannosamine	ManNAc	GLYCON, Germany	3
N-acetylgalactosamine	GalNAc	GLYCON, Germany	3
Diacetyl-chitobiose	β-D-GlcNAc*p*-(1→4)-D-GlcNAc	Megazyme, Ireland	2, 3
Hexosamine			
Galactosamine	GalN	GLYCON, Germany	3
Glucosamine	GlcN	GLYCON, Germany	3
Chitosanbiose	β-D-GlcN*p*-(1→4)-D-GlcN	Megazyme, Ireland	2, 3
Glycerol, xylitol, sorbitol, mannitol		Sigma-Aldrich, USA	3
Aliphatic and aromatic alcohols			
Methanol, ethanol, hexanol, octanol		Sigma-Aldrich, USA	3
2-Propanol, 2-butanol, 2-hexanol, 2-octanol		Sigma-Aldrich, USA	3
Benzyl alcohol		Sigma-Aldrich, USA	3
4-Hydroxybenzyl alcohol		Sigma-Aldrich, USA	3
Anisyl alcohol		Sigma-Aldrich, USA	3
3,4-Dimethoxybenzyl alcohol		Sigma-Aldrich, USA	3
4-Hydroxy-3-methoxybenzyl alcohol		Sigma-Aldrich, USA	3
3,5-Dimethoxy-4-hydroxybenzyl alcohol		Biosynth, USA	3
Cinnamyl alcohol		Sigma-Aldrich, USA	3

Electron donors	Structure	Manufacturer	Study
Coniferyl alcohol		Sigma-Aldrich, USA	3
p-Coumaryl alcohol		Kindly provided by Dr. Anna Happonen	3
Caffeyl alcohol		TransMIT, USA	3
Sinapyl alcohol		Sigma-Aldrich, Germany	3
Hydroxymethyl furfural		Sigma-Aldrich, Germany	3

3.2 Production and purification of fungal AA3 proteins

The gene construction and production of the fungal AA3 proteins are described in the publications [1–3]. Table 4 provides an overview of all the AA3 proteins successfully produced in those studies and characterized in this thesis. Except for *Tm*XdhA, the AA3 proteins were constructed with a C-terminal 6* His tag and expressed in *Pichia pastoris* strain KM71H. In contrast, *Tm*XdhA was expressed in an engineered *Aspergillus niger* strain CSFG_9057 without any tag. For the proteins with a His tag, affinity chromatography was used for purification, with *Ab*PDH1 additionally purified through anion-exchange chromatography and size exclusion chromatography [1,3]. *Tm*XdhA was purified solely by size exclusion chromatography as described in [2]. After purification, all protein samples were transferred to 10 mM sodium acetate buffer at pH 5.5 with continuous dilution and concentration using 10 kDa Vivaspin centrifuge filters. The protein concentration was determined using the Bradford method [1] and the BCA method [2,3], and protein purity was confirmed with SDS-PAGE. Additionally, the purity of *Tm*XdhA was further assessed using 2D electrophoresis with pH 3–10 strips and Criterion TGX 4–20% gel. The spots from the 2D gel were analyzed using matrix-assisted laser-desorption/ionization time of flight mass spectrometry (MALDI-TOF-MS), and protein identification was conducted by comparing the *A. niger* database from UniProt with the *TmxdhA* sequence. After purification, the enzymes were snap-frozen using liquid nitrogen and stored at −80 °C.

3.3 Enzymatic assays

The dehydrogenase activity of an AA3 protein was assayed using BQ, DCIP, or/and ferrocenium hexafluorophosphate (Fc^+). The oxidase activity was screened by coupling the H_2O_2 formation to the oxidation of ABTS by HRP. The specific reaction conditions, wavelengths, and corresponding extinction coefficients were detailed in [1–3]. All activity measurements were monitored using an Eon plate reader (BioTek, Winooski, VT, USA).

*Ab*PDH1 and *Am*PDH1 were mainly assessed for their substrate specificity toward xylooligosaccharides, whereas *Tm*XdhA was screened for its activity towards a list of

monosachharides, disaccharides, and oligosaccharides [1–2]. The remaining AA3_2s were tested for their activity against 52 substrates, including monosaccharides, disaccharides, alcohols, and polyols, with a two-level screening design [3]. Briefly, the AA3_2s were screened on 14 substrate mixtures at the first level. The substrates present in the oxidized mixtures were subsequently individually screened at the second level, each with the corresponding protein and electron acceptor.

To determine the pH profile of each AA3 protein with at least moderate activity, the best electron acceptor and electron donor were employed. Steady-state kinetic constants were then measured in triplicates at the optimum pH for each protein using the corresponding electron acceptor. The reduction rate of the electron acceptor or the formation rate of the oxidized electron donor was plotted against substrate concentration (a minimum of eight data points). The Michaelis–Menten constant (K_M) was estimated by fitting the data to the Michaelis–Menten equation using GraphPad Prism 6.0 (GraphPad Software, La Jolla, CA, USA). For laccase activity measurements, hydroquinone (HQ) was used as the substrate at a concentration of 5 mM. The oxidation of HQ was followed in a 250 µl reaction, with an absorption coefficient (ε_{abs249}) of 17.25 $mM^{-1}cm^{-1}$. Enzyme unit (U) is defined as the amount of enzyme that catalyzed the conversion of one micromole of substrate per minute.

Table 4. Summary of proteins produced and characterized in the studies covered in this thesis.

Protein name	Sub-family	Sequence ID	Organism	CBM family	Purification	Study
*Ab*PDH1	2	NCBI_AAW92124	*Agaricus bisporus*	N	Affinity chromatography+ Anion exchange+ size exclusion	1
*Am*PDH1	2	NCBI_AAW82997	*Leucoagaricus meleagris*	N	Affinity chromatography	1
*Tm*XdhA	1	csfg_Myrth2p4_000359	*Thermothelomyces myriococcoides*	N	Size exclusion	2
*Ab*AA3_2A	2	jgi_Agbis_177008	*Agaricus bisporus var bisporus*	N	Affinity chromatography	3
*Ps*AaoA	2	jgi|Punst1|143069	*Punctularia strigosozonata*	N	Affinity chromatography	3
*Ap*GoxA	2	csfg_Aurpu2p4_000012	*Aureobasidium pullulans*	N	Affinity chromatography	3
*Pc*AA3_2A	2	jgi_Phaca1|179599	*Phanerochaete carnosa*	N	Affinity chromatography	3
*As*AadhA	2	jgi|Aurde3_1|1328312	*Auricularia subglabra*	1	Affinity chromatography	3
*As*AadhB	2	jgi|Aurde3_1|1407644	*Auricularia subglabra*	1	Affinity chromatography	3
*Ap*AA3_2B	2	csfg_Aurpu2p4_000585	*Aureobasidium pullulans*	N	Affinity chromatography	3
*Ap*Aa3_2C	2	csfg_Aurpu2p4_010615	*Aureobasidium pullulans*	N	Affinity chromatography	3
*Mc*GdhA	2	csfg_Malci1p7_002451	*Malbranchea cinnamomea*	N	Affinity chromatography	3
*Ms*AA3_2A	2	csfg_Corse1p7_015851	*Myceliophthora sepedonium*	N	Affinity chromatography	3
*Ta*GdhA	2	csfg_Theau2p4_003545	*Thermoascus aurantiacus*	N	Affinity chromatography	3
*Ki*OdhA	2	jgi_Kocim1_624823	*Kockovaella imperatae*	13	Affinity chromatography	3

N in the CBM column indicates proteins that lacked a CBM.

3.4 Product identification and quantification

Figure 11 illustrates the workflow for characterizing AA3 enzymes in terms of ability to oxidize various electron donors using diverse electron acceptors. Different strategies for product analysis were employed in each study to ensure accurate identification and quantification of the products.

3.4.1 Product analysis of *Ab*PDH1 and *Am*PDH1 oxidized xylooligosaccharides (Study 1)

*Ab*PDH1 and *Am*PDH1 were subjected to reactions with neutral and acidic xylooligosaccharides using BQ as the electron acceptor. The depletion rate of the substrates was monitored at different time points (1, 4, and 8 h for neutral substrates, and 24 h for acidic substrates) using high-performance anion-exchange chromatography coupled with pulsed electrochemical detection (HPAEC-PAD). The oxidations introduced by PDHs can lead to multiple potential products that might further react with water, complicating mass spectra interpretation. To simplify the data analysis, sodium borodeuteride ($NaBD_4$) was added to the reactions to reduce carbonyls back to hydroxyls. The samples were then desalted using a porous graphitic carbon (PGC) column. The oxidized positions were revealed using electron spray ionization coupled with multiple-level tandem mass spectrometry (ESI-MS^n) in the negative mode, and an ultra-high-performance liquid chromatography method coupled with a mass spectrometry and evaporative light scattering detector (UPLC-MS-ELSD) method was developed for quantifying the multiple oxidation products. Detailed analysis parameters and quantitative interpretation of mass spectra are described in [1].

3.4.2 Product analysis of *Tm*XdhA oxidized oligosaccharides (Study 2)

*Tm*XdhA activity was tested using 29 different carbohydrates. The reaction products, as well as the oxidation positions, were confirmed using ESI-MS/MS in the negative mode. Additionally, the efficiency of *Tm*XdhA in oxidizing cellooligosaccharides and xylooligosaccharides was compared both individually and in mixtures. Time course sampling was performed at 1, 3, 7, and 24 h, and the formation of reaction products was quantified using a hydrophilic interaction chromatography (HILIC) method coupled with ELSD and semi-quantified using ESI-MS. Detailed analysis parameters are described in [2].

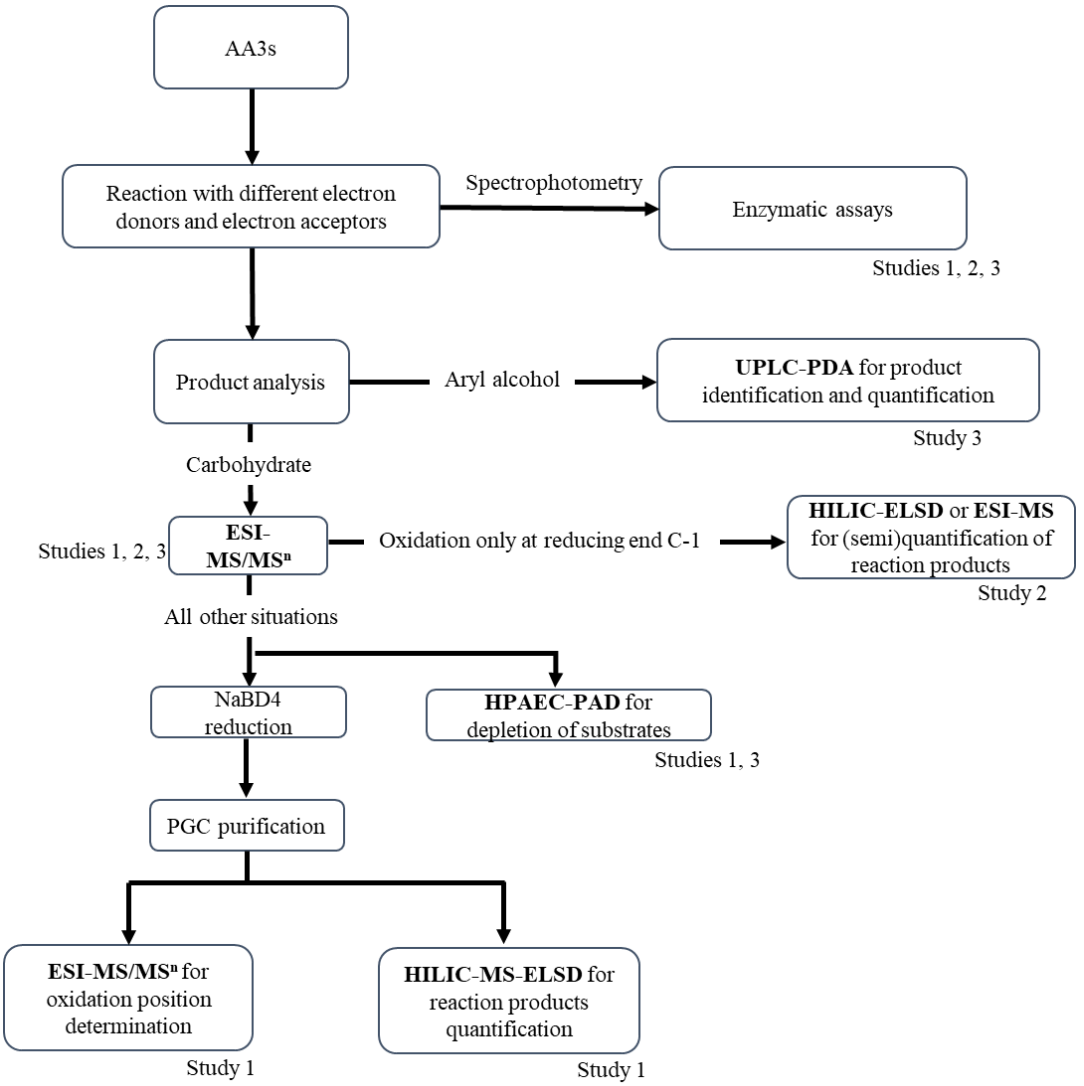


Figure 11. Workflow for characterizing AA3s in their ability to utilize diverse electron donors and electron acceptors. The analytical methods used for the product analyses are shown in bold.

3.4.3 Product analysis of AA3_2 oxidized carbohydrate and aryl alcohols (Study 3)

Both carbohydrate-oxidizing and aryl-alcohol-oxidizing enzymes were found in the AA3_2 subfamily. For the AA3_2 oxidized carbohydrates, the reaction product(s) were analyzed using ESI-MS^n in the negative mode. Substrate depletion for *Ki*OdhA oxidized carbohydrates over a 24-h reaction was analyzed with HPAEC-PAD. Instead, the AA3_2 oxidized aryl alcohols were injected in a UPLC HSS pentafluorophenyl (PFP) column (100 Å, 1.8 µm, 2.1 mm × 100 mm; Waters, MA, USA). The reaction products were identified and quantified with corresponding standards using a photodiode array detector (PAD). The purification method, elution parameters, and detector settings are described in [3].

3.5 Utilization of phenoxy radicals by AA3_2s

The experiments were conducted at pH 5.5 and 30 ℃ in 20 mM ammonium acetate with 0.1 mM ferulic acid, laccase from *T. versicolor* at a concentration of 40 U/l, and either 5 mM glucose or 5 mM anisyl alcohol. The AA3_2 enzymes were tested at various concentrations ranging from 20 U/l to 10,000 U/l. Negative controls were included using boiled AA3_2 enzymes, and in some reactions, catalase at a concentration of 2 U/ml was added to eliminate hydrogen peroxide. The remaining ferulic acid was measured at 320 nm, and the formation of ferulic acid dimer was measured at 350 nm for 60 min with 10-min intervals. The data were averaged, and standard deviations were calculated from three replicate reactions ($n = 3$).

3.6 Sequence and structure analysis

The sequence similarity network was generated using the SSNpipe and was visualized by cystoscope using the layout of yFiles Organic (Viborg et al. 2019). Multi-sequence alignment was performed using MUSCLE v5 (Edgar 2022), and the informative sites were selected using ClipKit with default settings (Steenwyk et al. 2020). The conservation of key amino acids was visualized using WebLogo (Crooks et al. 2004). The model structures were generated using AlphaFold2 and visualized with PyMOL V2.0 (Jumper et al. 2021).

3.7 Statistical analysis

Averages and standard deviations were calculated over three replicate reactions ($n = 3$). One-way ANOVA ($p < 0.05$; GraphPad) with F-test and Tukey's test were performed to ascertain the differences in specific activities toward different substrates and kinetic values.

4. Results

4.1 Production and purification of fungal AA3 proteins

The AA3_2 proteins studied in this thesis were produced in *P. pastoris* KM71H, while the AA3_1 *Tm*XdhA was produced in *A. niger* CSFG_9057. Out of the 30 recombinant protein production attempts, 15 were successful. All the *Pichia*-produced proteins were constructed with a His tag on the C-terminus, allowing them to be purified using affinity chromatography. *Ab*PDH1 was additionally purified using anion exchange and size exclusion chromatography. In contrast, the *A. niger* strain CSFG_9057 was genetically modified to remove most of the secreted proteins. Also, the *Tm*XdhA was produced without any tag, and it was purified using solely size exclusion chromatography. The purity of the proteins was confirmed using SDS-PAGE (Figure 12). However, 2D electrophoretic analysis of *Tm*XdhA revealed the presence of a protein impurity (Figure 12D, two spots in the 2D electrophoretic gel). MALDI-TOF-MS analysis of the tryptic peptides confirmed that spot 2 was *Tm*XdhA, while spot 1 was predicted to be an endogenous *A. niger* hydrolase (UniProt: AoA370CB09) [2]. Efforts to remove the hydrolase were not successful due to the similarities of the molecular weight and pI of the two proteins. Consequently, the hydrolytic activity was tested using five different pNP-glycosides, and minimal activity was observed on pNP-β-D-glucopyranoside, pNP-β-D-xylopyranoside, and pNP-β-D-mannopyranoside, while activities were detected on pNP-α-L-arabinofuranoside (0.52 U/mg) and pNP-α-D-glucopyranoside (0.12 U/mg). To minimize this α-glucosidase activity, 0.1 mM castanospermine was introduced to the reactions, which did not influence the oxidoreductase activity, and the α-arabinofuranosidase activity remained unchanged, albeit at a low level [2]. Following the production and purification of fungal AA3 enzymes, the subsequent sections of the thesis focus on characterizing the ability of these proteins to oxidize lignocellulosic materials, particularly oligosaccharides.

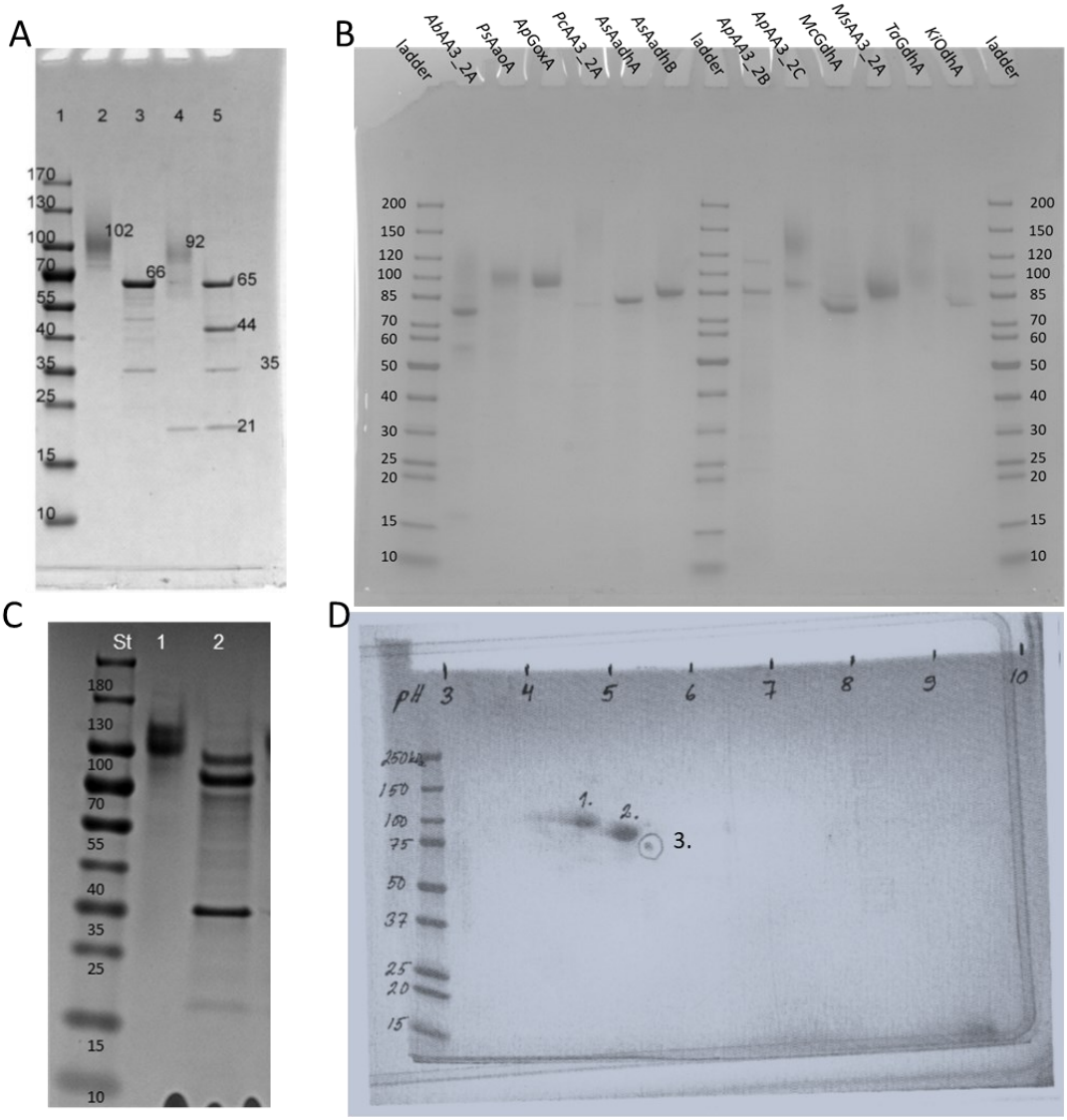


Figure 12. SDS-PAGE A), B), and C), as well as the 2D electrophoresis gel separation D), of all proteins that were studied for this thesis. A) Lane 1 is a molecular weight ladder; lane 2, *Am*PDH1; lane 3, deglycosylated *Am*PDH1; lane 4, *Ab*PDH1; lane 5, deglycosylated *Ab*PDH1. B) The newly discovered and purified AA3_2 proteins. C) Lane 1 is native *Tm*XdhA; lane 2, deglycosylated *Tm*XdhA. D) Purified *Tm*XdhA (pH 3–10 strip, Criterion TGX+gel 4–20%). Spot 1, *A. niger* glycoside hydrolase (Uniport: A0A370CB09); spot 2, *Tm*XdhA; spot 3, contaminants from staining. This figure was originally published in [1–3].

4.2 Oxidation of xylooligosaccharides by AA3_2 *Ab*PDH1 and *Am*PDH1

*Ab*PDH1 and *Am*PDH1 are the two most studied AA3_2 enzyme families and are known for oxidizing various monosaccharides, cellooligosaccharides, and maltooligosaccharides. However, their ability to oxidize xylooligosaccharides longer than xylobiose remains unexplored (Gonaus et al. 2016; Morrison et al. 1999; Sygmund et al. 2008; Volc et al. 2000). In this study, the *Ab*PDH1 and *Am*PDH1 produced in-house demonstrated activity comparable to previously studied enzymes when using glucose as the substrate [1]. Subsequently, the activity on xylose and xylooligosaccharides was measured for each PDH. The activity on xylose for both enzymes (43–45 U/mg, Figure 13) was found to be similar to that previously reported for the native *Am*PDH1 (39 U/mg), indicating the successful production of both PDHs with appropriate activity (Sygmund et al. 2008). This part of the research had two main objectives: (1) characterize both PDHs for their activity towards xylooligosaccharides and (2) understand the regioselectivity of both PDHs towards xylooligosaccharides.

4.2.1 *Ab*PDH1 and *Am*PDH1 were able to oxidize xylooligosaccharides

Both PDHs exhibited activity on X_2–X_4 and A^3X at pH 7.5 using Fc^+ as an electron acceptor (Figure 13). The initial activity measurements revealed that the overall activity decreased with an increase in the degree of polymerization for linear xylooligosaccharides for both PDHs. Notably, the activity of *Ab*PDH1 towards A^3X was greater than that toward X_3, and *Ab*PDH1 activity towards A^2XX and XA^3XX was approximately 40% and 55%, respectively, in comparison to the corresponding unsubstituted X_4. Similarly, *Am*PDH1's activity towards A^3X was double its activity towards X_3. In contrast, initial activity values were not measurable for *Am*PDH1 for oxidizing A^2XX or XA^3XX under the tested conditions. Initial activities were not obtained for *Ab*PDH1 and *Am*PDH1 towards $U^{4m2}XX$ or $XU^{4m2}XX$ under the tested conditions. However, the oxidation of all tested xylooligosaccharides by both PDHs was observed with prolonged incubation time and after reaction optimization.

To maximize xylooligosaccharide oxidation, both PDHs were incubated with the corresponding substrate for 24 h, and the Fc^+ electron acceptor in the initial activity measurements was replaced with BQ that could be regenerated using laccase (Baminger, Ludwig, et al. 2001). The laccase was dosed in the same amount (0.2 U/ml) for PDHs, and all subsequent reactions were performed at pH 5.5, which is close to the pH optima of both PDHs and laccase.

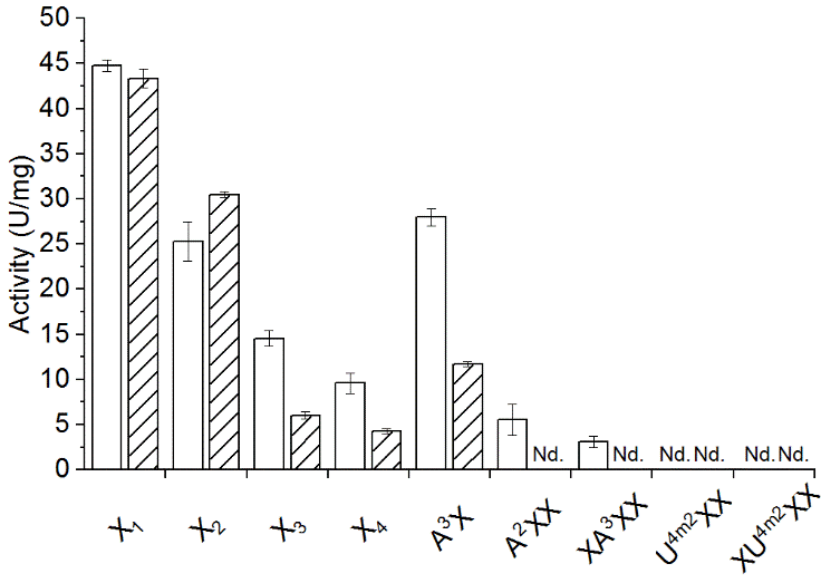


Figure 13. Initial activity of *Ab*PDH1 (white) and *Am*PDH1 (with diagonal stripes) on 10 mM of neutral or 2 mM of acidic xylooligosaccharides at pH 7.5 using Fc^+ ion as the electron acceptor. X, xylose; X_2, xylobiose; X_3, xylotriose; X_4, xylotetraose; A^3X, 3^2-α-L-arabinofuranosyl-xylobiose; A^2XX, 2^3-α-L-arabinofuranosyl-xylotriose; XA^3XX, 3^3-α-L-arabinofuranosyl-xylotetraose; $U^{4m2}XX$, 2^3-(4-O-methyl-α-D-glucuronyl)-xylotriose; $XU^{4m2}XX$, 2^3-(4-O-methyl-α-D-glucuronyl)-xylotetraose. Error bars represent standard deviation of three replicate reactions. Reactions with $U^{4m2}XX$ and $XU^{4m2}XX$ were conducted in duplicate. Nd. indicates no activity detected under these conditions after 24 h. This figure was originally published in [1].

The substrate conversion over a 24 h incubation period was monitored by measuring the depletion of substrates (Figure 14). Consistent with the initial activity measurements, both *Ab*PDH1 and *Am*PDH1 showed the most rapid oxidation of X_2, with *Ab*PDH1 converting 62% and *Am*PDH1 converting 95% after the first hour of the reaction. The substrate conversion decreased with the increase in degree of polymerization for the linear xylooligosaccharides within the first hour (Figure 14A–C). After 8 h of incubation, both *Ab*PDH1 and *Am*PDH1 fully depleted X_2, and by 24 h, they fully converted X_3. *Ab*PDH1 also fully depleted xylotetraose by 24 h, while *Am*PDH1 oxidized 77% of X_4 by the same time point (Figure 14A–C). Consistent with the higher initial rates of *Ab*PDH1 and *Am*PDH1 oxidizing A^3X than in oxidizing X_3, full depletion of A^3X by both PDHs was achieved at 8 h time points (Figure 14D). A^2XX and XA^3XX were oxidized by both PDHs during this extended incubation period. *Ab*PDH1's conversion of A^2XX was 1.6 times higher than *Am*PDH1 after 24 h (Figure 14E), and both *Ab*PDH1 and *Am*PDH1 had transformed approximately 60% of XA^3XX after 24 h (Figure 14F).

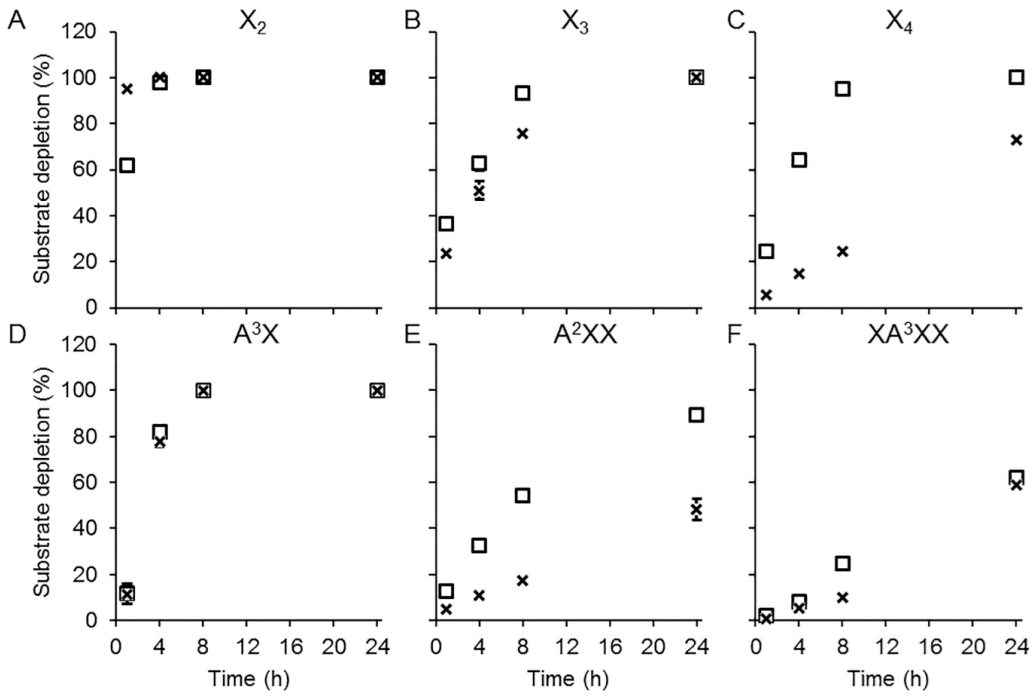


Figure 14. Substrate depletion by *Ab*PDH1 (square) and *Am*PDH1 (cross) followed by HPAEC-PAD. Substrates: (A) xylobiose, X_2; (B) xylotriose, X_3; (C) xylotetraose, X_4; (D) 3^2-α-L-arabinofuranosyl-xylobiose A^3X; (E) 2^3-α-L-arabinofuranosyl-xylotriose, A^2XX; and (F) 3^3-α-L-arabinofuranosyl-xylotetraose XA^3XX. Error bars show the data range of duplicate reactions. Error bars are not visible when the data range fits inside the drawn data point. This figure was originally published in [1].

The same enzyme loading (0.2 U/ml) was also applied to the acidic xylooligosaccharides, $U^{4m2}XX$ and $XU^{4m2}XX$, but neither *Ab*PDH1 or *Am*PDH1 could oxidize either substrate at a quantifiable level. However, when the enzyme loading was increased to 2 U/ml (10 times higher), *Ab*PDH1 fully depleted both $U^{4m2}XX$ and $XU^{4m2}XX$ substrates, whereas *Am*PDH1 only depleted around 30% and 20% of $U^{4m2}XX$ and $XU^{4m2}XX$, respectively [1]. Given the higher oxidation of neutral substrates by both PDHs, the products formed after 24 h of oxidation were analyzed in detail, focusing on the degree and positions of oxidation.

4.2.2 *Ab*PDH1 and *Am*PDH1 introduced multiple oxidations to the xylooligosaccharides

To facilitate the interpretation of MS spectra, the oxidized xylooligosaccharide samples were reduced by sodium borodeuteride ($NaBD_4$). The samples were then desalted and analyzed using electrospray ionization coupled with tandem mass spectrometry (ESI-MS) in negative mode, which has been proven to be better for complex oligosaccharide structural analysis than the typically used positive

mode (Juvonen et al. 2019). Because $NaBD_4$ reduced the carbonyls in the oxidized products, a PDH oxidation at a secondary hydroxyl is equivalent to one Dalton difference in mass between the oxidized product and the original substrate after $NaBD_4$ reduction. Similarly, double oxidation at secondary hydroxyls is indicated by a two Dalton increase. In contrast, oxidation at the reducing end C-1 forms a carboxyl group, which is resistant to $NaBD_4$ reduction. The quantification of different oxidized products was conducted based on peak intensity and isotopic abundance of the naturally present substrates. The detailed explanation and equations for this calculation are described in publication [1].

A total of six reaction species were quantified in the analysis: non-oxidized substrate, single oxidation at a secondary hydroxyl, double oxidations at secondary hydroxyls, single oxidation at the reducing end C-1, one oxidation at the reducing end C-1 with one oxidation at a secondary hydroxyl, and one oxidation at the reducing end C-1 with two oxidations at secondary hydroxyls (Figure 15). However, the ratio between the neutral products and the acidic products were not calculable.

Both PDHs were found to oxidize all of the tested xylooligosaccharides at secondary hydroxyls and at the reducing end C-1, producing various oxidized products. For neutral products with only oxidation at secondary hydroxyls, both PDHs introduced a maximum of two ketones (Figure 15A). Double-keto products were dominant for X_2 and X_3, while A^3X, A^2XX, and XA^3XX showed minimal oxidation at two secondary hydroxyls for both PDHs. Interestingly, *Ab*PDH1 produced slightly more double oxidized products compared to *Am*PDH1. Both PDHs were also found to oxidize xylooligosaccharides at the reducing end C-1, generating acidic reaction products after 24 h of incubation. The acidic products from linear xylooligosaccharide oxidation by *Ab*PDH1 and *Am*PDH1 were typically double oxidized, with oxidation at the reducing end C-1 and a secondary hydroxyl. The only exception was observed when X_2 was oxidized by *Am*PDH1, where more than 50% of the acidic products had triple oxidation (C-1 oxidation + two ketones) (Figure 15B). In contrast, most of the acidic products from Ara*f*-substituted xylooligosaccharide oxidation by both PDHs had a single oxidation specifically at the reducing end C-1 (Figure 15B).

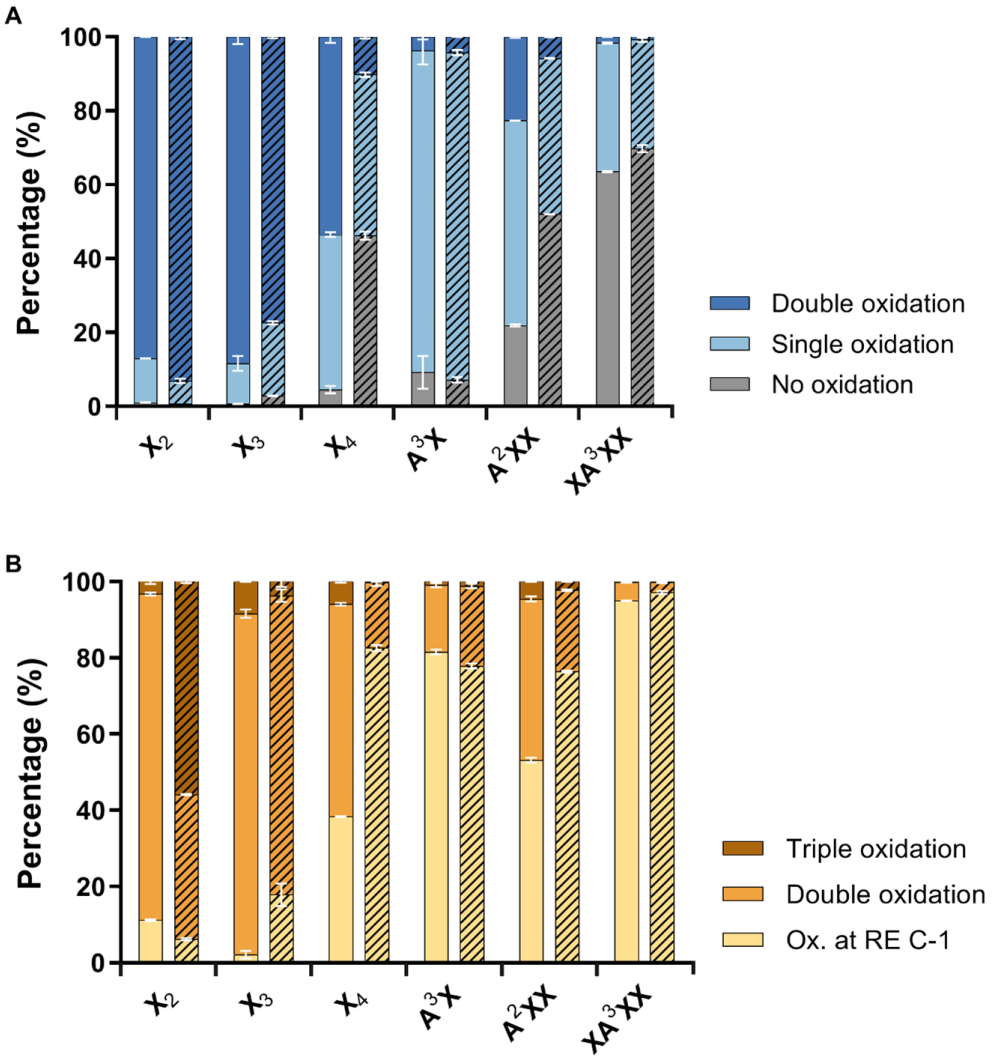


Figure 15. Distribution of A) neutral products (unreacted substrate and oxidations at secondary hydroxyls) and B) acidic products (reducing end C-1 oxidation with zero, one, or two secondary hydroxyl oxidations). Reactions with *Ab*PDH1 are indicated by solid color, and reactions with *Am*PDH1 are indicated by diagonal stripes. This figure was originally published in [1].

4.2.3 *Ab*PDH1 and *Am*PDH1 oxidized xylooligosaccharides at both ends

The successful separation and quantification of acidic and neutral reaction products were achieved using HILIC-ELSD. However, it should be noted that X_2 posed a challenge due to the coelution of acidic products with salt, thus preventing proper quantification [1]. In general, the acidic products resulting from oxidation at the anomeric C-1 position accounted for less than 25% of the total reaction products in the case of *Ab*PDH1-oxidized X_3, X_4, A^2X, and A^3XX, as well as *Am*PDH1-oxidized X_3, A^2X, and A^3XX (Figure 16). The primary product species observed in the oxidation of X_3 by both PDHs was the double oxidation at two secondary hydroxyls, which constituted 81% and 56% of the products oxidized by *Ab*PDH1 and *Am*PDH1, respectively. A similar observation was made for *Ab*PDH1-oxidized X_4, where 48% of the products contained two oxidations at secondary hydroxyls. In contrast, the dominant reaction product species for both PDHs in the oxidation of A^2X and A^3XX carried only one carbonyl group after a 24-h incubation. In the case of AmPDH1-oxidized X4, the acidic products accounted for approximately 55% of the total reaction products, and most of these acidic products did not carry a ketone group. Notably, XA^3XX exhibited a less specific oxidation pattern at secondary hydroxyls by both *Ab*PDH1 and *Am*PDH1, with 45% and 55% of the reaction products, respectively, being oxidized at the reducing end C-1 (Figure 16).

The determination of oxidized positions for each reaction product species was achieved by analyzing the distribution of deuteride(s) in the $NaBD_4$-reduced oxidation products using ESI-MS^n. However, it is important to note that while the oxidation on secondary hydroxyls can be identified in terms of the specific glycosyl residue involved, it is not possible to distinguish which hydroxyl (C-1/C-2/C-3/C-4) within that glycosyl residue has undergone oxidation. The oxidation patterns of xylooligosaccharides (X_2, X_3, and X_4) by both *Ab*PDH1 and *Am*PDH1 mainly occurred at both end xylosyl units rather than the internal xylopyranosyl (Xyl*p*) residues. Double oxidation was distributed between the reducing and non-reducing ends, and there were no indications of reaction products with two oxidations occurring at a single xylosyl residue. Single oxidation on X_3 primarily occurred at the secondary hydroxyls on the non-reducing end, while single oxidation on X_4 mainly occurred at the reducing end C-1 position or the secondary hydroxyls of the reducing end. The only triple-oxidized product detected was formed from X_2 by *Am*PDH1 oxidation, and it consisted of one ketone at the non-reducing end Xyl*p* unit and one ketone at the reducing xylosyl unit, with the reducing end C-1 oxidized to lactone (ultimately forming an acid).

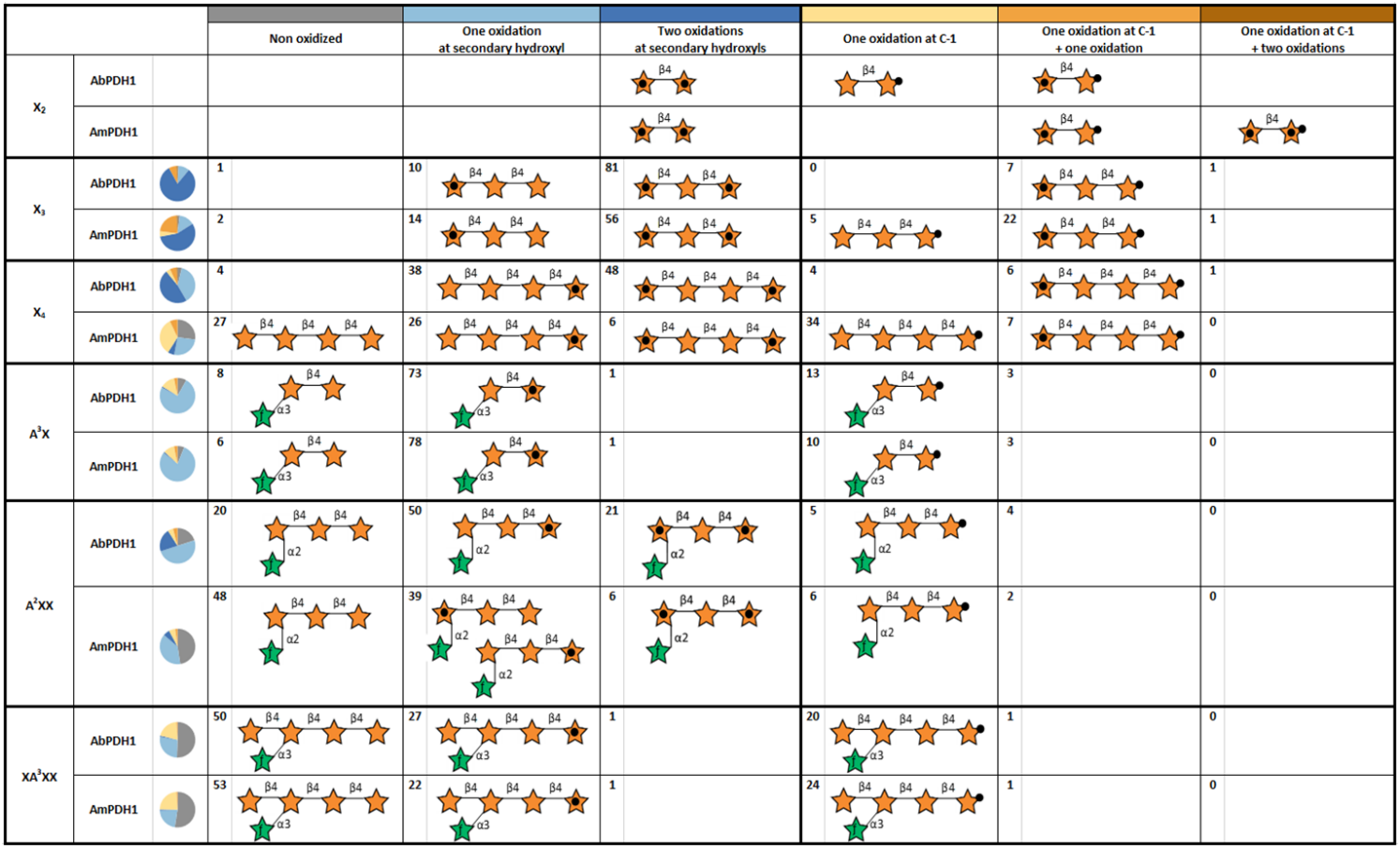


Figure 16. Summary of main oxidation products and oxidized positions following xylooligosaccharide treatment by *Ab*PDH1 and *Am*PDH1. Representative product structures are drawn for those representing > 5% of the reaction mixture; the symbol nomenclature for glycans was adopted from Varki et al. (2015). A black dot in the center of a star represents a secondary hydroxyl oxidation, and a black dot at the tip of a star represents oxidation at the reducing end C-1. The proportion of each reaction product is shown by the number in each cell and summarized by the pie chart shown in each row. This figure was originally published in [1].

For the Ara*f*-substituted xylooligosaccharides, both PDHs primarily induced single oxidation after a 24-h treatment. In A^3X and XA^3XX, which contained an α-3-linked Ara*f* substitution at the non-reducing side Xyl*p* unit, both PDHs oxidized primarily at the secondary hydroxyls, or the C-1 position of the reducing end xylosyl unit. Similarly, A^2XX with an α-2-linked Ara*f* substitution was also oxidized at the secondary hydroxyls and C-1 of the reducing end by both PDHs. In *Am*PDH1-induced monooxidation of A^2XX, oxidation at the secondary hydroxyls of the Xyl*p* unit linked to the Ara*f* substituent was also observed. However, no clear oxidation of Ara*f* residue was detected in any of the samples.

4.3 Biochemical characterization of a novel AA3_1 xylooligosaccharide dehydrogenase, *Tm*XdhA

Previously, all the characterized enzymes from AA3 subfamily 1 were cellobiose dehydrogenases with comparably low activity towards xylooligosaccharides. *Thermothelomyces myriococcoides* CBS 389.93 (syn. *Crassicarpon hotsonii, and Myriococcum thermophilum*) is an ascomycete that originated from the surface of heated compost in Switzerland (Koukol 2016; Wang et al. 2022). It encodes 17 AA3s, among which four genes are predicted to encode enzymes belonging to family AA3_1 (Gene accession codes *Myrth2p4_000359*, *Myrth2p4_001304*, *Myrth2p4_007444*, and *Myrth2p4_005287*; CSFG database). *Myrth2p4_001304* has been previously characterized and was found to encode a cellobiose dehydrogenase called *Mt*CDH (UniProt: A9XK88), mainly oxidizing cellooligosaccharides and lactose (Pricelius et al. 2009; Zámocký et al. 2008). In this study, *Myrth2p4_000359* was selected for recombinant protein production and functional characterization with the aim of understanding its specificity towards xylooligosaccharides. The protein is named *Tm*XdhA according to its preferential activity towards xylooligosaccharides.

4.3.1 *Tm*XdhA oxidized diverse mono-, di- and oligosaccharides at the anomeric carbon

The pH optima of *Tm*XdhA was measured for cellobiose, and the most activity was observed between pH 5 and 6, similar to the pH preference reported for *Mt*CDH [1] (Zámocký et al. 2008). Cellobiose oxidation by *Tm*XdhA was more efficient using BQ as the electron acceptor rather than DCIP. While *Tm*XdhA was found to utilize oxygen as an electron acceptor, its oxidase activity was limited and not quantifiable with the spectrophotometric assay. Therefore, subsequent biochemical characterizations of *Tm*XdhA were performed using BQ as the electron acceptor and 10 mM ammonium acetate buffer (pH 5.5).

To investigate the substrate specificity of *Tm*XdhA, it was incubated with various monosaccharides, disaccharides, and oligosaccharides for 24 h. The oxidized products were analyzed using ESI-Q-

TOF-MS in negative mode, where oxidation at the reducing anomeric center resulted in negatively charged peaks $[M\text{-}H]^-$ and neutral substrates were detected as chlorine adducts $[M + Cl]^-$. Thus, the oxidation at the anomeric center of the neutral substrates is equivalent to a 20 Da decrease in the mass spectrum. For instance, the glucose giving peak at mass-to-charge ratio (*m/z*) 215 were oxidized to gluconic acid giving peak at *m/z* 195 (Table 5). The acidic substrates $U^{4m2}X$ and $U^{4m2}XX$ carrying methyl-α-D-glucuronyl residue were detected as deprotonized forms $[M–H]^-$ with peaks at m/z 471 and m/z 603, respectively. The oxidation of $U^{4m2}XX$ introduced a second carboxylic acid at the reducing end, hence, the oxidized $U^{4m2}XX$ can be both single charged $[M–H]^-$ and doubly charged $[M–2H]^{2-}$ and was detected as peaks at *m/z* 619 and *m/z* 309, respectively (Table 5). Based on the mass spectra, *Tm*XdhA oxidation was found to be solely towards reducing end C-1 and *Tm*XdhA did not show any activity on C-1 methylated cellobiose and lactose (Table 5).

*Tm*XdhA oxidized 18 out of 29 tested substrates in 24 h to varying extents. Hexoses were efficiently oxidized, and disaccharides and oligosaccharides with β-(1→4) linkage were preferred. Gluco-disaccharides with α/β-(1→2), α/β-(1→3), and α/β-(1→6) glucosidic bonds were not oxidized, but a small amount of maltobionic acid was detected for the oxidation of α-(1→4)-linked maltose. Partial oxidation was observed for mannobiose and β-(1→4)-linked glycosyl-mannose, while β-(1→4)-linked galactobiose and chitosanbiose were not accepted as substrates by *Tm*XdhA. Complete oxidation was observed for lactose and β-(1→4)-linked cellooligosaccharides from dimer to tetramer, while glucosyl-(1→3)-β-D-cellobiose showed partial oxidation.

*Tm*XdhA fully oxidized various neutral and acidic xylooligosaccharides, including X_2, X_3, X_4, and $U^{4m2}XX$, after 24 h of reaction. However, the oxidation of $U^{4m2}X$ was not detected. When testing *Tm*XdhA activity on Ara*f*-substituted xylooligosaccharides A^3X and A^2XX, the residual α-arabinofuranosidase activity completely hydrolyzed A^3X and A^2XX during the 24 h treatment. During a shorter 3 h incubation, *Tm*XdhA was found to only oxidize A^2XX, and no oxidation of A^3X was detected [1].

Table 5. Oxidation of monosaccharides, disaccharides, and oligosaccharides by *Tm*XdhA after 24 h, with product detection by ESI-Q-TOF-MS in the negative mode. Detected oxidation is indicated as Y and no oxidation as N. The table was originally published in [2].

	Substrate	Linkage	Oxidation	Substrate *m/z*	Oxidized product *m/z*	Degree of oxidation %
Monosaccharides	Glucose		Y	215	195	~90
	Xylose		Y	**	165	**
	Mannose		Y	215	195	~90
	Galactose		Y	215	195	~90
Disaccharides	Cellobiose	β 1→4	Y	377	357	100
	Sophorose	β 1→2	N	377		-
	Laminaribiose	β 1→3	N	377		-
	Gentiobiose	β 1→6	N	377		-
	Maltose*	α 1→4	Y (Trace)	377	357	<5
	Kojibiose*	α 1→2	N	377		-
	Nigerose*	α 1→3	N	377		-
	Isomaltose*	α 1→6	N	377		-
	Xylobiose	β 1→4	Y	317	297	100
	Lactose	β 1→4	Y	377	357	100
	Galactobiose	β 1→4	N	377		-
	Mannobiose	β 1→4	Y	377	357	~50
	Glucosyl-mannose	β 1→4	Y	377	357	~90
	Chitosanbiose	β 1→4	N	375		-
Oligosaccharides	Cellotriose	β 1→4	Y	539	519	100
	Cellotetraose	β 1→4	Y	701	681	100
	Glucosyl-(1→3)-β-D-cellobiose	β 1→3/4	Y	539	519	~80
	Xylotriose	β 1→4	Y	449	429	100
	Xylotetraose	β 1→4	Y	581	561	100
Acidic	$U^{4m2}X$	β 1→4; α 1→2	N	471		-
	$U^{4m2}XX$	β 1→4; α 1→2	Y	603	619, 309	100
C-1 methylated disaccharides	Methylated-cellobiose	β 1→4	N	391		0
	Methylated-lactose	β 1→4	N	391		0

* Castanospermine included in the reactions.

** Xylose does not give a clear peak possibly due to the low ionization capacity; hence, the percentage was not calculable. This table was originally published in [2].

4.3.2 *Tm*XdhA prefers linear xylooligosaccharides over cellooligosaccharides

The substrates subjected to 24 h reactions as listed in Table 5 were subsequently analyzed for their specific activities. Initial velocity measurements revealed no quantifiable activity towards glucose, galactose, mannose, and mannobiose (Figure 17). Compared to the specific activities between 8.4 and 11 U/mg of *Tm*XdhA in oxidizing C_2–C_4, X_2–X_4 and $U^{4m2}XX$, the *Tm*XdhA oxidized glucosyl-(1→3)-β-D-cellobiose (3.1 U/mg) and glucosyl-(1→4)-β-D-mannose (6.0 U/mg) had a significantly lower rate (Figure 17). Among the specific activities observed, *Tm*XdhA demonstrated the highest specific activity (10.8 U/mg), which was statistically higher than the specific activity towards X_2 (9.0 ± 0.3 U/mg) and cellotriose (8.4 U/mg). However, this activity was not significantly different from its activities on C_2 and C_4 (9.6 U/mg and 10.4 U/mg, respectively).

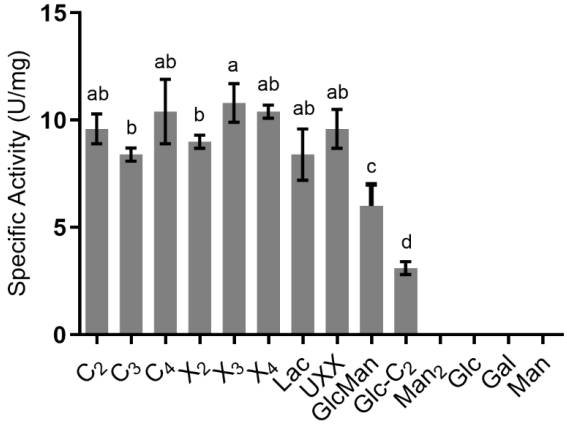


Figure 17. Specific activity of *Tm*XdhA towards different substrates ($n = 3$). No activity was detected for mannobiose (Man_2), glucose (Glc), galactose (Gal), and mannose (Man). Error bars represent standard deviation of three replicate reactions. Significance in activities ($p < 0.05$) is shown by different lowercase letters (a–d). Cellobiose, C_2; cellotriose, C_3; cellotetraose, C_4; xylobiose, X_2; xylotriose, X_3; xylotetraose, X_4; lactose, Lac; 2^3-(4-O-methyl-α-d-glucuronyl)-xylotriose, UXX; Glucosyl-(1→4)-β-D-mannose, GlcMan; Glucosyl-(1→3)-β-D-cellobiose, Glc-C_2. This figure was originally published in [2].

The kinetic parameters of *Tm*XdhA were assessed for both linear cellooligosaccharides and xylooligosaccharides, and the results are presented in Table 6. Overall, *Tm*XdhA displayed higher catalytic efficiency with xylooligosaccharides than cellooligosaccharides. This difference in catalytic efficiency was primarily driven by *Tm*XdhA's 3–5 times better binding affinity (K_M) towards xylooligosaccharides than cellooligosaccharides. The turnover rate (k_{cat}) increased with the rise in degree of polymerization, while the K_M values dropped with an increase in the length of

cellooligosaccharides. In contrast, *Tm*XdhA exhibited the greatest affinity to X_3 (0.11 mM) compared to X_2 (0.16 mM) and X_4 (0.13 mM). Interestingly, the catalytic efficiency (k_{cat}/K_M) indicated that X_3 and X_4 were the most favorable substrates, while cellotriose was the least favorable of the tested substrates.

Table 6. Kinetic parameters of *Tm*XdhA for cellooligosaccharides and xylooligosaccharides. The table was originally published in [2].

Substrate	K_M (mM)	k_{cat} (s^{-1})	k_{cat}/K_M ($s^{-1}\cdot mM^{-1}$)
Cellobiose	0.36 ± 0.04	16.7 ± 0.7	46.2 ± 5.8
Cellotriose	0.43 ± 0.04	17.6 ± 0.6	40.1 ± 4.2
Cellotetraose	0.53 ± 0.04	23.8 ± 1.1	45.1 ± 4.0
Xylobiose	0.16 ± 0.01	17.5 ± 0.4	108.9 ± 9.5
Xylotriose	0.11 ± 0.01	22.3 ± 0.4	200.9 ±14.5
Xylotetraose	0.13 ± 0.01	25.0 ± 0.5	187.7 ± 15.2

After the kinetic analyses, *Tm*XdhA was used in reactions with cellooligosaccharides and xylooligosaccharides to evaluate its ability with substrate conversion during a 24 h reaction. The product formation was semi-quantified by calculating the relative ratio of the product peak to the remaining substrate peak in the mass spectra. This MS-based semi-quantification method was verified for accuracy by comparing the results with a quantitative HILC-ELSD method. Although the MS method tended to slightly overestimate the percentage of product formation, it was simpler and faster than the HILC-ELSD method, making it suitable for following the substrate conversion. A detailed comparison of both methods can be found in [2].

When each oligosaccharide was individually converted by *Tm*XdhA over time, it was observed that all tested oligosaccharides were oxidized at a similar rate and were fully converted to corresponding aldonic acids after 24 h (Figure 18). Subsequently, the selectivity of *Tm*XdhA for converting specific substrates in a mixture of oligosaccharides was studied. Three substrates were mixed and incubated with *Tm*XdhA in equal molarity. Interestingly, in the mixtures, the oxidation pattern was length dependent, with the longest substrates (C_4 and X_4) being oxidized at a faster rate than the dimers and trimers in both cellooligosaccharide (Figure 19A) and xylooligosaccharide mixtures (Figure 19B). Moreover, when mixing xylooligosaccharides and cellooligosaccharides together, *Tm*XdhA clearly exhibited a preference for xylooligosaccharides in all three mixtures (Figure 19C, D, E).

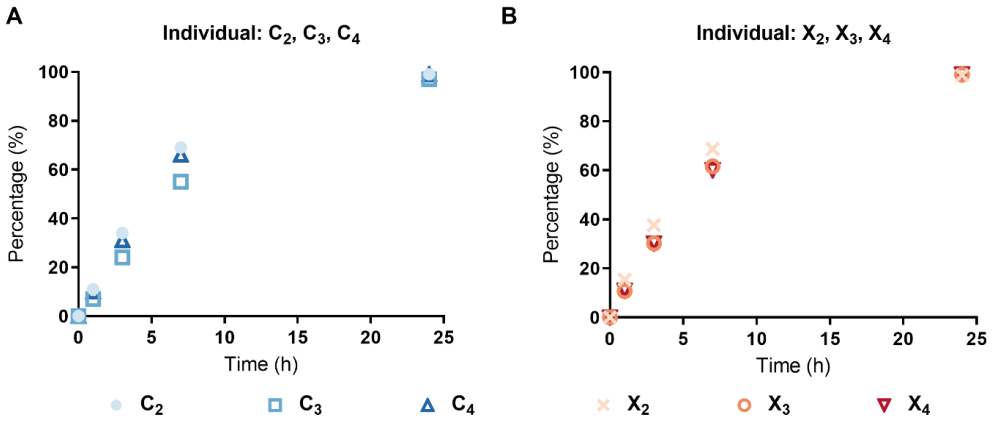


Figure 18. Product formation in the individual oxidations of linear oligosaccharides by *Tm*XdhA followed with mass spectra. A) Reactions with cellobiose (C_2), cellotriose (C_3), and cellotetraose (C_4). B) Reactions with xylobiose (X_2), xylotriose (X_3), and xylotetraose (X_4). Error bars represent standard deviation of three replicate reactions. This figure was originally published in [2].

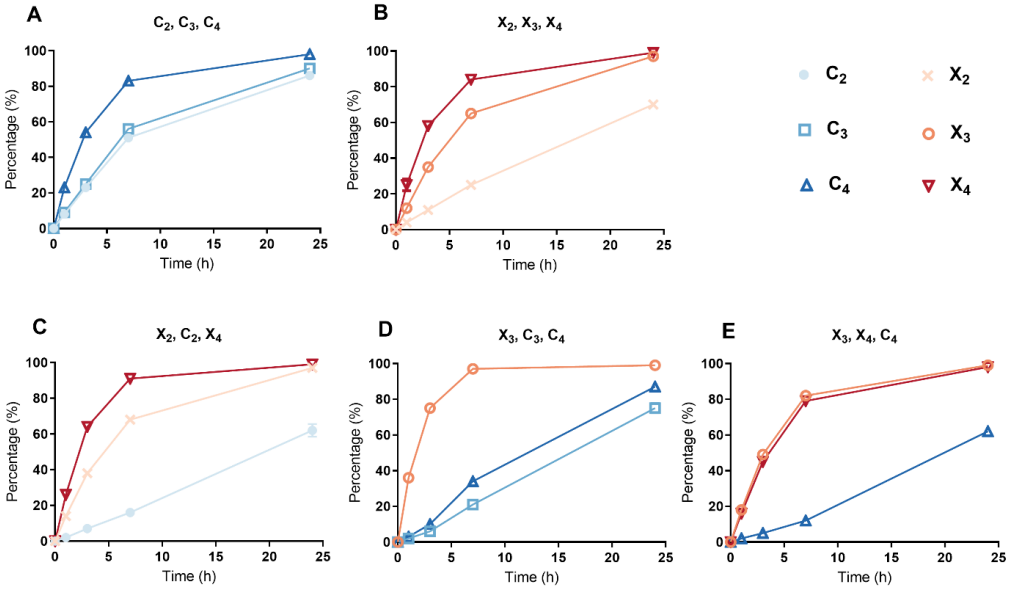


Figure 19. Product formation during *Tm*XdhA oxidation of cellooligosaccharide and xylooligosaccharide mixtures followed by the MS method. Reactions contained the following oligosaccharides as substrates: A) Cellobiose (C_2), cellotriose (C_3), and cellotetraose (C_4). B) Xylobiose (X_2), xylotriose (X_3), and xylotetraose (X_4). C) Xylobiose, cellobiose, and xylotetraose. D) Xylotriose, cellotriose, and cellotetraose. E) Xylotriose, xylotetraose, and cellotetraose. Error bars represent standard deviation of three replicate reactions. This figure was originally published in [2].

4.3.3 The structure model of *Tm*XdhA suggests that a glutamine residue could facilitate *Tm*XdhA's binding to pentose sugar

To gain insights into the unique activity of *Tm*XdhA towards xylooligosaccharides among AA3_1 enzymes, a structure model of *Tm*XdhA was predicted using AlphaFold2, which is a highly accurate protein structure predictor (Jumper et al. 2021). The majority of the residues in the predicted *Tm*XdhA structure were modeled with a high per-residue confidence (pLDDT) score (> 90) and a low predicted aligned error (PAE) (< 5).

The predicted structure of *Tm*XdhA reveals an architecture with an active-site pocket, as shown in Figure 20A. By performing a basic local alignment search tool (BLAST) analysis, it was found that *Tm*XdhA shared the most sequence identity with its isoform, *Mt*CDH. Comparing the *Tm*XdhA model with the dehydrogenase domain of *Mt*CDH (PDB: 4QI4), both proteins folded in a similar manner, and they exhibited conservation with a histidine residue positioned near the flavin ring to facilitate the reductive half-reaction (Figure 19B, C; Hallberg et al. 2003).

The primary difference between *Tm*XdhA and *Mt*CDH lies in a single amino acid residue within the substrate-binding domain, where *Tm*XdhA has a glutamine residue (Q406), while *Mt*CDH has a threonine residue at the corresponding position (Figure 20C). According to previous findings (Tan et al. 2015), the threonine residue in *Mt*CDH indirectly binds to the C-6 of the reducing moiety through the mediation of a water molecule, and all five hydrogen bonds in this hydrogen bond system fall within the ideal binding distance (2.6–2.9 Å) (Figure 20D). However, in *Tm*XdhA, the space between the water molecule and OE1 of Q406 is limited (1.3 Å), suggesting the need for a new hydrogen bond system to facilitate the binding to the pentose moiety.

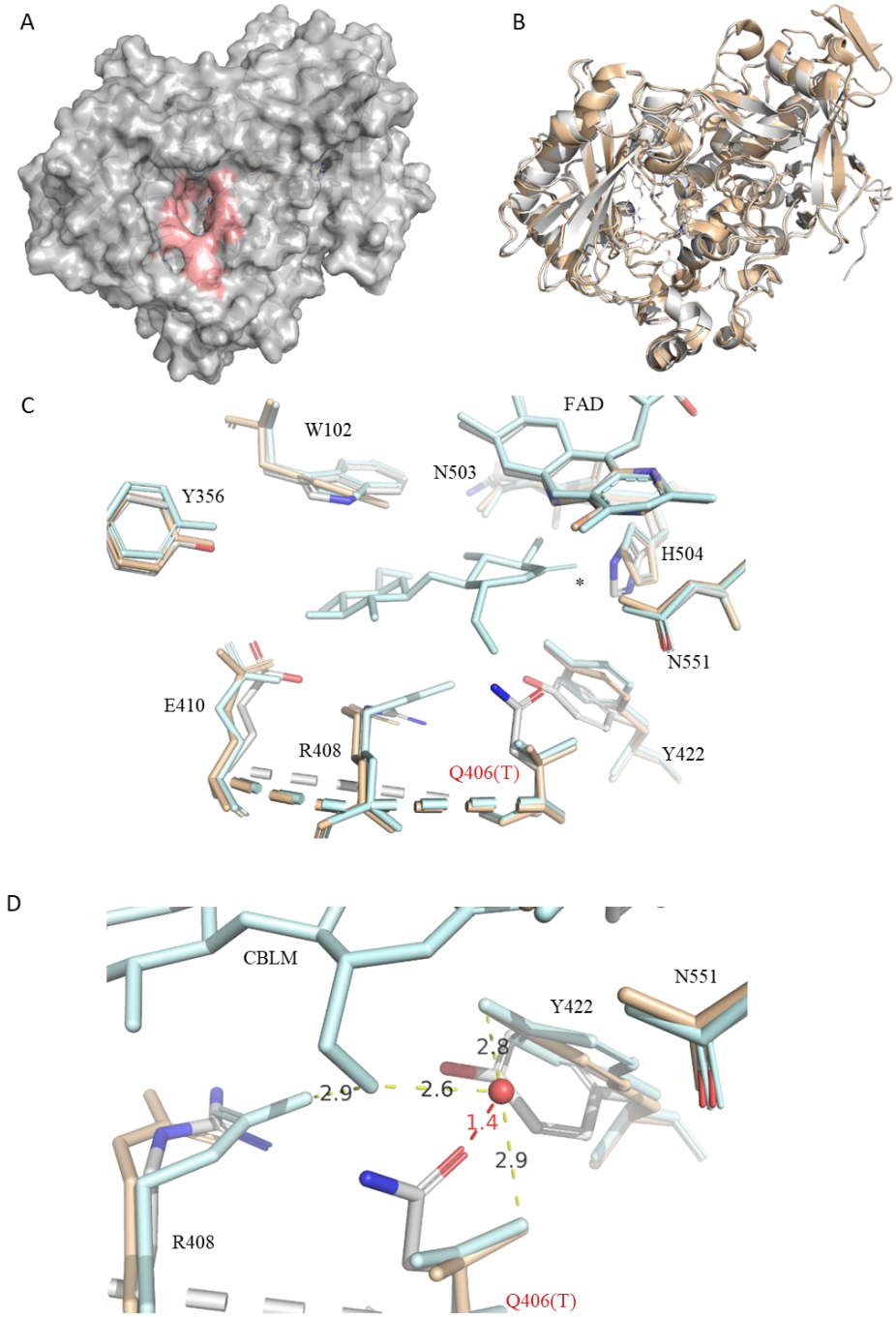


Figure 20. Structural comparison of *Tm*XdhA predicted model and *Mt*CDH (PDB code 4QI4). A) The predicted structure of *Tm*XdhA created with AlphaFold2; the surface of active site is colored red. B) Superimposition of the *Tm*XdhA predicted model structure with the structure of the dehydrogenase domain of *Mt*CDH (PDB code 4QI4). The structure of *Mt*CDH is shown in light yellow, and the structure of *Tm*XdhA is shown in gray. C) Alignment for the active site of *Tm*XdhA (white), substrate free *Mt*CDH (yellow), and *Mt*CDH-cellobionolactam (blue; PDB

code 4QI5). The asterisk marks the position of the hydroxyl being abstracted by CDHs in cellobiose. D) Alignment for the reducing end moiety C-6 binding site of the *Tm*XdhA (white) and *Mt*CDH–CBLM complex (blue). The water molecule mediating the hydrogen bond (dashed yellow line) system is shown as a red sphere. The distance between the OE1 of Q406 and the water molecule is shown as a dashed red line. This figure was originally published in [2].

4.4 Screening for substrate specificity among AA3_2 subclusters

In the last two years, it has been discovered that AA3_2 GOx/GDHs also exhibits activity on disaccharides such as maltose, laminaribiose, and gentiobiose, opening up possibilities for utilizing these enzymes in disaccharide and oligosaccharide tailoring and upgrading (Cerutti et al. 2021; Wijayanti et al. 2021). Additionally, given the diverse specific activities identified within AA3_2s, predicting enzymatic function though homology-based approaches remains challenging.

To address this knowledge gap and identify new AA3_2 enzymes with novel activities, phylogenetic analyses were conducted on fungal AA3_2 sequences to guide the sequence selection. Subsequently, successfully produced recombinant AA3_2 proteins were characterized for their substrate specificities towards various monosaccharides, disaccharides, aliphatic and aryl alcohols, and polyols. Three electron acceptors were tested in this step, including BQ, DCIP, and oxygen. Although oligosaccharides longer than disaccharides were not tested in this study, the insights gained from how these proteins oxidized the tested substrates will provide valuable guidance for potential future applications of these enzymes in oligosaccharide bio-upgrade processes.

4.4.1 Sequence selection based on sequence similarity network

A total of 4590 putative fungal AA3_2 sequences were collected from various databases and published papers, including JGI, CSFG, and MycoCLAP [3]. To analyze these sequences, an SSN was constructed using a bit-score threshold of 420. Figure 21 shows that cluster II contained biochemically characterized PDHs and AAO/AADHs, indicating a close phylogenetic relationship between these two types of enzymatic functionalities. The sequences situated between these characterized enzymes were considered possible transitional structures with the potential for dual functionality, oxidizing both carbohydrates and alcohols (Sützl et al. 2019). Therefore, nine sequences from this cluster were chosen for recombinant production.

In addition to cluster II, clusters VI, XI, and XII contained previously characterized GDHs and GOxs with oligosaccharide-oxidizing activities. Thus, an additional nine sequences from clusters VI and XI were selected. Furthermore, nine sequences from clusters IV, XV, XXX, and XXIV, which had limited known activities, were chosen with the goal of identifying novel enzymatic functions. The

selection process aimed to cover a diverse range of fungal species from both Ascomycota and Basidiomycota, representing different ecological and habitat backgrounds [3].

Out of the 27 selected proteins, 12 were successfully produced in *P. pastoris* KM71H, and the production and purification were described in Section 4.1. Table 4 provides a summary of all the purified proteins. The presence of the oxidized FAD was confirmed by characteristic peaks at approximately 375 nm and 440 nm for *Ab*AA3_2A, *Ps*AaoA, *Ap*GoxA, *As*AadhA, *As*AadhB, *Mc*GdhA, *Ms*AA3_2A, *Ta*GdhA, and *Ki*OdhA [3]. However, the oxidized FAD was not clearly observed for *Ap*AA3_2C. Consequently, exogenous FAD was added to *Ap*AA3_2C for the subsequent activity assays. The *Pc*AA3_2A and *Ap*AA3_2B stock concentrations (2.2 and 2.44 mg/ml, respectively) were below the detection threshold for FAD using spectroscopy-based methods.

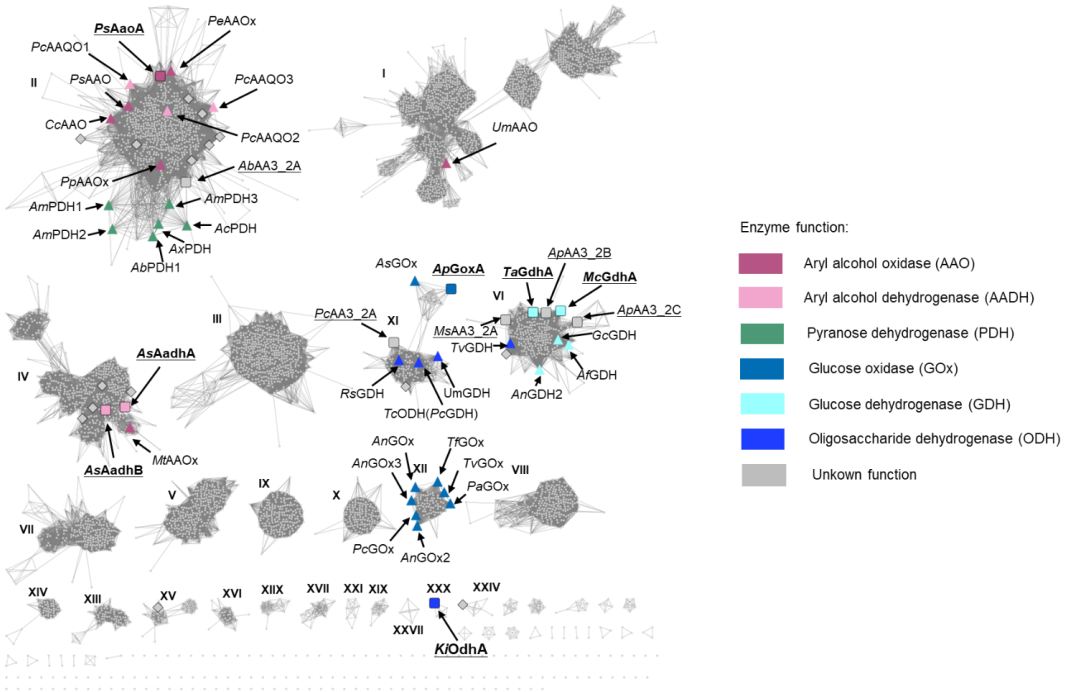


Figure 21. Sequence similarity network at a bit-score cut-off of 420. The clusters were numbered based on the number of individual sequences in the cluster. The previously biochemically characterized sequences (detailed in [3]) and the sequences selected by this study are shown with large symbols, while the remaining sequences are represented by gray dots. The sequences were colored based on specificity, and the shape reveals the characterization status (triangle: previously characterized; diamond: failed in production; square: successful production). The successfully produced enzymes with characterized activities are in bold and underlined, while

the produced proteins without any detected activity are solely underlined. The clusters were numbered based on the number of individual sequences in the cluster. This figure was adapted from [3].

4.4.2 Primary activity screening

The substrate specificity of the purified proteins was screened using a high throughput approach with 15 substrate mixtures containing a total of 52 distinct substrates at pH 5 (Figure 22). Both dehydrogenase and oxidase activity were screened using three different electron acceptors, including BQ, DCIP, and oxygen. Notably, the oxygen level was not controlled in these tests.

With regard to the protein activities, all proteins showed some level of activity except *Ap*AA3_2C. In general, four enzymes demonstrated high activity levels. Among them, *Ps*AaoA had the ability to utilize all three tested electron acceptors. It exhibited high oxidation activity towards aryl alcohol mixtures but had limited activity towards carbohydrates when using oxygen as the electron acceptor. In contrast, three carbohydrate-oxidizing enzymes were identified during the primary screening with high activity levels, including, *Ap*GoxA, *Ta*GdhA, and *Ki*OdhA. *Ap*GoxA effectively utilized all tested electron acceptors and showed the most activity with a mixture of monosaccharides, followed by a mixture of β-glucodisaccharides. *Ta*GdhA displayed the most dehydrogenase activity with a mixture of monosaccharides and showed less specificity, oxidizing both α and β-glucodisaccharides as well as galactodisaccharides. Interestingly, *Ki*OdhA exhibited the most activity in oxidizing a mixture of β-glucodisaccharides when using BQ as the electron acceptor, indicating its role as an oligosaccharide dehydrogenase.

4.4.3 Secondary activity screening

After the initial activity screening with mixtures, further analysis was conducted on individual substrates for enzymes that displayed at least low activity levels, along with their corresponding electron acceptors (Figure 23). Among them, *Ps*AaoA showed the most activity with cinnamyl alcohol, *p*-anisyl alcohol, and benzyl alcohol. Additionally, it had low activity with hexanol. In contrast, *As*AadhA and *AsA*adhB oxidized 4-hydroxybenzyl alcohol, coniferyl alcohol, and *p*-coumaryl alcohol, but not cinnamyl alcohol.

The carbohydrate-oxidizing enzymes displayed distinct oxidation profiles, but all exhibited activity with both glucose and gentiobiose. *Ta*GdhA had the most activity with glucose and xylose, followed by gentiobiose and mannose. Notably, *Ta*GdhA exhibited high mannose oxidation rates when BQ was used as the electron acceptor, but no activity was detected on mannose when DCIP was used. Similar results were observed for gentiobiose, where more activity was observed with DCIP (1.7 U/mg) than BQ (0.5 U/mg). In contrast, *Ap*GoxA used both oxygen and BQ when oxidizing

glucose, whereas DCIP was not preferred. Unlike *Ta*GdhA, *Ap*GoxA exhibited more activity only with glucose, and other carbohydrates were oxidized at slower rates. *Ki*OdhA showed the most activity with gentiobiose, followed by medium activity with glucose and medium-low activity with xylose and galactose. *Ap*AA3_2B, *Ab*AA3_2A, *As*AadhA, *As*AadhB, *Mc*GdhA, and *Ms*AA3_2A only displayed low to limited levels of activity on tested substrates that were not quantitatively significant, leading to their exclusion from further analysis.

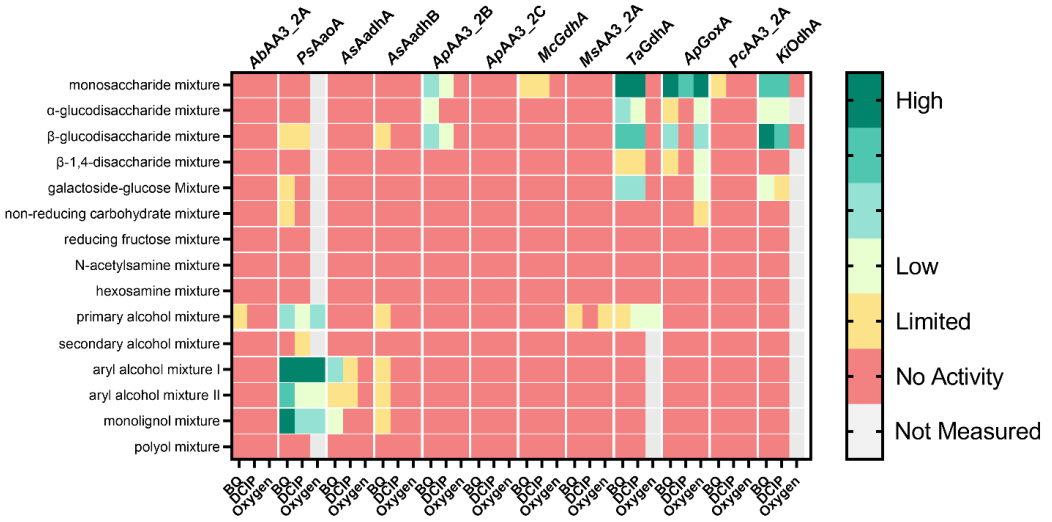


Figure 22. Activity heat map of fungal AA3_2 proteins at pH 5 and 30 °C with the substrate mixtures. The oxidase activity was screened by coupling the H_2O_2 production to the oxidation of ABTS by HRP, and the dehydrogenase activity was screened using BQ and DCIP as electron acceptors. The levels of activity were defined based on the ratio of absorbance change during the first hour of reaction compared to in the background., High: Ratio > 100; Medium: Ratio > 20; Moderate: Ratio > 3; Low: Ratio > 1.2. For cases where limited activity was observed, it signified a minimum of 10% difference in the absorbance between the reaction and the background after overnight incubation. This figure was adapted from [3].

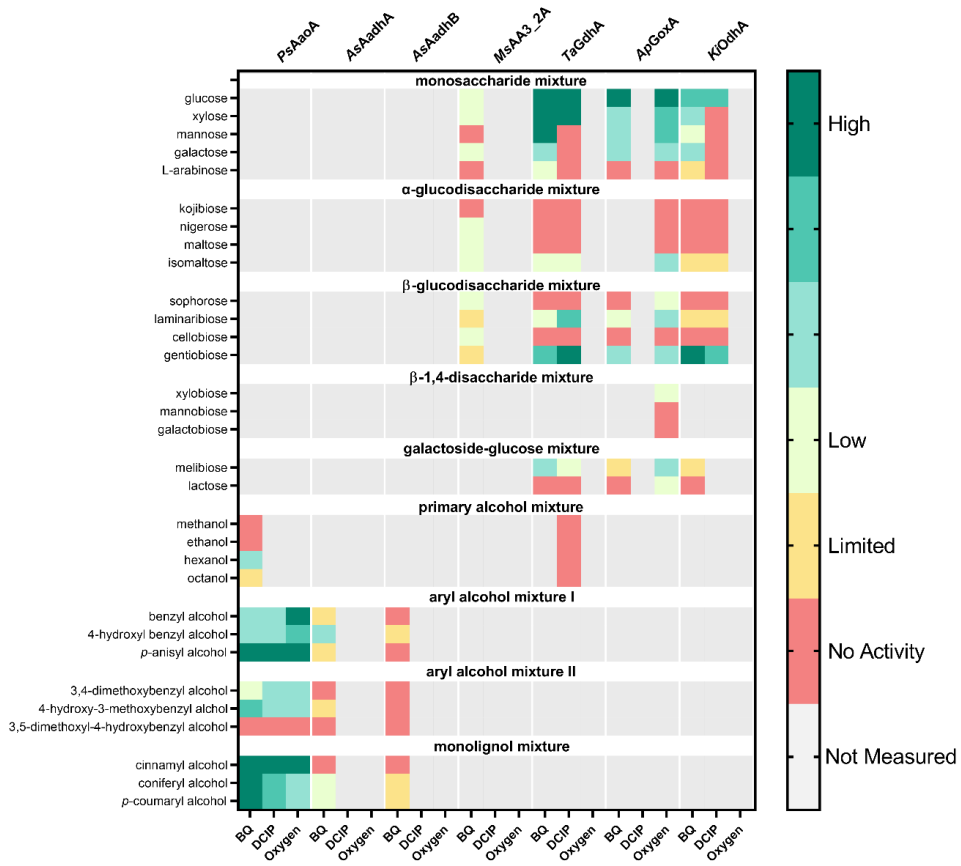


Figure 23. Activity heat map of fungal AA3_2 proteins at pH 5 and 30 °C with the individual substrates. This figure was adapted from [3].

4.4.4 Detailed characterization of the new carbohydrate oxidase and dehydrogenases

*Ap*GoxA displayed the greatest catalytic efficiency with glucose. Although it is named glucose oxidase due to its ability to use oxygen as an electron acceptor, it achieved a fivefold greater catalytic efficiency when using BQ as the electron acceptor (Table 7). Though *Ap*GoxA was able to oxidize gentiobiose from specific activity assays, the corresponding kinetic parameters were not measurable due to the unreachable plateau. Both *Ta*GdhA and *Ki*OdhA were dehydrogenases, as they did not use oxygen as an electron acceptor but preferred BQ. *Ta*GdhA displayed the most catalytic efficiency when oxidizing both glucose and xylose, with a 20-fold to 30-fold lower catalytic efficiency with gentiobiose (Table 8). Conversely, *Ki*OdhA oxidized gentiobiose with the highest rate (3500 $M^{-1}s^{-1}$), followed by glucose (130 $M^{-10}s^{-1}$). Kinetic parameters with xylose and mannose were not measurable for *Ki*OdhA (Table 8). All the carbohydrate-oxidizing enzymes studied here oxidized carbohydrates

solely at the reducing end C-1, confirmed by MS analysis, and no activity was detected when using α/β-methyl-glucose as substrates [3]. Due to the unique characteristics of *Ki*OdhA, additional studies were undertaken to evaluate its capacity to reduce monosaccharides and disaccharides during 24-h incubations using HPAEC-PAD [3]. Among the substrates that were examined, the most substantial reduction was observed in the case of gentiobiose at 78.6%, followed by melibiose at 5.1% and glucose at 3.7%.

Table 7. Kinetic parameters of *Ap*GoxA on carbohydrate substrates. Oxygen and BQ were used as the electron acceptors. All reactions were conducted at pH 5.5.

Substrate	*Ap*GoxA-Oxygen			*Ap*GoxA-BQ		
	K_M (mM)	k_{cat} (s^{-1})	k_{cat}/K_M ($M^{-1}\cdot s^{-1}$)	K_M (mM)	k_{cat} (s^{-1})	k_{cat}/K_M ($M^{-1}\cdot s^{-1}$)
Glucose	7.3±0.5	15.5±0.5	(2.1±0.2)×10^3	2.9±0.1	41.4±0.8	(1.5±0.6)×10^4
Xylose	81.3±4.4	3.1±0.1	38±2	105.5±14.9	3.1±0.2	29±10
Mannose	435.6±23.4	9.2±0.2	21±2	(1.4±0.1)×10^3	21.6±0.8	15±10
Gentiobiose		n.m.			n.m.	

n.m. = Not measurable

Table 8. Kinetic parameters of *Ta*GdhA and *Ki*OdhA on carbohydrate substrates. BQ was used as the electron acceptor. All reactions were conducted at pH 5.5.

Substrate	*Ta*GdhA			*Ki*OdhA		
	K_M (mM)	k_{cat} (s^{-1})	k_{cat}/K_M ($M^{-1}\cdot s^{-1}$)	K_M (mM)	k_{cat} (s^{-1})	k_{cat}/K_M ($M^{-1}\cdot s^{-1}$)
Glucose	3.1±0.2	92.5±1.9	(3.0±1.0)×10^4	69.0±11.3	9.0±0.8	130±68
Xylose	1.2±0.1	24.3±0.2	(2.0±0.6)×10^4		n.m.	
Mannose	524.8±19.2	36.4±0.5	69±25		n.m.	
Gentiobiose	1.7±0.8	1.4±0.2	818±290	3.1±0.7	10.7±1.2	(3.5±1.5)×10^3

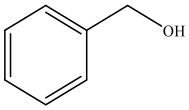
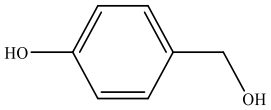
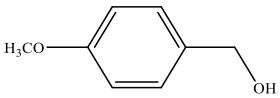
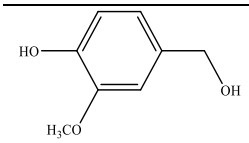
n.m. = Not measurable

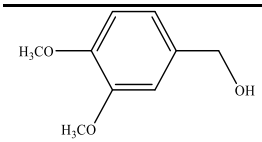
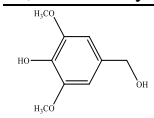
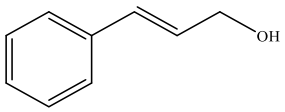
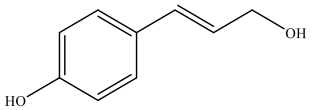
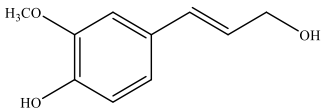
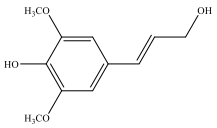
4.4.5 *Ps*AaoA is an aryl alcohol oxidase

UPLC analysis showed that *Ps*AaoA oxidized aryl alcohols to corresponding aldehydes [3]. The conversion rate after 8 h oxidation of each substrate by PsAaoA was calculated with corresponding standards (Table 9). In general, *Ps*AaoA possesses a very board substrate specificity and converted all tested aryl alcohols, and its kinetic constants for oxidizing various aryl alcohols are reported in Table 9. Specifically, *Ps*AaoA exhibited greater kinetic efficiency (k_{cat}/K_M) and better binding affinity (K_M) with monolignols containing hydroxypropylene side chains than with the simple aryl alcohols containing hydroxymethyl side chains. The best kinetic efficiency (2.2×10^5 $M^{-1} \times s^{-1}$) and binding affinity (0.05 mM) were observed on cinnamyl alcohol, followed by coniferyl alcohol and *p*-coumaryl

alcohol, being $3.2 \times 10^4\ M^{-1} \times s^{-1}$, 0.14 mM and $2.1 \times 10^4\ M^{-1} \times s^{-1}$, 0.15 mM, respectively. In contrast, the kinetic efficiency with simple aryl alcohols was at the level of hundreds $M^{-1} \times s^{-1}$ and the lowest K_M was 0.47 mM for *p*-anisyl alcohol. Consistent with the kinetic analysis, *Ps*AaoA oxidized the cinnamyl alcohol (89%), coniferyl alcohol (84%), and *p*-coumaryl alcohol (74%) more efficiently compared to benzyl alcohol (29%), *p*-anisyl alcohol (64%), 3,4-dimethoxybenzyl alcohol (56%), 4-hydroxy-3-methoxybenzyl alcohol (47%), and 4-hydroxybenzyl alcohol (29%). The highest turnover rate (k_{cat}) was recorded on the benzyl alcohol (12.4 s^{-1}), followed by cinnamyl alcohol (10.5 s^{-1}). The kinetic parameters cannot be measured for 3,5-dimethoxy-4-hydroxybenzyl alcohol and sinapyl alcohol, which carry substituents at three, four, and five position on the benzyl ring. Caffeoyl alcohol and 5-hydroxymethylfurfural were also found to be oxidized by *Ps*AaoA, 19% and 23%, respectively, after 8 h incubation. However, the kinetic parameters were not measurable (data not shown).

Table 9. Kinetic parameters of *Ps*AaoA on aryl alcohols and substrate conversion after 8h incubation. Oxygen was used as the electron acceptor, and catalase was added to remove hydrogen peroxide. The substrate conversion was calculated from the product formation. This table was adapted from [3].

Substrate	K_M (mM)	k_{cat} (s^{-1})	k_{cat}/K_M ($M^{-1} \cdot s^{-1}$)	Conversion rate (%)
 benzyl alcohol	1.6±0.7	12.4±1.5	$(7.8\pm3.7)\times10^3$	29
 4-hydroxybenzyl alcohol	9.9±2.0	2.1±0.2	209±47	29
 *p*-anisyl Alcohol	0.47±0.06	4.7±0.1	$(1.0\pm0.1)\times10^4$	64
 4-hydroxy-3-methoxybenzyl alcohol	8.7±1.6	1.7±0.1	200±40	47

Substrate	K_M (mM)	k_{cat} (s^{-1})	k_{cat}/K_M ($M^{-1}s^{-1}$)	Conversion rate (%)
 3,4-dimethoxybenzyl alcohol	4.0±1.3	1.1±0.1	269±93	56
 3,5-dimethoxy-4-hydroxybenzyl alcohol (Syringyl alcohol)	n.m.	n.m.	n.m.	3
 cinnamyl alcohol	0.05±0.01	10.5±0.4	$(2.2\pm0.4)\times10^5$	89
 *p*-coumaryl alcohol	0.15±0.02	3.3±0.02	$(2.1\pm0.3)\times10^4$	74
 coniferyl alcohol	0.14±0.01	4.7±0.1	$(3.2\pm0.3)\times10^4$	84
 sinapyl alcohol	n.m.	n.m.	n.m.	5

n.m. = Not measurable

4.5 AA3_2s can use phenoxy radical as electron acceptor

The AA3_2s were tested for their ability to use phenoxy radicals as an electron acceptor. The radical that tested in this study was generated from the laccase oxidation of ferulic acid. Without the presence of AA3_2s, the laccase oxidized ferulic acid to radicals, which further polymerized. The disappearance of ferulic acid was observed with the decrease in light absorption at 320 nm, while the formation of dimerized ferulic acid was indicated by the rise of light absorption at 350 nm (Figure 24).

The four active AA3_2s were found to regenerate ferulic acid during the oxidation by laccase at different levels by utilizing the laccase-generated phenoxy radical as an electron acceptor (Figure 24). Around half of the ferulic acid was polymerized with the presence of *Ta*GdhA at a ratio of 1:5 after 1 h reaction (Figure 24A). An increased dosage of *Ta*GdhA at a ratio of 1:250 improved ferulic acid regeneration but only to a minor extent. Conversely, *Ki*OdhA exhibited the highest ferulic acid radical recycling rate, achieving a remarkable 98.7% recycling at a laccase-to-*Ki*OdhA ratio of 1:2 after 1 h reaction (Figure 24B, Table 10).

Interestingly, both oxidases (*Ap*GoxA and *As*AaoA) appeared to inhibit ferulic acid from dimerization (Figure 24C, D). When used at a 1:10 ratio with laccase, *Ap*GoxA and *As*AaoA retained 85.8% and 71.0%, respectively, of ferulic acid after 1 h incubation (Table 10). However, in aerobic conditions, oxygen was used by both oxidases as an electron acceptor, which led to the generation of hydrogen peroxide, which is known to inhibit laccase activity (Milton and Minteer 2014). To mitigate this inhibitory effect, excess catalase was added to the reactions. The inclusion of excess catalase had minimal effects on ferulic acid regeneration for both dehydrogenases (Table 10). When hydrogen peroxide was removed by catalase in reactions involving *Ap*GoxA and *As*AaoA, both oxidases still regenerated 46.4% and 50.7% of the ferulic acid after a 1 h incubation, respectively (Table 10). This suggests that *Ap*GoxA and *As*AaoA can employ phenoxy radicals as electron acceptors under competition with molecular oxygen.

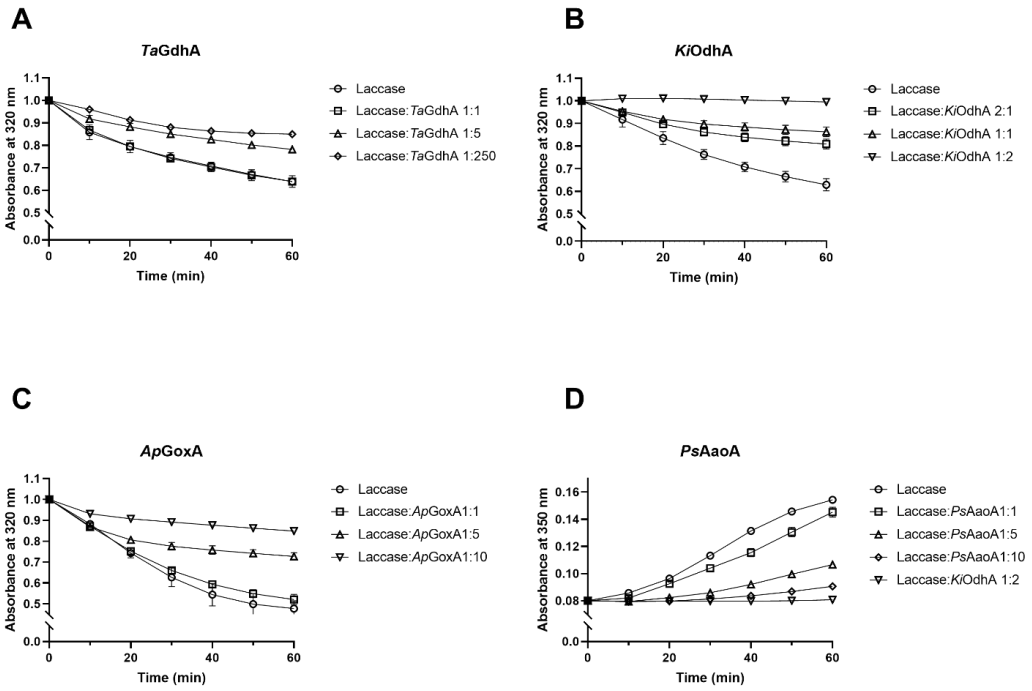


Figure 24. The ability of each AA3_2 to use laccase-generated radicals as an electron acceptor. Reactions with A) *Ta*GdhA, B) *Ki*OdhA, and C) *Ap*GoxA were followed at 320 nm for the depletion of ferulic acid. D) *Ps*AaoA was followed at 350 nm for the formation of ferulic acid dimer. The enzymes were dosed according to the specific activity of laccase and AA3_2s. The specific activity of *Ta*GdhA and *Ki*OdhA using BQ and the specific activity of *Ap*GoxA and *Ps*AaoA employing oxygen were used. This figure was adapted from [3].

Table 10. The percentages of remaining ferulic acid after 1 h reaction with/without the addition of catalase in excess amount. Control reactions did not contain catalase. The table was adapted from [3].

	Remaining ferulic acid (%)			
	Laccase:*Ta*GdhA 1:250	**Laccase:*Ki*OdhA 1:2**	**Laccase:*Ap*GoxA 1:10**	**Laccase:*Ps*AaoA 1:10**
control	58.3 ± 0.7	98.7 ± 2.8	71.0 ± 3.9	85.8 ± 0.2
+catalase	52.7 ± 1.8	97.8 ± 3.1	46.4 ± 4.4	50.7 ± 0.2

5. Discussion

This thesis focused on the discovery and characterization of fungal AA3 enzymes that can be utilized in lignocellulosic biomass upgrades. In the following discussion, the characterized enzymes from this study are directly compared to the other biocatalysts in terms of their ability to oxidize lignocellulosic biomass, especially on the xylooligosaccharides, simple sugars, and aryl alcohols. The discussion starts with *Ab*PDH1 and *Am*PDH1 in their regioselectivity to oxidize diverse xylooligosaccharides, both liner and branched, acid and neutral. Subsequently, the unique xylooligosaccharide oxidizing *Tm*XdhA from AA3_1 is compared with other AA3_1 cellobiose dehydrogenases and the xylooligosaccharide oxidizing enzymes from other AA families. Next, the newly discovered fungal AA3_2s in this thesis is compared to other phylogenetically closely related enzymes. In particular, the recent findings on how the carbohydrate-oxidizing enzymes oxidize oligosaccharides are discussed. Lastly, the potential biological functions of the fungal AA3s are discussed.

5.1 *Ab*PDH1 and *Am*PDH1 for xylooligosaccharide conversion

*Ab*PDH1 and *Am*PDH1, being among the first discovered PDHs, have undergone biochemical characterizations with a wide range of monosaccharides, glucodisaccharides, and selected oligosaccharides (Graf et al. 2017; Morrison et al. 1999; Sygmund et al. 2008; Volc et al. 1997; Volc et al. 1998). This study demonstrates the ability of *Am*PDH1 and *Ab*PDH1 to oxidize the xylooligosaccharides in an effort to guide the synthesis of telechelic building blocks derived from xylan fragments.

In accordance with previous studies on *Ab*PDH1 and *Am*PDH1, which demonstrated their broad specificity with ability to oxidize xylose, xylobiose, glucooligosaccharides, and maltooliogosaccharides, it is no surprise that both *Ab*PDH1 and *Am*PDH1 in this study exhibited oxidation of the tested xylooligosaccharides (Gonaus et al. 2016; Peterbauer and Volc 2010; Rafighi et al. 2019; Sygmund et al. 2008; Volc et al. 1997). Similar to *Am*PDH1 activity towards cellooligosaccharides and maltooligosaccharides, the specific activity of *Ab*PDH1 and *Am*PDH1, as well as the rate of substrate depletion over time, decreased with the increase in degree of polymerization (Gonaus et al. 2016; Rafighi et al. 2019; Sygmund et al. 2008). Additionally, the Ara*f* and MeGlc*p*A substitutions led to a decline in specific activity. The only exception was observed when both *Ab*PDH1 and *Am*PDH1 oxidized A^3X. In both cases, the activities with A^3X were higher than with X_3, and *Ab*PDH1 even oxidized A^3X with more activity than X_2.

*Ab*PDH1 and *Am*PDH1 primarily target the xylosyl residues of xylooligosaccharides at both ends. Previous studies have shown that L-arabinose can be oxidized by *Ac*PDH, *Ax*PDH, *Ab*PDH1, and *Am*PDH1. Among these enzymes, *Ab*PDH1 and *Am*PDH1 exhibited the most catalytic efficiency with L-arabinose (Gonaus et al. 2016; Staudigl et al. 2013; Sygmund et al. 2008). Specifically, *Am*PDH1 was found to oxidize L-arabinose at the C-2 position (Sedmera et al. 2006). However, in the present study, it was observed that *Ab*PDH1 and *Am*PDH1 only oxidized the xyl*p* residues of arabinofuranose-substituted xylooligosaccharides, and no oxidation was detected on the Ara*f* residues. This suggests that the presence of the pyranose ring in the substrate is crucial for the action of these PDH enzymes.

Based on the modeling of xylose in the active site, *Am*PDH1 was found to be able to oxidize at C-1, C-2, C-3, and C-4 of xylose, yet the oxidation at C-1 and C-4 was not experimentally proven (Tan et al. 2013). In this study, it was identified that both *Ab*PDH1 and *Am*PDH1 were able to oxidize at the reducing end C-1 of xylooligosaccharides. Similar oxidation patterns were observed previously for the *Am*PDH1-oxidized cellobiose, maltose, and lactose, where both secondary hydroxyls and the anomeric carbon were oxidized together (Sedmera et al. 2006; Sygmund, Gutmann, et al. 2012; Volc et al. 2004).

*Ab*PDH1 and *Am*PDH1 displayed some differences in their patterns of oxidizing xylooligosaccharides. For instance, the impact of substrate length on activity was more pronounced for *Am*PDH1 than for *Ab*PDH1. Additionally, *Am*PDH1 generated more products with reducing end C-1 being oxidized. A homology model of *Ab*PDH1 based on the solved structure of *Am*PDH1 revealed two amino acid deletions in the loop 1 region, differences in the loop 3 region, and substitution of Phe508 in *Am*PDH1 with the smaller Val505 in *Ab*PDH1 (Gonaus et al. 2016). These differences resulted in variations in the amino acid composition in the loop regions at the entrance of the substrate-binding pocket, which could impact the accessibility of the active site. However, the underlying structural basis for these differences remains to be determined and requires further investigation, including solving the structure of *Ab*PDH1 and studying enzyme-substrate complexes within this enzyme family.

In addition to AA3_2 PDHs, another type of enzyme called pyranose 2-oxidase (POx) from the CAZy AA3_4 subfamily also displayed the ability to introduce a ketone group to carbohydrates (Giffhorn 2000). However, POxs primarily oxidize the monosaccharides, especially glucose, at the C-2 position and, in rare cases, at the C-3 position (Kujawa et al. 2006). When tested with disaccharides such as gentiobiose, isomaltose, and melibiose, only gentiobiose was converted by POxs, but at a much lower

conversion rate than glucose (Giffhorn 2000). Therefore, the unique ability of both PDHs to perform single and double oxidations on various lignocellulosic-derived xylooligosaccharides make them promising for biofuel cell applications and for the generation of telechelic oligosaccharide building blocks (Aumala et al. 2019; Tasca et al. 2010).

5.2 *Tm*XdhA as the first xylooligosaccharide dehydrogenase in AA3_1

The AA3_1 enzymes have previously been extensively studied for their enzymatic functions, and all previously discovered AA3_1 enzymes primarily oxidized cellobiose. Hence, the AA3_1s were also referred to as cellobiose dehydrogenases (Henriksson, Johansson, and Pettersson 2000; Scheiblbrandner and Ludwig 2020). In this thesis, *Tm*XdhA was identified as having preferential activity with xylooligosaccharides, making it the first xylooligosaccharide dehydrogenase discovered in CAZy AA3_1.

All AA3_1 CDHs and *Tm*XdhA share a preference for substrates with a β-(1→4) linkage and specifically oxidize at the reducing end C-1. The predicted model of *Tm*XdhA displayed a similar structure as other CDHs, with a conserved histidine residue that plays a crucial role in the reductive half-reaction (Hallberg et al. 2003). Redirecting the oxidation of *Tm*XdhA to positions other than the reducing end C-1 by methylation at the reducing end C-1 was unsuccessful [2]. *Tm*XdhA activity is reduced for trisaccharides when the non-reducing sugar residue is linked via linkages other than β-(1→4) (e.g., as in the case of A^3X, $U^{4m2}X$, and glucosyl-β-(1→3)-cellobiose). Additionally, the equatorial position of the C-4 hydroxyl group and the unoccupied equatorial position of the C-2 hydroxyl group are also important for *Tm*XdhA activity, similar to other CDHs, including *Mt*CDH and *Pc*CDH from *Phanerochaete chrysosporium* K3 (Hallberg et al. 2003; Kujawa et al. 2006).

AA3_1 enzymes exhibit variations in their ability to oxidize xylooligosaccharides. For example, *Pc*CDH mainly accepts cellobiose but cannot oxidize xylobiose, xylotriose, or Glc–Glc–Xyl, Xyl–Glc–Xyl, and Glc–Xyl–Xyl, while *Nc*CDHs and *Hi*CDHs can oxidize xylobiose but with much lower catalytic efficiency compared to cellobiose (Igarashi et al. 2020; Schou et al. 1998; Sygmund, Kracher, et al. 2012). In contrast, *Tm*XdhA shows greater affinity and catalytic efficiency for xylobiose, xylotriose, and xylotetraose compared to all previously characterized CDHs (Scheiblbrandner and Ludwig 2020). By comparison to the *Tm*XdhA structure model with the crystal structure of *Mt*CDH and *Nc*CDH, a single amino acid residue (T406Q) substitution was identified. This difference affects the hydrogen bonding and the binding of substrates, potentially leading to different substrate preferences (Tan et al. 2015). Additionally, *Tm*XdhA demonstrates a greater affinity and catalytic

efficiency with oligosaccharides with a higher degree of polymerization. It exhibits faster oxidation rates and kinetic efficiency for xylotriose and xylotetraose compared to xylobiose in oligosaccharide mixtures. In the case of cellooligosaccharides, although the catalytic efficiency is similar for cellobiose, cellotriose, and cellotetraose, cellotetraose was oxidized at the highest rate during a 24 h incubation. However, it is important to note that further experimental evidence is required to fully understand and support these observations.

The ability to oxidize oligosaccharides at the reducing end C-1 position has also been found for enzymes belonging to the CAZy AA7 family, yet none of them can beat *Tm*XdhA in the preferential oxidation of xylooligosaccharides. For instance, AA7 oligosaccharide oxidase from *Sarocladium strictum* T1 possesses similar catalytic efficiency with both cellooligosaccharide and xylooligosaccharides (Vuong et al. 2013). Another AA7 oxidase, from *Myceliophthora thermophile* C1, did exhibit a strong substrate preference toward xylooligosaccharides. However, this AA7 xylooligosaccharide oxidase has 10 times lower catalytic efficiency with xylooligosaccharides than *Tm*XdhA (Ferrari et al. 2016). These unique features of *Tm*XdhA make it particularly suitable for applications where the preferential oxidation of xylooligosaccharides, especially those with a high degree of polymerization, is desired.

5.3 Mining for novel activities within AA3_2

5.3.1 Correlation between enzyme specificity and SSN clustering

The CAZy AA3_2 is a large subfamily that contains a wide range of enzymes with diverse enzymatic functionalities. However, previous sequence analysis on the fungal AA3_2s only explored a limited portion of the sequence space, covering less than 25% of the total fungal AA3_2 sequences (Figure 7) (Sützl et al. 2019). To deepen the understanding of the AA3_2 subfamily in regard to enzymatic function, AA3_2s sequences retrieved from JGI, CSFG, and MycoCLAP databases were divided into multiple clusters by SSN analysis at a bit score of 420. By annotating previously characterized AA3_2 enzymes and those characterized in this study within the SSN, a clear correlation between enzymatic function and SSN clustering was observed (Figure 21).

Specifically, aryl-alcohol-oxidizing activities are found within clusters I and IV. Cluster II displays both AAO/AADH and PDH activities, with these two distinct activities located on different sides of the cluster. Similarly, cluster XI contains both ODH and GOx activities, with GOx sequences being somewhat separated from the ODH sequences. Additionally, clusters XII and XXX comprise solely GOx and ODH sequences, respectively. GDHs and ODHs were found within cluster VI. Moreover,

there were clusters that lacked any known activities, indicating the need for biochemical investigation to uncover the enzymatic functions within those clusters. This clustering of AA3_2 sequences using SSN provides valuable guidance for future biochemical characterization of novel AA3_2 sequences.

5.3.2 AA3_2 GDH/GOx activities are not restricted to glucose

Three new carbohydrate-oxidizing enzymes with high activity levels were identified in clusters VI, XI, and XXX with one oxidase (*Ap*GoxA) and two dehydrogenases (*Ta*GdhA and *Ki*OdhA). In general, it was observed that GOxs exhibited a greater preference for glucose over xylose, while GDHs displayed significant activity on both glucose and xylose (Mori et al. 2011; Sode et al. 2017; Sygmund et al. 2011). In this study, *Ta*GdhA showed greater affinity towards xylose (1.2 mM) than glucose (3 mM), making it a promising candidate to be used in biosensors for xylose detection. However, some engineering effort is required since *Ta*GdhA reacts equally well to glucose. The threonine or serine residue (Thr110) present in *An*GOx and *Pc*GOx (PDB 1GPE) forms a hydrogen bond with the C6 of glucose, whereas *Ta*GdhA and *Af*GDH have an alanine in the same position, possibly contributing to their relaxed substrate preferences (Wohlfahrt et al. 1999; Yoshida et al. 2015).

In addition to their activity with glucose and monosaccharides, *Ta*GdhA, *Ap*GoxA, and *Ki*OdhA all showed activity with disaccharides, especially on gentiobiose with β-(1→6) linkage. Among them, *Ki*OdhA showed a clear preference for gentiobiose, with more affinity (3.1 mM) and better catalytic efficiency (3500 $M^{-1}s^{-1}$). This represents the highest gentiobiose oxidizing activity reported to date, being at least 15 times higher in affinity and 5 times higher in catalytic efficiency than *Um*GDH (86 mM, 122 $M^{-1}s^{-1}$) (Reyre et al. 2022; Wijayanti et al. 2021). Such oligosaccharide-oxidizing activities only gained attention since the re-annotation of *Tc*ODH (*Pc*GDH), which was found to oxidize β-(1→3) linked laminaribiose the best (Cerutti et al. 2021). Unlike *Af*GDH or *An*GOx, which bind with the enzyme via hydrogen bonds, *Tc*ODH mainly binds laminaribiose via sugar–aromatic stacking (Cerutti et al. 2021). The superposition of *Tc*ODH and the structure model of *Ki*OdhA revealed the conservation of two aromatic amino acid residues (Phe416/Phe435 and Trp430/Trp448) to be responsible for this stacking force [3]. These residues are highly conserved within clusters XI, XII, and XXX, with the latter also being conserved in cluster VI, suggesting the importance of sugar–aromatic stacking in all enzymes within these clusters [3]. A phenylalanine (Phe421) shifted around 17 Å towards the active site upon the binding of laminaribiose to establish the sugar–aromatic stacking towards the non-reducing glucosyl moiety for *Tc*ODH. However, *Ki*OdhA, *Ta*GdhA, *Ap*GoxA are occupied by glycine in the same position, which potentially explains their lower activity

with laminaribiose. Further structural analysis of *Ki*OdhA would be valuable for understanding its binding with gentiobiose. Other than laminaribiose and gentiobiose, *Tv*GDH, recently identified and located within cluster VI, was found to oxidize maltose at the highest rates, indicating novel oligosaccharide-oxidizing activities are still to be discovered within AA3_2 (Wijayanti et al. 2021).

5.3.3 *Ps*AaoA oxidized a wide range of aryl alcohols

In this study, a new aryl-alcohol-oxidizing enzyme (*Ps*AaoA) was identified. Unlike *Pe*AAOx, which comprises three aromatic residues (Tyr92, Phe397 and Phe501) that restrict access to the inner cavity of the active site, *Ps*AaoA does not share conservation in all three positions [3] (Fernández et al. 2009). Specifically, in *Ps*AaoA, Tyr92 is replaced by an aromatic phenylalanine (Phe122), Phe397 is replaced by a hydrophobic alanine (Ala427), and Phe501 is replaced by an aromatic tryptophan (Trp529). The hydrophobic alanine provided *Ps*AaoA an opener inner cavity on the active side compared to *Pe*AAOx.

*Ps*AaoA displayed activity with a comparatively broad range of electron donors and electron acceptors, displaying its best catalytic efficiency when using oxygen as an electron acceptor with cinnamyl alcohol, coniferyl alcohol, and *p*-coumaryl alcohol. This is in contrast to *Pe*AAOx, which showed minimal activity with cinnamyl alcohol but demonstrated more activity with simple aryl alcohols containing hydroxymethyl side chains (Ferreira et al. 2005). The greater activities of *Ps*AaoA compared to *Pe*AAOx when acting on monolignols with hydroxypropylene side chains could potentially be attributed to the modification of the substrate access tunnel. This modification is a result of the substitution of an amino acid residue, Phe397 (*Pe*AAOx), with Ala427 (*Ps*AaoA). This is supported by the activities measured for *Mt*AAOx and *Cc*AAOx, where the equivalent position is occupied by alanine and leucine, respectively. In both of these cases, the enzymes exhibited more activities when acting on substrates with hydroxypropylene side chains than on substrates with hydroxymethyl side chains (Kadowaki et al. 2020; Tamaru et al. 2018).

Two aromatic residues, Phe122 and Trp529 in *Ps*AaoA, are expected to be crucial for its reactivity with oxygen. Both *As*AadhA and *As*AadhB have hydrophobic residues (Gly123 and Met556 for AsAadhA, and Gly144 and Ala576 for AsAadhB) in the same position, which do not show any activity with oxygen. Furthermore, site-direct mutagenesis of Phe501 to alanine in *Pe*AAOx significantly reduced *Pe*AAOx's reactivity with oxygen (Hernández-Ortega et al. 2011).

The FDCA, a promising green chemical building block, can be produced from 5-HMF by the oxidation of AAO and UPO (Dijkman and Fraaije 2014; Kamm 2007). *Ps*AaoA oxidized 5-HMF; however, its activity on furan was not comparable to the activity on aromatic alcohols [3].

5.4 The biological function of AA3s

So far, the biological role of AA3s have been associated with the promotion of lignocellulose decay. Specifically, AA3 oxidases are responsible for continuous generation of H_2O_2, while AA3 dehydrogenases serve to reduce quinones to hydroquinone. The generation of H_2O_2 can directly drive/fuel other ligninolytic peroxidases, while hydroquinone can act as a mediator to drive the same reactions (Garajova et al. 2016; Kracher et al. 2016; Mathieu et al. 2016; Piumi et al. 2014; Sygmund et al. 2011).

However, it needs to be noted that the classification of oxidase and dehydrogenase are artificial. Dehydrogenases may exhibit trace oxygen activity, and oxidases can utilize quinones as electron acceptors. Previous research has showed that AA3_2 dehydrogenases can utilize the phenoxy radicals as electron acceptors (Mathieu et al. 2016; Piumi et al. 2014). In this study, it was found that not only the AA3_2 dehydrogenases with limited or no activity on oxygen can recycle the phenolic radicals, but the AA3_2 oxidases (*Ap*GoxA and *As*AaoA) can also participate in this radical redox cycle in aerobic environments.

This versatile characteristic of AA3 enzymes enables them to contribute to lignocellulose degradation through multiple pathways. For instance, when oxygen is utilized in nature as the electron acceptor, the H_2O_2 is produced to drive peroxidase and LPMOs or to start a Fenton reaction for the oxidative degradation of lignocellulose (Ferreira et al. 2023; Garajova et al. 2016; Kracher et al. 2016; Mathieu et al. 2016; Piumi et al. 2014; Sygmund et al. 2011). Furthermore, during plant defense events, when cytotoxic quinones are produced, AA3 enzymes can detoxify them to hydroquinones. These hydroquinones can then act as redox mediators for electron transfer to LPMOs. Additionally, under conditions of high oxidative stress, AA3 enzymes may reduce phenoxy radicals, thereby preventing potential radical cytotoxicity and the repolymerization of semiquinones and other lignin radicals (Gómez-Toribio et al. 2009). These results highlight the multifunctionality of AA3_2 enzymes and their involvement in multiple stages of lignocellulose degradation.

The gentiobiose/laminaribiose activity from the AA3_2s suggests a potential role of AA3_2s in modification of the fungal cell wall, as the fungal cell wall consists of β-(1→3)/(1→6) linked glucans. Notably, *Ki*OdhA comprises an N-terminal, CBM13, which has a β-trefoil fold structure and is

primarily associated with GH16 enzymes that display endo-β-1,3-glucanase and chitin-β-1,6-glucanosyltransferase activity (Fujimoto 2013; Viborg et al. 2019). The high efficiency of *Ki*OdhA in eliminating phenoxy radicals also suggests that it might prevent radical damage to the fungus itself. Such an idea is supported by the recent finding on a maize pathogen, *Ustilago maydis*, where the co-expression of a GH hydrolyzing β-(1→3)/(1→6) glucans, and *Um*GDH oxidizing both laminaribiose and gentiobiose was found (Reyre et al. 2022). As most previous research of AA3_2s only focused on their role in interplay with other enzymes in plant cell wall degradation, research effort is needed to study their linkage with fungal cell walls to fully uncover their physiological role.

6. Future research aspects

Utilizing and engineering the characterized AA3 oxidoreductases for biotechnological applications

The discovery and characterization of AA3 enzymes expanded the biocatalytic tool box for future biotechnological applications. For instance, the ability of *Ab*PDH1 and *Am*PDH1 to oxidize at both ends of xylooligosaccharides opens up new applications for PDHs in transforming underutilized xylan streams into telechelic molecules suitable for polymerization. AA3 oxidoreductases are known for their ability to boost LPMO for oxidative degradation of cellulose (Garajova et al. 2016; Kracher et al. 2016). The discovery of *Tm*XdhA adds potential to fuel xylan-active LPMOs for oxidative degradation of xylan. Furthermore, the carbohydrate-oxidizing AA3_2s all displayed activity with disaccharides such as laminaribiose and gentiobiose. Therefore, it is worth investigating their activity with β-glucan and oligomers with β-(1→3) and (1→6) linkages. In addition to these carbohydrate-active oxidoreductases, *Ps*AaoA displayed activity on HMF, making it a potential candidate to produce FDCA, so that it is a promising candidate to produce FDCA, a green chemical to substitute terephthalic acid for the production of bio-based plastics. Moreover, the ability of *Ps*AaoA to oxidize monolignols to monolignaldehydes provides the possibility of utilizing such enzymes in tailoring the structure of artificial lignin. However, it is worth noting that further efforts to engineer these AA3 enzymes for improved activity, thermostability, and specificity could yield valuable benefits.

Characterize fungal AA3 proteins from unknow SSN clusters

Within the SSN of fungal AA3_2 enzymes constructed in this research, a correlation between enzymatic function and sequence similarity was observed. Nevertheless, out of the top 15 clusters, only six clusters contain enzymes that have undergone biochemical characterization. This highlights the importance of exploring the uncharacterized clusters, aiming to not only fill existing knowledge gaps but also to uncover potential novel enzymatic activities.

CAZy AA3s from bacteria and plants

While fungal AA3 enzymes have been studied over the years, the exploration of bacterial AA3 enzymes is a relatively recent development and growing area of interest. Bacterial AA3s (*As*POx and *Ka*POx) were initially identified from soil bacteria, specifically *Arthrobacter siccitolerans,* now reclassified as *Pseudoarthrobacter siccitolerans*, and *Kitasatospora aureofaciens.* These enzymes, recognized as pyranose 2-oxidases, possess the ability to oxidize aldopyranose sugars at the C-2 position, resulting in the formation of 2-keto sugars (Herzog et al. 2019; Mendes et al. 2016). Interestingly, *Ka*POx was found to be secreted to the extracellular space and is believed to provide H_2O_2 to fuel peroxidase for lignin depolymerization (Virginia and Peterbauer 2023). More recently, two additional FAD-dependent bacterial enzymes (*Mt*CarA from *Microbacterium trichothecenolyticum* and *Sc*POx from *Streptomyces canus*) have been characterized from the same sequence space. Both of these enzymes have demonstrated substantial activity with C-glycosides and/or O-glycosides (Kostelac et al. 2023; Kumano 2021). *As*POx was also renamed to *Ps*G3Ox, as it was found to have a 50,000-fold greater specificity on mangiferin (a C-glycoside) than D-glucose (Taborda et al. 2023). These findings suggest that there is potentially a wealth of untapped enzymatic function awaiting diversity within bacterial AA3s.

Surprisingly, very little attention has been devoted to AA3 enzymes derived from plants. In 2014, the establishment of the plant CAZyme database (https://bcb.unl.edu/plantcazyme/) brought to light a substantial collection of 43,790 plant CAZymes, among which 539 AA3 proteins were identified, originating from 35 different plant species (Ekstrom et al. 2014). It is important to note that these plant AA3 proteins are phylogenetically distinct from fungal AA3s, preventing their classification in any established subgroups. The expression and characterization of these plant AA3 enzymes hold the potential to enhance our comprehension of their evolutionary significance and elucidate their physiological role within plants. To date, only two plant AA3 enzymes have undergone biochemical characterization. *At*Fao3 from *Arabidopsis thaliana* was identified as a fatty alcohol oxidase, capable of oxidizing 1-dodecanol *in vitro* (Cheng et al. 2004). Reverse genetic studies involving *At*Fao3 and its homologs have demonstrated morphological alterations related to stem cuticular waxes (Yang et al. 2022). Another notable plant AA3 enzyme, *Nm*Nec3 from *Nesocodon mauritianus*, was found to facilitate the oxidation of sinapyl alcohol to sinapyl aldehyde, a crucial step in the formation of the red pigment found in nectar (Roy et al. 2021). The characterization of plant-derived AA3 enzymes could unravel new insights into plant biology and their applications.

Gentiobiose as a plant signaling molecule

The previous study on AA3_2 GOx/GDH mainly focused on their activities towards monosaccharides. However, in this study, the newly characterized AA3_2 carbohydrate-active oxidoreductases consistently displayed activity with gentiobiose, a disaccharide composed of β-D-Glcp-(1→6)-D-Glc. Disaccharides and oligosaccharides act as signal molecules to regulate plant metabolism. For instance, glucose oligosaccharides derived from pathogen invasion can serve as signals to trigger plant defense responses (Shibuya and Minami, 2001). Additionally, certain β-(1→3) glycans, such as laminarin, have been observed to induce defense responses in various plants, including rice, tobacco, alfalfa, and grapevine (Trouvelot et al. 2014). Gentiobiose and gentiooligosaccharides are abundantly present in some Gentianaceae species, and studies have revealed their involvement in regulating bud dormancy in the herbaceous perennial *Gentiana* (Takahashi et al. 2014). Although gentiobiose is relatively uncommon in plants outside the Gentianaceae family, gentiobiose have been reported to expedite fruit ripening in tomato and capsicum (Aizat et al, 2014; Dumville and Fry, 2003).

Further illustration of the biological role of AA3s in regulating reactive oxygen species (ROS)

Maintaining an optimal level of oxidative stress is important for the normal functioning of fungi. ROS such as H_2O_2 and hydroxyl radicals, while cytotoxic at excessive levels, play critical roles in fungal extracellular redox reactions (Bissaro et al. 2018). The fine-tuning of extracellular ROS is achieved through a complex interplay between ROS producing and eliminating enzymes (Mattila et al. 2022). Fungal AA3 enzymes have traditionally been classified as ROS producers; they can supply H_2O_2 and hydroquinones, which support ROS-quenching enzymes like LPMO (Garajova et al. 2016). At the same time, certain AA3 enzymes, such as AAOs and GOxs, generate H_2O_2, which, in turn, triggers the Fenton reaction, leading to the production of hydroxyl radicals (Sützl et al. 2018).

In this study, AA3_2 oxidases and dehydrogenases were identified that have the ability to utilize phenolic radicals as electron acceptors. This finding has led to the hypothesis that these enzymes may also function as ROS utilizers under conditions of high oxidative stress, potentially reducing free radicals, including hydroxyl radicals. However, to validate this hypothesis, further research is required, including transcriptome and secretome analysis of fungi subjected to varying levels of oxidative stress and *in vitro* experiments designed to investigate the ability of fungal AA3s to utilize free radicals as electron acceptors.

7. Conclusions

This study focused on the discovery and characterization of fungal carbohydrate oxidoreductases from the CAZyme families AA3_1 and AA3_2. Through successful biochemical characterization, this research provided valuable insights into the potential applications of these enzymes and enhanced our understanding of their potential physiological roles. The key findings and outputs of this study are as follows:

A method to study the regioselectivity of PDHs was developed based on chromatographic and mass spectra analyses after sodium borodeuteride reduction of the reaction products. With this method, AA3_2 *Ab*PDH1 and *Am*PDH1 were found to exhibit varying degrees of oxidation for xylooligosaccharides, and the oxidation by both PDHs was restricted to both terminal xylosyl units.

This study successfully expressed and characterized an AA3_1 enzyme, *Tm*XdhA, which showed a unique preference for xylooligosaccharides, making it the first discovered xylooligosaccharide dehydrogenase within the AA3_1 family. Structural predictions highlighted the potential role of amino acid Q406 in promoting the binding between *Tm*XdhA and the xylopyranosyl-reducing end moiety.

By applying an SSN analysis at a cutoff of e^{-420}, the distinct enzymatic functions within AA3_2 were grouped into separate clusters. This functional clustering of AA3_2s was confirmed by biochemical characterization of AA3_2 proteins and will serve as a basis for predicting enzymatic functions of putative AA3_2 sequences.

Three highly active carbohydrate-oxidizing AA3_2s (*Ap*GoxA, *Ta*GdhA, and *Ki*OdhA) and one aryl alcohol-oxidizing AA3_2 enzyme (*Ps*AaoA) were biochemically characterized. Although new enzymes to target xylooligosaccharides were not found, the characterized AA3_2s displayed potential to oxidize oligosaccharides with β-(1→6) linkage. In particular, the discovery of *Ki*OdhA as a gentiobiose dehydrogenase suggests its potential role in modifying fungal cell walls, a biological role that has thus far been largely overlooked. Notably, the ability of AA3_2s to utilize diverse electron acceptors, including phenoxy radicals, sheds light on their functional versatility.

References

Adams, E. C., Mast, R. L., & Free, A. H. (1960). Specificity of glucose oxidase. *Archives of Biochemistry and Biophysics*, *91*(2), 230–234. https://doi.org/10.1016/0003-9861(60)90495-1

Adler, P. R., Del Grosso, S. J., & Parton, W. J. (2007). Life-cycle assessment of net greenhouse-gas flux for bioenergy cropping systems. *Ecological Applications*, *17*(3), 675–691. https://doi.org/10.1890/05-2018

Aizat, W. M., Dias, D. A., Stangoulis, J. C. R., Able, J. A., Roessner, U., & Able, A. J. (2014). Metabolomics of capsicum ripening reveals modification of the ethylene related-pathway and carbon metabolism. *Postharvest Biology and Technology*, *89*, 19–31. https://doi.org/10.1016/j.postharvbio.2013.11.004

Alonso, S., Rendueles, M., & Díaz, M. (2013). Bio-production of lactobionic acid: Current status, applications and future prospects. *Biotechnology Advances*, *31*(8), 1275–1291. https://doi.org/10.1016/j.biotechadv.2013.04.010

Andberg, M., Mollerup, F., Parikka, K., Koutaniemi, S., Boer, H., Jovonen, M., Master, E., Tenkanen, M., & Kruus, K. (2017). A novel *Colletotrichum graminicola* raffinose oxidase in the AA5 family. *Applied and Environmental Microbiology*, *83*(20), 1–17. https://doi.org/10.1128/AEM .01383-17

Aumala, V., Mollerup, F., Jurak, E., Blume, F., Karppi, J., Koistinen, A. E., Schuiten, E., Voß, M., Bornscheuer, U., Deska, J., & Master, E. R. (2019). Biocatalytic production of amino carbohydrates through oxidoreductase and transaminase cascades. *ChemSusChem*, *12*(4), 848–857. https://doi.org/10.1002/cssc.201802580

Baminger, U., Ludwig, R., Galhaup, C., Leitner, C., Kulbe, K. D., & Haltrich, D. (2001). Continuous enzymatic regeneration of redox mediators used in biotransformation reactions employing flavoproteins. *Journal of Molecular Catalysis - B Enzymatic*, *11*(4–6), 541–550. https://doi.org/10.1016/S1381-1177(00)00034-5

Baminger, U., Subramaniam, S. S., Renganathan, V., & Haltrich, D. (2001). Purification and characterization of cellobiose dehydrogenase from the plant pathogen *Sclerotium (Athelia) rolfsii*. *Applied and Environmental Microbiology*, *67*(4), 1766–1774. https://doi.org/10.1128/AEM.67.4.1766

Bannwarth, M., Bastian, S., Heckmann-Pohl, D., Giffhorn, F., & Schulz, G. E. (2004). Crystal structure of pyranose 2-oxidase from the white-rot fungus *Peniophora sp. Biochemistry*, *43*(37), 11683–11690. https://doi.org/10.1021/bi048609q

Barnett, J. R., & Bonham, V. A. (2004). Cellulose microfibril angle in the cell wall of wood fibres. *Biological Reviews of the Cambridge Philosophical Society*, *79*(2), 461–472. https://doi.org/10.1017/S1464793103006377

Bissaro, B., Røhr, Å. K., Müller, G., Chylenski, P., Skaugen, M., Forsberg, Z., Horn, S. J., Vaaje-Kolstad, G., & Eijsink, V. G. H. (2017). Oxidative cleavage of polysaccharides by monocopper enzymes depends on H_2O_2. *Nature Chemical Biology*, *13*(10), 1123–1128. https://doi.org/10.1038/nchembio.2470

Bissaro, B., Várnai, A., Røhr, Å. K., & Eijsink, V. G. H. (2018). Oxidoreductases and reactive oxygen species in conversion of lignocellulosic biomass. *Microbiology and Molecular Biology Reviews*, *82*(4).

https://doi.org/10.1128/MMBR.00029-18

Bragd, P. L., Besemer, A. C., & Van Bekkum, H. (2000). Bromide-free TEMPO-mediated oxidation of primary alcohol groups in starch and methyl alpha-D-glucopyranoside. *Carbohydrate Research*, *328*(3), 355–363. https://doi.org/10.1016/S0008-6215(00)00109-9

Carpita, N. C., Ralph, J., & McCann, M. C. (2015). The cell wall. In *Biochemistry and molecular biology of plants* (Second Edi, pp. 45–110).

Carro, J., Martínez-Júlvez, M., Medina, M., Martínez, A. T., & Ferreira, P. (2017). Protein dynamics promote hydride tunnelling in substrate oxidation by aryl-alcohol oxidase. *Physical Chemistry Chemical Physics*, *19*(42), 28666–28675. https://doi.org/10.1039/c7cp05904c

Cavener, D. R. (1992). GMC oxidoreductases. A newly defined family of homologous proteins with diverse catalytic activities. *Journal of Molecular Biology*, *223*(3), 811–814. https://doi.org/10.1016/0022-2836(92)90992-S

Cerutti, G., Gugole, E., Montemiglio, L. C., Turbé-Doan, A., Chena, D., Navarro, D., Lomascolo, A., Piumi, F., Exertier, C., Freda, I., Vallone, B., Record, E., Savino, C., & Sciara, G. (2021). Crystal structure and functional characterization of an oligosaccharide dehydrogenase from *Pycnoporus cinnabarinus* provides insights into fungal breakdown of lignocellulose. *Biotechnology for Biofuels*, *14*(1), 1–18. https://doi.org/10.1186/s13068-021-02003-y

Chen, C., Chen, J., Geng, Z., Wang, M., Liu, N., & Li, D. (2018). Regioselectivity of oxidation by a polysaccharide monooxygenase from *Chaetomium thermophilum*. *Biotechnology for Biofuels*, *11*(1), 1–16. https://doi.org/10.1186/S13068-018-1156-2

Cheng, Q., Liu, H.-T., Bombelli, P., Smith, A., & Slabas, A. R. (2004). Functional identification of *At*Fao3, a membrane bound long chain alcohol oxidase in *Arabidopsis thaliana*. *FEBS Letters*, *574*(1–3), 62–68. https://doi.org/10.1016/J.FEBSLET.2004.07.086

Chung, H., Yang, J. E., Ha, J. Y., Chae, T. U., Shin, J. H., Gustavsson, M., & Lee, S. Y. (2015). Bio-based production of monomers and polymers by metabolically engineered microorganisms. *Current Opinion in Biotechnology*, *36*, 73–84. https://doi.org/10.1016/J.COPBIO.2015.07.003

Cinquin, P., Gondran, C., Giroud, F., Mazabrard, S., Pellissier, A., Boucher, F., Alcaraz, J. P., Gorgy, K., Lenouvel, F., Mathé, S., Porcu, P., & Cosnier, S. (2010). A glucose biofuel cell implanted in rats. *PLoS ONE*, *5*(5), 1–7. https://doi.org/10.1371/journal.pone.0010476

Cleveland, M. E., Mathieu, Y., Ribeaucourt, D., Haon, M., Mulyk, P., Hein, J. E., Lafond, M., Berrin, J. G., & Brumer, H. (2021). A survey of substrate specificity among Auxiliary Activity Family 5 copper radical oxidases. *Cellular and Molecular Life Sciences*, *78*(24), 8187–8208. https://doi.org/10.1007/s00018-021-03981-w

Cleveland, M., Lafond, M., Xia, F. R., Chung, R., Mulyk, P., Hein, J. E., & Brumer, H. (2021). Two *Fusarium* copper radical oxidases with high activity on aryl alcohols. *Biotechnology for Biofuels*, *14*(1), 1–19. https://doi.org/10.1186/s13068-021-01984-0

Couturier, M., Mathieu, Y., Li, A., Navarro, D., Drula, E., Haon, M., Grisel, S., Ludwig, R., & Berrin, J. G.

(2016). Characterization of a new aryl-alcohol oxidase secreted by the phytopathogenic fungus *Ustilago maydis*. *Applied Microbiology and Biotechnology*, *100*(2), 697–706. https://doi.org/10.1007/S00253-015-7021-3

Couturier, M., Navarro, D., Olivé, C., Chevret, D., Haon, M., Favel, A., Lesage-Meessen, L., Henrissat, B., Coutinho, P. M., & Berrin, J. G. (2012). Post-genomic analyses of fungal lignocellulosic biomass degradation reveal the unexpected potential of the plant pathogen *Ustilago maydis*. *BMC Genomics*, *13*(1), 1–14. https://doi.org/10.1186/1471-2164-13-57

Cragg, S. M., Beckham, G. T., Bruce, N. C., Bugg, T. D. H., Distel, D. L., Dupree, P., Etxabe, A. G., Goodell, B. S., Jellison, J., McGeehan, J. E., McQueen-Mason, S. J., Schnorr, K., Walton, P. H., Watts, J. E. M., & Zimmer, M. (2015). Lignocellulose degradation mechanisms across the Tree of Life. *Current Opinion in Chemical Biology*, *29*, 108–119. https://doi.org/10.1016/J.CBPA.2015.10.018

Crooks, G., Hon, G., Chandonia, J., & Brenner, S. (2004). NCBI GenBank FTP Site\nWebLogo: a sequence logo generator. *Genome Research*, *14*, 1188–1190. https://doi.org/10.1101/gr.849004.1

Del Río, J., Rencoret, J., Gutiérrez, A., Elder, T., Kim, H., & Ralph, J. (2020). Lignin Monomers from beyond the Canonical Monolignol Biosynthetic Pathway: Another Brick in the Wall. *ACS Sustainable Chemistry & Engineering*, *8*(13), 4997-5012. https://doi.org/10.1021/acssuschemeng.0c01109

Demerec, M., Adelberg, E. A., Clark, A. J., & Hartman, P. E. (1966). A proposal for a uniform nomenclature in bacterial genetics. *Genetics*, *54*, 61–76. https://doi.org/10.1093/genetics/54.1.61

Dijkman, W. P., & Fraaije, M. W. (2014). Discovery and characterization of a 5-hydroxymethylfurfural oxidase from *Methylovorus sp.* strain MP688. *Applied and Environmental Microbiology*, *80*(3), 1082–1090. https://doi.org/10.1128/AEM.03740-13

Drula, E., Garron, M. L., Dogan, S., Lombard, V., Henrissat, B., & Terrapon, N. (2022). The carbohydrate-active enzyme database: functions and literature. *Nucleic Acids Research*, *50*(D1), D571–D577. https://doi.org/10.1093/NAR/GKAB1045

Duarte, J. C., Costa-Ferreira, M., & Sena-Martins, G. (1999). Cellobiose dehydrogenase. Possible roles and importance for pulp and paper biotechnology. *Bioresource Technology*, *68*(1), 43–48. https://doi.org/10.1016/S0960-8524(98)00080-7

Dumville, J. C., & Fry, S. C. (2003). Gentiobiose: A novel oligosaccharin in ripening tomato fruit. *Planta*, *216*(3), 484–495. https://doi.org/10.1007/s00425-002-0869-3

Edgar, R. C. (2022). Muscle5: High-accuracy alignment ensembles enable unbiased assessments of sequence homology and phylogeny. *Nature Communications*, *13*(1), 0–1. https://doi.org/10.1038/s41467-022-34630-w

Ekstrom, A., Taujale, R., McGinn, N., & Yin, Y. (2014). PlantCAZyme: A database for plant carbohydrate-active enzymes. *Database*, *2014*, 79. https://doi.org/10.1093/DATABASE/BAU079

Eriksson, K.-E. L., Blanchette, R. A., & Ander, P. (1990). Morphological aspects of wood degradation by fungi and bacteria. In *Microbial and enzymatic degradtion of wood and wood components* (pp. 1–74).

Farmer, V. C., Henderson, M. E., & Russell, J. D. (1960). Aromatic-alcohol-oxidase activity in the growth

medium of *Polystictus versicolor*. *The Biochemical Journal*, *74*(2), 257–262. https://doi.org/10.1042/bj0740257

Felice, A. K. G., Schuster, C., Kadek, A., Filandr, F., Laurent, C. V. F. P., Scheiblbrandner, S., Schwaiger, L., Schachinger, F., Kracher, D., Sygmund, C., Man, P., Halada, P., Oostenbrink, C., & Ludwig, R. (2021). Chimeric cellobiose dehydrogenases reveal the function of cytochrome domain mobility for the electron transfer to lytic polysaccharide monooxygenase. *ACS Catalysis*, *11*, 517–532. https://doi.org/10.1021/acscatal.0c05294

Fernández, I. S., Ruíz-Duẽas, F. J., Santillana, E., Ferreira, P., Martínez, M. J., Martínez, Á. T., & Romero, A. (2009). Novel structural features in the GMC family of oxidoreductases revealed by the crystal structure of fungal aryl-alcohol oxidase. *Acta Crystallographica Section D: Biological Crystallography*, *65*(11), 1196–1205. https://doi.org/10.1107/S0907444909035860

Ferrari, A. R., Rozeboom, H. J., Dobruchowska, J. M., Van Leeuwen, S. S., Vugts, A. S. C., Koetsier, M. J., Visser, J., Fraaije, M. W., & Hart, G. (2016). Discovery of a xylooligosaccharide oxidase from *myceliophthora thermophila* C1. *Journal of Biological Chemistry*, *291*(45), 23709–23718. https://doi.org/10.1074/jbc.M116.741173

Ferreira, P., Carro, J., Balcells, B., Martinez, A. T., & Serrano, A. (2023). Expanding the physiological role of aryl-alcohol flavooxidases. *Applied and Environmental Microbiology*, *89*(5). https://doi.org/doi.org/10.1128/aem.01844-22

Ferreira, P., Hernández-Ortega, A., Herguedas, B., Rencoret, J., Gutiérrez, A., Martínez, M. J., Jiménez-Barbero, J., Medina, M., & Martínez, Á. T. (2010). Kinetic and chemical characterization of aldehyde oxidation by fungal aryl-alcohol oxidase. *Biochemical Journal*, *425*(3), 585–593. https://doi.org/10.1042/BJ20091499

Ferreira, P., Medina, M., Guillén, F., Martínez, M. J., Van Berkel, W. J. H., & Martínez, Á. T. (2005). Spectral and catalytic properties of aryl-alcohol oxidase, a fungal flavoenzyme acting on polyunsaturated alcohols. *Biochemical Journal*, *389*(3), 731–738. https://doi.org/10.1042/BJ20041903

Ferreira, P., Ruiz-Dueñas, F. J., Martínez, M. J., Van Berkel, W. J. H., & Martínez, A. T. (2006). Site-directed mutagenesis of selected residues at the active site of aryl-alcohol oxidase, an H_2O_2-producing ligninolytic enzyme. *FEBS Journal*, *273*(21), 4878–4888. https://doi.org/10.1111/j.1742-4658.2006.05488.x

Froidevaux, V., Negrell, C., Caillol, S., Pascault, J. P., & Boutevin, B. (2016). Biobased amines: From synthesis to polymers; present and future. *Chemical Reviews*, *116*(22), 14181–14224. https://doi.org/10.1021/ACS.CHEMREV.6B00486

Fujimoto, Z. (2013). Structure and function of carbohydrate-binding module families 13 and 42 of glycoside hydrolases, comprising a β-trefoil fold. *Bioscience, Biotechnology and Biochemistry*, *77*(7), 1363–1371. https://doi.org/10.1271/bbb.130183

Galperin, I., Javeed, A., Luig, H., Lochnit, G., & Rühl, M. (2016). An aryl-alcohol oxidase of *Pleurotus sapidus*: heterologous expression, characterization, and application in a 2-enzyme system. *Applied Microbiology and Biotechnology*, *100*(18), 8021–8030. https://doi.org/10.1007/s00253-016-7567-8

Garajova, S., Mathieu, Y., Beccia, M. R., Bennati-Granier, C., Biaso, F., Fanuel, M., Ropartz, D., Guigliarelli, B., Record, E., Rogniaux, H., Henrissat, B., & Berrin, J. G. (2016). Single-domain flavoenzymes trigger lytic polysaccharide monooxygenases for oxidative degradation of cellulose. *Scientific Reports*, *6*(28276). https://doi.org/10.1038/srep28276

Giffhorn, F. (2000). Fungal pyranose oxidases: Occurrence, properties and biotechnical applications in carbohydrate chemistry. *Applied Microbiology and Biotechnology*, *54*(6), 727–740. https://doi.org/10.1007/s002530000446

Glushkov, D. O., Nyashina, G. S., Anand, R., & Strizhak, P. A. (2021). Composition of gas produced from the direct combustion and pyrolysis of biomass. *Process Safety and Environmental Protection*, *156*, 43–56. https://doi.org/10.1016/j.psep.2021.09.039

Godjevargova, T., Dayal, R., & Turmanova, S. (2004). Gluconic acid production in bioreactor with immobilized glucose oxidase plus catalase on polymer membrane adjacent to anion-exchange membrane. *Macromolecular Bioscience*, *4*(10), 950–956. https://doi.org/10.1002/MABI.200400058

Gómez-Toribio, V., García-Martín, A. B., Martínez, M. J., Martínez, Á. T., & Guillén, F. (2009). Induction of extracellular hydroxyl radical production by white-rot fungi through quinone redox cycling. *Applied and Environmental Microbiology*, *75*(12), 3944–3953. https://doi.org/10.1128/AEM.02137-08

Gonaus, C., Kittl, R., Sygmund, C., Haltrich, D., & Peterbauer, C. (2016). Transcription analysis of pyranose dehydrogenase from the basidiomycete *Agaricus bisporus* and characterization of the recombinantly expressed enzyme. *Protein Expression and Purification*, *119*, 36–44. https://doi.org/10.1016/J.PEP.2015.11.003

Graf, M. M. H., Bren, U., Haltrich, D., & Oostenbrink, C. (2013). Molecular dynamics simulations give insight into D-glucose dioxidation at C2 and C3 by *Agaricus meleagris* pyranose dehydrogenase. *Journal of Computer-Aided Molecular Design*, *27*(4), 295–304. https://doi.org/10.1007/s10822-013-9645-7

Graf, M. M. H., Sucharitakul, J., Bren, U., Chu, D. B., Koellensperger, G., Hann, S., Furtmüller, P. G., Obinger, C., Peterbauer, C. K., Oostenbrink, C., Chaiyen, P., & Haltrich, D. (2015). Reaction of pyranose dehydrogenase from *Agaricus meleagris* with its carbohydrate substrates. *FEBS Journal*, *282*(21), 4218–4241. https://doi.org/10.1111/febs.13417

Graf, M. M. H., Weber, S., Kracher, D., Kittl, R., Sygmund, C., Ludwig, R., Peterbauer, C., & Haltrich, D. (2017). Characterization of three pyranose dehydrogenase isoforms from the litter-decomposing basidiomycete *Leucoagaricus meleagris* (syn. *Agaricus meleagris*). *Applied Microbiology and Biotechnology*, *101*(7), 2879–2891. https://doi.org/10.1007/s00253-016-8051-1

Guillén, F., Martínez, A. T., & Martínez, M. J. (1992). Substrate specificity and properties of the aryl-alcohol oxidase from the ligninolytic fungus *Pleurotus eryngii*. *European Journal of Biochemistry*, *209*(2), 603–611. https://doi.org/10.1111/j.1432-1033.1992.tb17326.x

Haddad Momeni, M., Fredslund, F., Bissaro, B., Raji, O., Vuong, T. V., Meier, S., Nielsen, T. S., Lombard, V., Guigliarelli, B., Biaso, F., Haon, M., Grisel, S., Henrissat, B., Welner, D. H., Master, E. R., Berrin, J.-G., & Abou Hachem, M. (2021). Discovery of fungal oligosaccharide-oxidising flavo-enzymes with

previously unknown substrates, redox-activity profiles and interplay with LPMOs. *Nature Communications*, *12*(2132). https://doi.org/10.1038/s41467-021-22372-0

Hallberg, B. M., Henriksson, G., Pettersson, G., & Divne, C. (2002). Crystal structure of the flavoprotein domain of the extracellular flavocytochrome cellobiose dehydrogenase. *Journal of Molecular Biology*, *315*(3), 421–434. https://doi.org/10.1006/jmbi.2001.5246

Hallberg, B. M., Henriksson, G., Pettersson, G., Vasella, A., & Divne, C. (2003). Mechanism of the reductive half-reaction in cellobiose dehydrogenase. *Journal of Biological Chemistry*, *278*(9), 7160–7166. https://doi.org/10.1074/jbc.M210961200

Harmsen, P. F. H., Hackmann, M. M., & Bos, H. L. (2014). Green building blocks for bio-based plastics. *Biofuels, Bioproducts and Biorefining*, *8*(3), 306–324. https://doi.org/10.1002/BBB.1468

Harreither, W., Sygmund, C., Augustin, M., Narciso, M., Rabinovich, M. L., Gorton, L., Haltrich, D., & Ludwig, R. (2011). Catalytic properties and classification of cellobiose dehydrogenases from ascomycetes. *Applied and Environmental Microbiology*, *77*(5), 1804–1815. https://doi.org/10.1128/AEM.02052-10

Harris, P. J., & Stone, B. A. (2008). Chemistry and molecular organization of plant cell walls. In *Biomass Recalcitrance: Deconstructing the Plant Cell Wall for Bioenergy* (pp. 61–93). John Wiley & Sons, Ltd. https://doi.org/10.1002/9781444305418.CH4

Hayes, D. J. (2009). An examination of biorefining processes, catalysts and challenges. *Catalysis Today*, *145*(1–2), 138–151. https://doi.org/10.1016/j.cattod.2008.04.017

Henriksson, G., Johansson, G., & Pettersson, G. (2000). A critical review of cellobiose dehydrogenases. *Journal of Biotechnology*, *78*(2), 93–113. https://doi.org/10.1016/S0168-1656(00)00206-6

Henriksson, G., Pettersson, G., Johansson, G., Ruiz, A., & Uzcategui, E. (1991). Cellobiose oxidase from *Phanerochaete chrysosporium* can be cleaved by papain into two domains. *European Journal of Biochemistry*, *196*, 101–106. https://doi.org/10.1111/j.1432-1033.1991.tb15791.x

Hernández-Ortega, A., Ferreira, P., Merino, P., Medina, M., Guallar, V., & Martínez, A. T. (2012). Stereoselective hydride transfer by aryl-alcohol oxidase, a member of the GMC superfamily. *ChemBioChem*, *13*(3), 427–435. https://doi.org/10.1002/CBIC.201100709

Hernández-Ortega, A., Lucas, F., Ferreira, P., Medina, M., Guallar, V., & Martínez, A. T. (2011). Modulating O_2 reactivity in a fungal flavoenzyme: Involvement of aryl-alcohol oxidase Phe-501 contiguous to catalytic histidine. *Journal of Biological Chemistry*, *286*(47), 41105–41114. https://doi.org/10.1074/jbc.M111.282467

Herzog, P. L., Sützl, L., Eisenhut, B., Maresch, D., Haltrich, D., Obinger, C., & Peterbauer, C. K. (2019). Versatile oxidase and dehydrogenase activities of bacterial pyranose 2-oxidase facilitate redox cycling with manganese peroxidase *in vitro*. *Applied and Environmental Microbiology*, *85*(13). https://doi.org/10.1128/AEM.00390-19

Houfani, A. A., Anders, N., Spiess, A. C., Baldrian, P., & Benallaoua, S. (2020). Insights from enzymatic degradation of cellulose and hemicellulose to fermentable sugars– a review. *Biomass and Bioenergy*,

134(January), 105481. https://doi.org/10.1016/j.biombioe.2020.105481

Hüttner, S., Várnai, A., Petrovic, D. M., Bach, C. X., Dang Thi, K. A., Cu Nguyen, T., Eijsink, C. G. H., Larsbrink, J., & Olsson, L. (2019). Specific xylan activity revealed for AA9 lytic polysaccharide monooxygenases of the thermophilic fungus *Malbranchea cinnamonea* by functional characterization. *Applied and Environmental Microbiology*, *85*(23), 1–13. https://doi.org/10.1128/AEM .01408-19

Igarashi, K., Kaneko, S., Kitaoka, M., & Samejima, M. (2020). Effect of C-6 methylol groups on substrate recognition of glucose/xylose mixed oligosaccharides by cellobiose dehydrogenase from the Basidiomycete *Phanerochaete chrysosporium*. *Journal of Applied Glycoscience*, *67*, 51–57. https://doi.org/10.5458/jag.jag.jag-2020_0003

Igarashi, K., Samejima, M., & Eriksson, K. E. L. (1998). Cellobiose dehydrogenase enhances *Phanerochaete chrysosporium* cellobiohydrolase I activity by relieving product inhibition. *European Journal of Biochemistry*, *253*(1), 101–106. https://doi.org/10.1046/J.1432-1327.1998.2530101.X

Ishii, T. (1997). Structure and functions of feruloylated polysaccharides. *Plant Science*, *127*(2), 111–127. https://doi.org/10.1016/S0168-9452(97)00130-1

Ivnitski, D., Branch, B., Atanassov, P., & Apblett, C. (2006). Glucose oxidase anode for biofuel cell based on direct electron transfer. *Electrochemistry Communications*, *8*(8), 1204–1210. https://doi.org/10.1016/j.elecom.2006.05.024

Jankowski, N., Koschorreck, K., & Urlacher, V. B. (2020). High-level expression of aryl-alcohol oxidase 2 from *Pleurotus eryngii* in *Pichia pastoris* for production of fragrances and bioactive precursors. *Applied Microbiology and Biotechnology*, *104*(21), 9205–9218. https://doi.org/10.1007/s00253-020-10878-4

Johnson, R. K., Zink-Sharp, A., Renneckar, S. H., & Glasser, W. G. (2009). A new bio-based nanocomposite: Fibrillated TEMPO-oxidized celluloses in hydroxypropylcellulose matrix. *Cellulose*, *16*(2), 227–238. https://doi.org/10.1007/S10570-008-9269-6

Jumper, J., Evans, R., Pritzel, A., Green, T., Figurnov, M., Ronneberger, O., Tunyasuvunakool, K., Bates, R., Žídek, A., Potapenko, A., Bridgland, A., Meyer, C., Kohl, S. A. A., Ballard, A. J., Cowie, A., Romera-Paredes, B., Nikolov, S., Jain, R., Adler, J., … Hassabis, D. (2021). Highly accurate protein structure prediction with AlphaFold. *Nature*, *596*, 583–589. https://doi.org/10.1038/s41586-021-03819-2

Juvonen, M., Kotiranta, M., Jokela, J., Tuomainen, P., & Tenkanen, M. (2019). Identification and structural analysis of cereal arabinoxylan-derived oligosaccharides by negative ionization HILIC-MS/MS. *Food Chemistry*, *275*, 176–185. https://doi.org/10.1016/J.FOODCHEM.2018.09.074

Kadowaki, M. A. S., Higasi, P. M. R., de Godoy, M. O., de Araújo, E. A., Godoy, A. S., Prade, R. A., & Polikarpov, I. (2020). Enzymatic versatility and thermostability of a new aryl-alcohol oxidase from *Thermothelomyces thermophilus* M77. *Biochimica et Biophysica Acta - General Subjects*, *1864*(10), 129681. https://doi.org/10.1016/j.bbagen.2020.129681

Kamm, B. (2007). Production of platform chemicals and synthesis gas from biomass. *Angewandte Chemie - International Edition*, *46*(27), 5056–5058. https://doi.org/10.1002/anie.200604514

Kilpeläinen, P., Kitunen, V., Pranovich, A., Ilvesniemi, H., & Willför, S. (2013). Pressurized hot water flow-

through extraction of birch sawdust with acetate pH buffer. *BioResources*, *8*(4), 5202–5218.

Kisonen, V., Prakobna, K., Xu, C., Salminen, A., Mikkonen, K. S., Valtakari, D., Eklund, P., Seppälä, J., Tenkanen, M., & Willför, S. (2015). Composite films of nanofibrillated cellulose and O-acetyl galactoglucomannan (GGM) coated with succinic esters of GGM showing potential as barrier material in food packaging. *Journal of Materials Science*, *50*(8), 3189–3199. https://doi.org/10.1007/S10853-015-8882-7

Koch, C., Neumann, P., Valerius, O., Feussner, I., & Ficner, R. (2016). Crystal structure of alcohol oxidase from *Pichia pastoris*. *PLoS ONE*, *11*(2), 1–17. https://doi.org/10.1371/journal.pone.0149846

Kostelac, A., Sützl, L., Puc, J., Furlanetto, V., Divne, C., & Haltrich, D. (2022). Biochemical characterization of pyranose oxidase from *Streptomyces canus*—Towards a better understanding of pyranose oxidase homologues in bacteria. *International Journal of Molecular Sciences*, *23*(21). https://doi.org/10.3390/ijms232113595

Koukol, O. (2016). *Myriococcum* revisited: a revision of an overlooked fungal genus. *Plant Systematics and Evolution*, *302*, 957–969. https://doi.org/10.1007/s00606-016-1310-x

Kracher, D., Forsberg, Z., Bissaro, B., Gangl, S., Preims, M., Sygmund, C., Eijsink, V. G. H., & Ludwig, R. (2020). Polysaccharide oxidation by lytic polysaccharide monooxygenase is enhanced by engineered cellobiose dehydrogenase. *FEBS Journal*, *287*, 897–908. https://doi.org/10.1111/febs.15067

Kracher, D., & Ludwig, R. (2016). Cellobiose dehydrogenase: An essential enzyme for lignocellulose degradation in nature - A review. *Journal of Land Management, Food and Environment*, *67*(3), 145–163. https://doi.org/10.1515/boku-2016-0013

Kracher, D., Scheiblbrandner, S., Felice, A. K. G., Breslmayr, E., Preims, M., Ludwicka, K., Haltrich, D., Eijsink, V. G. H., & Ludwig, R. (2016). Extracellular electron transfer systems fuel cellulose oxidative degradation. *Science*, *352*(6289), 1098–1101. https://doi.org/10.1126/science.aaf3165

Kristiansen, K. A., Potthast, A., & Christensen, B. E. (2010). Periodate oxidation of polysaccharides for modification of chemical and physical properties. *Carbohydrate Research*, *345*(10), 1264–1271. https://doi.org/10.1016/J.CARRES.2010.02.011

Krondorfer, I., Lipp, K., Brugger, D., Staudigl, P., Sygmund, C., Haltrich, D., & Peterbauer, C. K. (2014). Engineering of pyranose dehydrogenase for increased oxygen reactivity. *PLOS ONE*, *9*(3), e91145. https://doi.org/10.1371/JOURNAL.PONE.0091145

Kujawa, M., Ebner, H., Leitner, C., Hallberg, B. M., Prongjit, M., Sucharitakul, J., Ludwig, R., Rudsander, U., Peterbauer, C., Chaiyen, P., Haltrich, D., & Divne, C. (2006). Structural basis for substrate binding and regioselective oxidation of monosaccharides at C3 by pyranose 2-oxidase. *Journal of Biological Chemistry*, *281*(46), 35104–35115. https://doi.org/10.1074/jbc.M604718200

Kumar, A., Adamopoulos, S., Jones, D., & Amiandamhen, S. O. (2021). Forest biomass availability and utilization potential in Sweden: A review. *Waste and Biomass Valorization*, *12*(1), 65–80. https://doi.org/10.1007/s12649-020-00947-0

Kumano, T., Hori, S., Watanabe, S., Terashita, Y., Yu, H. Y., Hashimoto, Y., Senda, T., Senda, M., &

Kobayashi, M. (2021). FAD-dependent C-glycoside–metabolizing enzymes in microorganisms: Screening, characterization, and crystal structure analysis. *Proceedings of the National Academy of Sciences of the United States of America*, *118*(40). https://doi.org/10.1073/pnas.2106580118

Laurent, C. V. F. P., Breslmayr, E., Tunega, D., Ludwig, R., & Oostenbrink, C. (2019). Interaction between cellobiose dehydrogenase and lytic polysaccharide monooxygenase. *Biochemistry*, *58*(9), 1226–1235. https://doi.org/10.1021/ACS.BIOCHEM.8B01178

Leppänen, A. S., Xu, C., Parikka, K., Eklund, P., Sjöholm, R., Brumer, H., Tenkanen, M., & Willför, S. (2014). Targeted allylation and propargylation of galactose-containing polysaccharides in water. *Carbohydrate Polymers*, *100*, 46–54. https://doi.org/10.1016/j.carbpol.2012.11.053

Loew, N., Tsugawa, W., Nagae, D., Kojima, K., & Sode, K. (2017). Mediator preference of two different FAD-dependent glucose dehydrogenases employed in disposable enzyme glucose sensors. *Sensors (Switzerland)*, *17*(11). https://doi.org/10.3390/s17112636

Lourenco, A., & Pereira, H. (2018). Compositional variability of lignin in biomass. In M. Peletto (Ed.), *Lignin - Trends and Applications* (pp. 65–85). InTech. https://doi.org/10.5772/INTECHOPEN.71210

Ludwig, R., Salamon, A., Varga, J., Zámocky, M., Peterbauer, C. K., Kulbe, K. D., & Haltrich, D. (2004). Characterisation of cellobiose dehydrogenases from the white-rot fungi *Trametes pubescens* and *Trametes villosa*. *Applied Microbiology and Biotechnology*, *64*, 213–222. https://doi.org/10.1007/s00253-003-1501-6

Maischberger, T., Nguyen, T. H., Sukyai, P., Kittl, R., Riva, S., Ludwig, R., & Haltrich, D. (2008). Production of lactose-free galacto-oligosaccharide mixtures: comparison of two cellobiose dehydrogenases for the selective oxidation of lactose to lactobionic acid. *Carbohydrate Research*, *343*(12), 2140–2147. https://doi.org/10.1016/j.carres.2008.01.040

Martínez, A. T., Ruiz-Dueñas, F. J., Camarero, S., Serrano, A., Linde, D., Lund, H., Vind, J., Tovborg, M., Herold-Majumdar, O. M., Hofrichter, M., Liers, C., Ullrich, R., Scheibner, K., Sannia, G., Piscitelli, A., Pezzella, C., Sener, M. E., Kılıç, S., van Berkel, W. J. H., … Alcalde, M. (2017). Oxidoreductases on their way to industrial biotransformations. *Biotechnology Advances*, *35*(6), 815–831. https://doi.org/10.1016/j.biotechadv.2017.06.003

Mathieu, Y., Piumi, F., Valli, R., Aramburu, J. C., Ferreira, P., Faulds, C. B., & Record, E. (2016). Activities of secreted aryl alcohol quinone oxidoreductases from *Pycnoporus cinnabarinus* provide insights into fungal degradation of plant biomass. *Applied and Environmental Microbiology*, *82*(8), 2411–2423. https://doi.org/10.1128/AEM.03761-15

Mattevi, A. (2006). To be or not to be an oxidase: challenging the oxygen reactivity of flavoenzymes. *Trends in Biochemical Sciences*, *31*(5), 276–283. https://doi.org/10.1016/j.tibs.2006.03.003

Mattila, H., Österman-Udd, J., Mali, T., & Lundell, T. (2022). Basidiomycota fungi and ROS: Genomic perspective on key enzymes involved in generation and mitigation of reactive oxygen species. *Frontiers in Fungal Biology*, *3*(March). https://doi.org/10.3389/ffunb.2022.837605

Mendes, S., Banha, C., Madeira, J., Santos, D., Miranda, V., Manzanera, M., Ventura, M. R., van Berkel, W.

J. H., & Martins, L. O. (2016). Characterization of a bacterial pyranose 2-oxidase from *Arthrobacter siccitolerans*. *Journal of Molecular Catalysis B: Enzymatic*, *133*, S34–S43. https://doi.org/10.1016/j.molcatb.2016.11.005

Mikkonen, K. S., Parikka, K., Ghafar, A., & Tenkanen, M. (2013). Prospects of polysaccharide aerogels as modern advanced food materials. *Trends in Food Science and Technology*, *34*(2), 124–136. https://doi.org/10.1016/j.tifs.2013.10.003

Milton, R. D., Giroud, F., Thumser, A. E., Minteer, S. D., & Slade, R. C. T. (2013). Hydrogen peroxide produced by glucose oxidase affects the performance of laccase cathodes in glucose/oxygen fuel cells: FAD-dependent glucose dehydrogenase as a replacement. *Physical Chemistry Chemical Physics*, *15*(44), 19371–19379. https://doi.org/10.1039/c3cp53351d

Milton, R. D., & Minteer, S. D. (2014). Investigating the reversible inhibition model of laccase by hydrogen peroxide for bioelectrocatalytic applications. *Journal of The Electrochemical Society, 161*(13), H3011–H3014. https://doi.org/10.1149/2.0031413jes

Miyauchi, S., Navarro, D., Grisel, S., Chevret, D., Berrin, J. G., & Rosso, M. N. (2017). The integrative omics of white-rot fungus *Pycnoporus coccineus* reveals co-regulated CAZymes for orchestrated lignocellulose breakdown. *PLOS ONE*, *12*(4), e0175528. https://doi.org/10.1371/JOURNAL.PONE.0175528

Mori, K., Nakajima, M., Kojima, K., Murakami, K., Ferri, S., & Sode, K. (2011). Screening of Aspergillus-derived FAD-glucose dehydrogenases from fungal genome database. *Biotechnology Letters*, *33*(11), 2255–2263. https://doi.org/10.1007/s10529-011-0694-5

Morrison, S. C., Wood, D. A., & Wood, P. M. (1999). Characterization of a glucose 3-dehydrogenase from the cultivated mushroom (*Agaricus bisporus*). *Applied Microbiology and Biotechnology*, *51*(1), 58–64. https://doi.org/10.1007/S002530051363

Muller, D. (1929). A new enzyme, glucoxidase II. *Kgl. Landbauhochschule, Kopenhagen. Biochem. Z*, *205*, 111–143.

Nekiunaite, L., Arntzen, M., Svensson, B., Vaaje-Kolstad, G., & Hachem, M. A. (2016). Lytic polysaccharide monooxygenases and other oxidative enzymes are abundantly secreted by *Aspergillus nidulans* grown on different starches. *Biotechnology for Biofuels*, *9*(1), 1–16. https://doi.org/10.1186/S13068-016-0604-0

Nyanhongo, G. S., Thallinger, B., & Guebitz, G. M. (2017). Cellobiose dehydrogenase-based biomedical applications. *Process Biochemistry*, *59*, 37–45. https://doi.org/10.1016/j.procbio.2017.02.023

Okolie, J. A., Mukherjee, A., Nanda, S., Dalai, A. K., & Kozinski, J. A. (2021). Next-generation biofuels and platform biochemicals from lignocellulosic biomass. *International Journal of Energy Research*, *45*(10), 14145–14169. https://doi.org/10.1002/er.6697

Oliveira, D. M., Mota, T. R., Salatta, F. V., Marchiosi, R., Gomez, L. D., McQueen-Mason, S. J., Ferrarese-Filho, O., & dos Santos, W. D. (2019). Designing xylan for improved sustainable biofuel production. *Plant Biotechnology Journal*, *17*(12), 2225–2227. https://doi.org/10.1111/PBI.13150

Parikka, K., Leppänen, A. S., Pitkänen, L., Reunanen, M., Willför, S., & Tenkanen, M. (2010). Oxidation of

polysaccharides by galactose oxidase. *Journal of Agricultural and Food Chemistry*, *58*(1), 262–271. https://doi.org/10.1021/jf902930t

Parikka, K., Nikkilä, I., Pitkänen, L., Ghafar, A., Sontag-Strohm, T., & Tenkanen, M. (2017). Laccase/TEMPO oxidation in the production of mechanically strong arabinoxylan and glucomannan aerogels. *Carbohydrate Polymers*, *175*, 377–386. https://doi.org/10.1016/J.CARBPOL.2017.07.074

Pazur, J. H., & Kleppe, K. (1964). The oxidation of glucose and related compounds by glucose oxidase from *Aspergillus niger*. *Biochemistry*, *3*(4), 578–583. https://doi.org/10.1021/bi00892a018

Peterbauer, C. K. (2020). Pyranose dehydrogenases: Rare enzymes for electrochemistry and biocatalysis. In *Bioelectrochemistry* (Vol. 132, p. 107399). Elsevier. https://doi.org/10.1016/j.bioelechem.2019.107399

Peterbauer, C. K., & Volc, J. (2010). Pyranose dehydrogenases: Biochemical features and perspectives of technological applications. *Applied Microbiology and Biotechnology*, *85*(4), 837–848. https://doi.org/10.1007/s00253-009-2226-y

Piumi, F., Levasseur, A., Navarro, D., Zhou, S., Mathieu, Y., Ropartz, D., Ludwig, R., Faulds, C. B., & Record, E. (2014). A novel glucose dehydrogenase from the white-rot fungus *Pycnoporus cinnabarinus*: production in *Aspergillus niger* and physicochemical characterization of the recombinant enzyme. *Applied Microbiology and Biotechnology*, *98*(24), 10105–10118. https://doi.org/10.1007/s00253-014-5891-4

Pricelius, S., Ludwig, R., Lant, N., Haltrich, D., & Guebitz, G. M. (2009). Substrate specificity of *Myriococcum thermophilum* cellobiose dehydrogenase on mono-, oligo-, and polysaccharides related to in situ production of H_2O_2. *Applied Microbiology and Biotechnology*, *85*, 75–83. https://doi.org/10.1007/s00253-009-2062-0

Rafighi, P., Bollella, P., Pankratova, G., Peterbauer, C. K., Conghaile, P., Leech, D., Haghighi, B., & Gorton, L. (2019). Substrate preference pattern of *Agaricus meleagris* pyranose dehydrogenase evaluated through bioelectrochemical flow injection amperometry. *ChemElectroChem*, *6*(3), 801–809. https://doi.org/10.1002/CELC.201801194

Ranji-Burachaloo, H., Reyhani, A., Gurr, P. A., Dunstan, D. E., & Qiao, G. G. (2019). Combined Fenton and starvation therapies using hemoglobin and glucose oxidase. *Nanoscale*, *11*(12), 5705–5716. https://doi.org/10.1039/c8nr09107b

Rastall, R. A., & Maitin, V. (2002). Prebiotics and synbiotics: towards the next generation. *Current Opinion in Biotechnology*, *13*(5), 490–496. https://doi.org/10.1016/S0958-1669(02)00365-8

Reyre, J. Lou, Grisel, S., Haon, M., Navarro, D., Ropartz, D., Le Gall, S., Record, E., Sciara, G., Tranquet, O., Berrin, J. G., & Bissaro, B. (2022). The Maize pathogen *Ustilago maydis* secretes glycoside hydrolases and carbohydrate oxidases directed toward components of the fungal cell wall. *Applied and Environmental Microbiology*, *88*(23), e0158122. https://doi.org/10.1128/aem.01581-22

Roy, R., Moreno, N., Brockman, S. A., Kostanecki, A., Zambre, A., Holl, C., Solhaug, E. M., Minami, A., Snell-Rood, E. C., Hampton, M., Bee, M. A., Chiari, Y., Hegeman, A. D., & Carter, C. J. (2022). Convergent evolution of a blood-red nectar pigment in vertebrate-pollinated flowers. *Proceedings of the*

National Academy of Sciences of the United States of America, *119*(5). https://doi.org/10.1073/pnas.2114420119

Rytioja, J., Hildén, K., Yuzon, J., Hatakka, A., de Vries, R. P., & Mäkelä, M. R. (2014). Plant-polysaccharide-degrading enzymes from Basidiomycetes. *Microbiology and Molecular Biology Reviews*, *78*(4), 614–649. https://doi.org/10.1128/mmbr.00035-14

Savino, S., & Fraaije, M. W. (2021). The vast repertoire of carbohydrate oxidases: An overview. *Biotechnology Advances*, *51*, 107634. https://doi.org/10.1016/j.biotechadv.2020.107634

Scheiblbrandner, S., & Ludwig, R. (2020). Cellobiose dehydrogenase: Bioelectrochemical insights and applications. *Bioelectrochemistry*, *131*, 107345. https://doi.org/10.1016/j.bioelechem.2019.107345

Scheller, H. V., & Ulvskov, P. (2010). Hemicelluloses. *Annual Review of Plant Biology*, *61*, 263–289. https://doi.org/10.1146/annurev-arplant-042809-112315

Schmer, M. R., Vogel, K. P., Mitchell, R. B., & Perrin, R. K. (2008). Net energy of cellulosic ethanol from switchgrass. *Proceedings of the National Academy of Sciences of the United States of America*, *105*(2), 464–469. https://doi.org/10.1073/PNAS.0704767105

Schou, C., Christensen, M. H., & Schülein, M. (1998). Characterization of a cellobiose dehydrogenase from *Humicola insolens*. *Biochemical Journal*, *330*, 565–571. https://doi.org/10.1042/bj3300565

Sedmera, P., Halada, P., Kubátová, E., Haltrich, D., Přikrylová, V., & Volc, J. (2006). New biotransformations of some reducing sugars to the corresponding (di)dehydro(glycosyl) aldoses or aldonic acids using fungal pyranose dehydrogenase. *Journal of Molecular Catalysis B: Enzymatic*, *41*(1–2), 32–42. https://doi.org/10.1016/j.molcatb.2006.04.004

Sedmera, P., Halada, P., Peterbauer, C., & Volc, J. (2004). A new enzyme catalysis: 3,4-dioxidation of some aryl β-D-glycopyranosides by fungal pyranose dehydrogenase. *Tetrahedron Letters*, *45*(47), 8677–8680. https://doi.org/10.1016/j.tetlet.2004.09.149

Semashko, T. V., Mikhailova, R. V., & Eremin, A. N. (2003). Extracellular glucose oxidase of *Penicillium funiculosum* 46.1. *Applied Biochemistry and Microbiology*, *39*(4), 368–374. https://doi.org/10.1023/A:1024512316571

Serrano, A., Calviño, E., Carro, J., Sánchez-Ruiz, M. I., Cañada, F. J., & Martínez, A. T. (2019). Complete oxidation of hydroxymethylfurfural to furandicarboxylic acid by aryl-alcohol oxidase. *Biotechnology for Biofuels*, *12*(1), 1–12. https://doi.org/10.1186/s13068-019-1555-z

Shaghaleh, H., Xu, X., & Wang, S. (2018). Current progress in production of biopolymeric materials based on cellulose, cellulose nanofibers, and cellulose derivatives. *RSC Advances*, *8*(2), 825–842. https://doi.org/10.1039/c7ra11157f

Shibuya, N., & Minami, E. (2001). Oligosaccharide signalling for defence responses in plant. *Physiological and Molecular Plant Pathology*, *59*(5), 223–233. https://doi.org/10.1006/pmpp.2001.0364

Singh, R. S., Singh, T., & Pandey, A. (2019). Microbial enzymes—An overview. In *Advances in Enzyme Technology* (1st ed., pp. 1–40). Elsevier. https://doi.org/10.1016/B978-0-444-64114-4.00001-7

Sode, K., Loew, N., Ohnishi, Y., Tsuruta, H., Mori, K., Kojima, K., Tsugawa, W., LaBelle, J. T., & Klonoff,

D. C. (2017). Novel fungal FAD glucose dehydrogenase derived from *Aspergillus niger* for glucose enzyme sensor strips. *Biosensors and Bioelectronics*, *87*, 305–311. https://doi.org/10.1016/j.bios.2016.08.053

Staudigl, P., Krondorfer, I., Haltrich, D., & Peterbauer, C. K. (2013). Pyranose dehydrogenase from *Agaricus campestris* and *Agaricus xanthoderma*: Characterization and applications in carbohydrate conversions. *Biomolecules*, *3*(3), 535–552. https://doi.org/10.3390/biom3030535

Steenwyk, J. L., Buida, T. J., Li, Y., Shen, X. X., & Rokas, A. (2020). ClipKIT: A multiple sequence alignment trimming software for accurate phylogenomic inference. *PLoS Biology*, *18*(12), 1–17. https://doi.org/10.1371/journal.pbio.3001007

Sulej, J., Osińska-Jaroszuk, M., Jaszek, M., Grąz, M., Kutkowska, J., Pawlik, A., Chudzik, A., & Bancerz, R. (2019). Antimicrobial and antioxidative potential of free and immobilised cellobiose dehydrogenase isolated from wood degrading fungi. *Fungal Biology*, *123*(12), 875–886. https://doi.org/10.1016/J.FUNBIO.2019.09.007

Sun, P., Laurent, C. V. F. P., Boerkamp, V. J. P., van Erven, G., Ludwig, R., van Berkel, W. J. H., & Kabel, M. A. (2022). Regioselective C4 and C6 double oxidation of cellulose by lytic polysaccharide monooxygenases. *ChemSusChem*, *15*(2), e202102203. https://doi.org/10.1002/CSSC.202102203

Sun, W., Shen, Y. H., Qi, D. W., Xiang, Z. H., & Zhang, Z. (2011). Molecular cloning and characterization of Ecdysone oxidase and 3-dehydroecdysone-3α-reductase involved in the ecdysone inactivation pathway of silkworm, *Bombyx mori*. *International Journal of Biological Sciences*, *8*(1), 125–138. https://doi.org/10.7150/ijbs.8.125

Sun, Y., & Cheng, J. (2002). Hydrolysis of lignocellulosic materials for ethanol production: A review. *Bioresource Technology*, *83*(1), 1–11. https://doi.org/10.1016/S0960-8524(01)00212-7

Sützl, L., Foley, G., Gillam, E. M. J., Bodén, M., & Haltrich, D. (2019). The GMC superfamily of oxidoreductases revisited: Analysis and evolution of fungal GMC oxidoreductases. *Biotechnology for Biofuels*, *12*, 118. https://doi.org/10.1186/s13068-019-1457-0

Sützl, L., Laurent, C. V. F. P., Abrera, A. T., Schütz, G., Ludwig, R., & Haltrich, D. (2018). Multiplicity of enzymatic functions in the CAZy AA3 family. *Applied Microbiology and Biotechnology*, *102*, 2477–2492. https://doi.org/10.1007/s00253-018-8784-0

Sygmund, C., Gutmann, A., Krondorfer, I., Kujawa, M., Glieder, A., Pscheidt, B., Haltrich, D., Peterbauer, C., & Kittl, R. (2012). Simple and efficient expression of *Agaricus meleagris* pyranose dehydrogenase in *Pichia pastoris*. *Applied Microbiology and Biotechnology*, *94*(3), 695–704. https://doi.org/10.1007/s00253-011-3667-7

Sygmund, C., Kittl, R., Volc, J., Halada, P., Kubátová, E., Haltrich, D., & Peterbauer, C. K. (2008). Characterization of pyranose dehydrogenase from *Agaricus meleagris* and its application in the C-2 specific conversion of D-galactose. *Journal of Biotechnology*, *133*(3), 334–342. https://doi.org/10.1016/J.JBIOTEC.2007.10.013

Sygmund, C., Klausberger, M., Felice, A. K., & Ludwig, R. (2011). Reduction of quinones and phenoxy

radicals by extracellular glucose dehydrogenase from *Glomerella cingulata* suggests a role in plant pathogenicity. *Microbiology*, *157*(11), 3203–3212. https://doi.org/10.1099/mic.0.051904-0

Sygmund, C., Kracher, D., Scheiblbrandner, S., Zahma, K., Felice, A. K. G., Harreither, W., Kittl, R., & Ludwig, R. (2012). Characterization of the two *Neurospora crassa* cellobiose dehydrogenases and their connection to oxidative cellulose degradation. *Applied and Environmental Microbiology*, *78*(17), 6161–6171. https://doi.org/10.1128/AEM.01503-12

Taborda, A., Frazão, T., Rodrigues, M. V., Fernández-Luengo, X., Sancho, F., Lucas3, M. F., Frazão, C., Ventura, M. R., Masgrau, L., Borges, P. T., & Martins, L. O. (2023). Mechanistic insights into glycoside 3-oxidases involved in C-glycoside metabolism in soil microorganisms. *PREPRINT*, 1–31. https://doi.org/10.21203/rs.3.rs-2662172/v1

Takahashi, H., Imamura, T., Konno, N., Takeda, T., Fujita, K., Konishi, T., Nishihara, M., & Uchimiya, H. (2014). The gentio-oligosaccharide gentiobiose functions in the modulation of bud dormancy in the Herbaceous perennial Gentiana. *Plant Cell*, *26*(10), 3949–3963. https://doi.org/10.1105/tpc.114.131631

Tamaru, Y., Umezawa, K., & Yoshida, M. (2018). Characterization of an aryl-alcohol oxidase from the plant saprophytic basidiomycete *Coprinopsis cinerea* with broad substrate specificity against aromatic alcohols. *Biotechnology Letters*, *40*(7), 1077–1086. https://doi.org/10.1007/s10529-018-2534-3

Tan, T. C., Kracher, D., Gandini, R., Sygmund, C., Kittl, R., Haltrich, D., Hällberg, B. M., Ludwig, R., & Divne, C. (2015). Structural basis for cellobiose dehydrogenase action during oxidative cellulose degradation. *Nature Communications*, *6*(May), 7524. https://doi.org/10.1038/ncomms8542

Tan, T. C., Spadiut, O., Wongnate, T., Sucharitakul, J., Krondorfer, I., Sygmund, C., Haltrich, D., Chaiyen, P., Peterbauer, C. K., & Divne, C. (2013). The 1.6 Å crystal structure of pyranose dehydrogenase from *Agaricus meleagris* rationalizes substrate specificity and reveals a flavin intermediate. *PLoS ONE*, *8*(1). https://doi.org/10.1371/journal.pone.0053567

Tasca, F., Gorton, L., Kujawa, M., Patel, I., Harreither, W., Peterbauer, C. K., Ludwig, R., & Nöll, G. (2010). Increasing the coulombic efficiency of glucose biofuel cell anodes by combination of redox enzymes. *Biosensors & Bioelectronics*, *25*(7), 1710–1716. https://doi.org/10.1016/J.BIOS.2009.12.017

Tasca, F., Timur, S., Ludwig, R., Haltrich, D., Volc, J., Antiochia, R., & Gorton, L. (2007). Amperometric biosensors for detection of sugars based on the electrical wiring of different pyranose oxidases and pyranose dehydrogenases with osmium redox polymer on graphite electrodes. *Electroanalysis*, *19*(2–3), 294–302. https://doi.org/10.1002/elan.200603740

Taylor, J. W. (2011). The poetry of mycological accomplishment and challenge. *Fungal Biology Reviews*, *25*(1), 3–13. https://doi.org/10.1016/j.fbr.2011.01.005

Terrett, O. M., & Dupree, P. (2019). Covalent interactions between lignin and hemicelluloses in plant secondary cell walls. *Current Opinion in Biotechnology*, *56*, 97–104. https://doi.org/10.1016/j.copbio.2018.10.010

Tonyushkina, K., & Nichols, J. H. (2009). Glucose meters: A review of technical challenges to obtaining accurate results. *Journal of Diabetes Science and Technology*, *3*(4), 971–980.

https://doi.org/10.1177/193229680900300446

Trouvelot, S., Héloir, M. C., Poinssot, B., Gauthier, A., Paris, F., Guillier, C., Combier, M., Trdá, L., Daire, X., & Adrian, M. (2014). Carbohydrates in plant immunity and plant protection: Roles and potential application as foliar sprays. *Frontiers in Plant Science*, *5*(November), 1–14. https://doi.org/10.3389/fpls.2014.00592

Urlacher, V. B., & Koschorreck, K. (2021). Pecularities and applications of aryl-alcohol oxidases from fungi. *Applied Microbiology and Biotechnology*, *105*(10), 4111–4126. https://doi.org/10.1007/s00253-021-11337-4

Varela, E., Böckle, B., Romero, A., Martínez, A. T., & Martínez, M. J. (2000). Biochemical characterization, cDNA cloning and protein crystallization of aryl-alcohol oxidase from *Pleurotus pulmonarius*. *Biochimica et Biophysica Acta - Protein Structure and Molecular Enzymology*, *1476*(1), 129–138. https://doi.org/10.1016/S0167-4838(99)00227-7

Varki, A., Cummings, R. D., Aebi, M., Packer, N. H., Seeberger, P. H., Esko, J. D., Stanley, P., Hart, G., Darvill, A., Kinoshita, T., Prestegard, J. J., Schnaar, R. L., Freeze, H. H., Marth, J. D., Bertozzi, C. R., Etzler, M. E., Frank, M., Vliegenthart, J. F. G., Lütteke, T., … Kornfeld, S. (2015). Symbol nomenclature for graphical representations of glycans. *Glycobiology*, *25*(12), 1323–1324. https://doi.org/10.1093/glycob/cwv091

Viborg, A. H., Terrapon, N., Lombard, V., Michel, G., Czjzek, M., Henrissat, B., & Brumer, H. (2019). A subfamily roadmap of the evolutionarily diverse glycoside hydrolase family 16 (GH16). *Journal of Biological Chemistry*, *294*(44), 15973–15986. https://doi.org/10.1074/jbc.RA119.010619

Viña-Gonzalez, J., Martinez, A. T., Guallar, V., & Alcalde, M. (2020). Sequential oxidation of 5-hydroxymethylfurfural to furan-2,5-dicarboxylic acid by an evolved aryl-alcohol oxidase. *Biochimica et Biophysica Acta - Proteins and Proteomics*, *1868*(1), 140293. https://doi.org/10.1016/j.bbapap.2019.140293

Virginia, L. J., & Peterbauer, C. (2023). Localization of pyranose 2-oxidase from *Kitasatospora aureofaciens*: A step closer to elucidate a biological role. *International Journal of Molecular Sciences*, *24*(3). https://doi.org/10.3390/ijms24031975

Vogel, J. (2008). Unique aspects of the grass cell wall. *Current Opinion in Plant Biology*, *11*(3), 301–307. https://doi.org/10.1016/j.pbi.2008.03.002

Volc, J., Kubátová, E., Wood, D. A., & Daniel, G. (1997). Pyranose 2-dehydrogenase, a novel sugar oxidoreductase from the basidiomycete fungus *Agaricus bisporus*. *Archives of Microbiology*, *167*(2–3), 119–125. https://doi.org/10.1007/s002030050424

Volc, J., Sedmera, P., Halada, P., Daniel, G., Přikrylová, V., & Haltrich, D. (2002). C-3 oxidation of non-reducing sugars by a fungal pyranose dehydrogenase: Spectral characterization. *Journal of Molecular Catalysis - B Enzymatic*, *17*(2), 91–100. https://doi.org/10.1016/S1381-1177(02)00014-0

Volc, J., Sedmera, P., Halada, P., Přikrylová, V., & Daniel, G. (1998). C-2 and C-3 oxidation of D-Glc, and C-2 oxidation of D-Gal by pyranose dehydrogenase from *Agaricus bisporus*. *Carbohydrate Research*,

310(1–2), 151–156. https://doi.org/10.1016/S0008-6215(98)00151-7

Volc, J., Sedmera, P., Halada, P., Přikrylová, V., & Haltrich, D. (2000). Double oxidation of D-xylose to D-glycero-pentos-2,3-diulose (2,3-diketo-D-xylose) by pyranose dehydrogenase from the mushroom *Agaricus bisporus*. *Carbohydrate Research*, *329*(1), 219–225. https://doi.org/10.1016/S0008-6215(00)00167-1

Volc, J., Sedmera, P., Kujawa, M., Halada, P., Kubátová, E., & Haltrich, D. (2004). Conversion of lactose to β-D-galactopyranosyl-(1 → 4)-D-arabino-hexos-2-ulose-(2-dehydrolactose) and lactobiono-1,5-lactone by fungal pyranose dehydrogenase. *Journal of Molecular Catalysis B: Enzymatic*, *30*(3–4), 177–184. https://doi.org/10.1016/j.molcatb.2004.05.006

Vuong, T. V., & Master, E. R. (2022). Enzymatic upgrading of heteroxylans for added-value chemicals and polymers. *Current Opinion in Biotechnology*, *73*, 51–60. https://doi.org/10.1016/j.copbio.2021.07.001

Vuong, T. V., Vesterinen, A. H., Foumani, M., Juvonen, M., Seppälä, J., Tenkanen, M., & Master, E. R. (2013). Xylo- and cello-oligosaccharide oxidation by gluco-oligosaccharide oxidase from *Sarocladium strictum* and variants with reduced substrate inhibition. *Biotechnology for Biofuels*, *6*(148). https://doi.org/10.1186/1754-6834-6-148

Wang, X. W., Han, P. J., Bai, F. Y., Luo, A., Bensch, K., Meijer, M., Kraak, B., Han, D. Y., Sun, B. D., Crous, P. W., & Houbraken, J. (2022). Taxonomy, phylogeny and identification of *Chaetomiaceae* with emphasis on thermophilic species. *Studies in Mycology*, *101*(1), 121–243. https://doi.org/10.3114/SIM.2022.101.03

Westermark, U. (1985). The occurrence of *p*-hydroxyphenylpropane units in the middle-lamella lignin of spruce (*Picea abies*). *Wood Science and Technology*, *19*(3), 223–232. https://doi.org/10.1007/BF00392051

Westermark, U., & Eriksson, K.-E. (1974). Cellobiose:quinone oxidoreductase, a new wood-degrading enzyme from white-rot fungi. *Acta Chemica Scandinavica B*, *28*, 209–214. https://doi.org/10.3891/acta.chem.scand.28b-0209

Westermark, U., & Eriksson, K.-E. (1975). Purification and properties of cellobiose: quinone oxidoreductase from *Sporotrichum pulverulentum*. *Acta Chemica Scandinavica B*, *29*(4), 419–424.

Wijayanti, S. D., Sützl, L., Duval, A., & Haltrich, D. (2021). Characterization of fungal fAD-dependent AA3_2 glucose oxidoreductases from hitherto unexplored phylogenetic clades. *Journal of Fungi*, *7*(10). https://doi.org/10.3390/jof7100873

Witt, S., Singh, M., & Kalisz, H. M. (1998). Structural and kinetic properties of nonglycosylated recombinant *Penicillium amagasakiense* glucose oxidase expressed in *Escherichia coli*. *Applied and Environmental Microbiology*, *64*(4), 1405. https://doi.org/10.1128/AEM.64.4.1405-1411.1998

Wohlfahrt, G., Witt, S., Hendle, J., Schomburg, D., Kalisz, H. M., & Hecht, H. J. (1999). 1.8 and 1.9 Å resolution structures of the *Penicillium amagasakiense* and *Aspergillus niger* glucose oxidases as a basis for modelling substrate complexes. *Acta Crystallographica Section D: Biological Crystallography*, *55*(5), 969–977. https://doi.org/10.1107/S0907444999003431

Yang, X., Cui, L., Li, S., Ma, C., Kosma, D. K., Zhao, H., & Lü, S. (2022). Fatty alcohol oxidase 3 (FAO3) and FAO4b connect the alcohol- and alkane-forming pathways in *Arabidopsis* stem wax biosynthesis. *Journal of Experimental Botany*, *73*(9), 3018–3029. https://doi.org/10.1093/jxb/erab532

Yoshida, H., Sakai, G., Mori, K., Kojima, K., Kamitori, S., & Sode, K. (2015). Structural analysis of fungus-derived FAD glucose dehydrogenase. *Scientific Reports*, *5*, 1–13. https://doi.org/10.1038/srep13498

Yu, Q., Wang, Y., Van Le, Q., Yang, H., Hosseinzadeh-Bandbafha, H., Yang, Y., Sonne, C., Tabatabaei, M., Lam, S. S., & Peng, W. (2021). An overview on the conversion of forest biomass into bioenergy. *Frontiers in Energy Research*, *9*(July), 1–10. https://doi.org/10.3389/fenrg.2021.684234

Zamil, M. S., & Geitmann, A. (2017). The middle lamella - More than a glue. *Physical Biology*, *14*(1). https://doi.org/10.1088/1478-3975/aa5ba5

Zámocký, M., Schümann, C., Sygmund, C., O'Callaghan, J., Dobson, A. D. W., Ludwig, R., Haltrich, D., & Peterbauer, C. K. (2008). Cloning, sequence analysis and heterologous expression in *Pichia pastoris* of a gene encoding a thermostable cellobiose dehydrogenase from *Myriococcum thermophilum*. *Protein Expression and Purification*, *59*, 258–265. https://doi.org/10.1016/j.pep.2008.02.007

Zebda, A., Gondran, C., Le Goff, A., Holzinger, M., Cinquin, P., & Cosnier, S. (2011). Mediatorless high-power glucose biofuel cells based on compressed carbon nanotube-enzyme electrodes. *Nature Communications*, *2*(1). https://doi.org/10.1038/ncomms1365

Zhang, J., Xia, W., Liu, P., Cheng, Q., Tahirou, T., Gu, W., & Li, B. (2010). Chitosan modification and pharmaceutical/biomedical applications. *Marine Drugs*, *8*(7), 1962–1987. https://doi.org/10.3390/MD8071962

Zhou, N., Thilakarathna, W. P. D. W., He, Q. S., & Rupasinghe, H. P. V. (2022). A review: Depolymerization of lignin to generate high-value bio-products: Opportunities, challenges, and prospects. *Frontiers in Energy Research*, *9*(January), 1–18. https://doi.org/10.3389/fenrg.2021.758744